

**Modeling the AppA/PpsR Signal Transduction  
System of *Rhodobacter sphaeroides***

**Dissertation**

zur Erlangung des akademischen Grades

**doctor rerum naturalium**

**(Dr. rer. nat.)**

genehmigt durch die Fakultät für Naturwissenschaften  
der Otto-von-Guericke-Universität Magdeburg

von **M. Tech. M. Sc. Rakesh Pandey**  
geb. am 1 July 1983 in Ballia, Uttar Pradesh, India

Gutachter: Jun.-Prof. Dr. rer. nat. Marcus J. B. Hauser  
Prof. Dr. rer. nat. Carsten Beta

eingereicht am: 25.06.2012

verteidigt am: 26.11.2012



*to my parents Shrimati Chandrawati Pandey and Shri  
Kameshwar Nath Pandey*



# Contents

<b>Abstract</b>	<b>v</b>
<b>Abstract (German)</b>	<b>vii</b>
<b>List of Abbreviations</b>	<b>x</b>
<b>1 Introduction</b>	<b>1</b>
1.1 Motivation and Task . . . . .	6
1.2 Thesis Outline . . . . .	7
<b>2 State of the Art</b>	<b>8</b>
<b>3 A Simple Model for the AppA/PpsR System</b>	<b>11</b>
3.1 Model Construction . . . . .	11
3.1.1 Reduction of PpsR by AppA . . . . .	12
3.1.2 Complex Formation between AppA and PpsR . . . . .	14
3.1.3 Redox Regulation of AppA . . . . .	16
3.1.4 Reoxidation of PpsR . . . . .	16
3.2 Model Equations . . . . .	17
3.3 Steady States when $K_{eq} \gg 1$ . . . . .	19
3.4 Meaning of the Parameters . . . . .	20
3.5 Results . . . . .	21
3.5.1 When $[A_T]/[P_T] < 2$ . . . . .	21
3.5.2 When $[A_T]/[P_T] \geq 2$ . . . . .	25
3.6 Discussion and Summary . . . . .	30
3.6.1 PS Gene Repression under Semi-Aerobic Conditions . . . . .	33
3.6.2 PS Gene Repression under Anaerobic Conditions . . . . .	33
3.6.3 Bistability in the AppA/PpsR System . . . . .	34
3.6.4 Possible Experiments to Verify Bistability . . . . .	35
3.6.5 Model Limitations . . . . .	35

---

<b>4</b>	<b>An Extended Model for the AppA/PpsR System</b>	<b>37</b>
4.1	Development of the Extended Model . . . . .	37
4.1.1	Reaction Steps from the Simple Model . . . . .	38
4.1.2	A Detailed Mechanism for the Light Regulation . . . . .	39
4.2	System Equations and Parameters . . . . .	41
4.3	Steady State Expressions . . . . .	45
4.4	Results . . . . .	46
4.4.1	Effect of the New Parameters in the Absence of Light . . . . .	47
4.4.2	Parameter Estimation for the Extended Model . . . . .	47
4.4.3	Peak Development in the Extended Model . . . . .	52
4.4.4	Repression of PS genes Under Semi-Aerobic Conditions . . . . .	55
4.4.5	Role of $\gamma$ on the Peak-Position and Bistability . . . . .	59
4.4.6	Role of $K_{eq}$ for the Peak of Reduced PpsR . . . . .	62
4.4.7	Light Response Curve of an AppA Mutant . . . . .	63
4.5	Discussion and Summary . . . . .	63
<b>5</b>	<b>Conclusions and Outlook</b>	<b>66</b>
	<b>Appendix A Reduction of PpsR with a 2:1 Stoichiometry</b>	<b>72</b>
A.1	Quasi-Steady State Approximation . . . . .	74
	<b>Appendix B Complex Formation as a Multi-Step Process</b>	<b>77</b>
B.1	Quasi-Equilibrium Approximation . . . . .	80
	<b>Appendix C Descartes' Rule of Signs</b>	<b>83</b>
	<b>Appendix D Roots of the Polynomial 3.15</b>	<b>84</b>
	<b>Appendix E Limit Point Bifurcation</b>	<b>87</b>
	<b>Appendix F The Principle of Detailed Balance</b>	<b>90</b>
	<b>Appendix G Methods</b>	<b>92</b>
	<b>List of Publications</b>	<b>100</b>
	<b>Curriculum Vitae</b>	<b>101</b>
	<b>Erklärung</b>	<b>103</b>

# Acknowledgement

First and foremost I would like to thank God. HE has given me the courage to believe in myself and pursue my dreams. I could never have done this without your blessings, the Almighty.

I would like to express my deepest gratitude to my supervisor Prof. Marcus J. B. Hauser. He provided me freedom and a friendly environment, which helped me a lot during this study. His enthusiastic and dedicated view of research inspired me to do my doctoral work.

I am deeply grateful to Dr. Ronny Straube without whom this work could not be shaped. A few lines are too short to make a complete account of my deep appreciation for him. He is so kind that he spent his precious time to clear my doubts whenever I approached him. He has given me his unequivocal support throughout. He provided inspiring guidance for the successful completion of my research work. I deem it as my privilege to work under his guidance. I ever remain grateful to him.

I do thank Dr. Barbara Witter for all the help she rendered me during my stay in Magdeburg to finish this work, and to Prof. Dietrich Flockerzi for developing a strong interest in me for dynamical systems. I owe sincere thanks to all staff and my colleagues of the Max Planck Institute for Dynamics of Complex Technical Systems, Magdeburg for their co-operation and help during this work. A special thanks to Anke Carius for her help during preparation of the thesis.

At this juncture, I think of my parents whose selfless sacrificial life and their great efforts with unceasing prayers has enabled me to reach the present position in my life. I am eternally grateful to my father who planted the seed of idea to do research and stood by me through the good times and bad. Unconditional love and blessings of my mother have been the greatest strength of my life. I would also like to thanks Priyanka whose patience and support helped me to overcome many crisis situations.

Rakesh Pandey

# Abstract

Purple non-sulfur bacteria, such as *Rhodobacter sphaeroides*, are remarkably versatile in their growth capabilities. They switch their energy generation mechanism from photosynthesis to respiration depending on the oxygen levels and light conditions. The AppA/PpsR system is one of the regulatory systems in *R. sphaeroides* which mediates this transition at the transcription level. It specifically represses the photosynthesis (PS) genes under aerobic conditions. Actually, under aerobic conditions, the PpsR protein binds cooperatively to the target promoters of the PS genes and inhibits their expression. The repressor activity of PpsR is antagonized by the flavoprotein AppA, which utilizes the two cofactors FAD and heme to sense blue light and oxygen, respectively. It is believed that the oxygen- and light-dependent interaction between AppA and PpsR leads to a unique phenotype under semi-aerobic conditions, where PS genes are repressed by sufficiently intense blue light irradiance ( $LI \geq 0.2 \mu\text{molm}^{-2}\text{s}^{-1}$ ).

To understand the molecular mechanism that may lead to such a phenotype, we developed a simple mathematical model for the AppA/PpsR system. The model is based on two experimental findings: (i) the AppA-mediated reduction of a disulfide bond in PpsR, and (ii) the light-inhibited complex formation between AppA and PpsR. A steady state analysis of the model equations shows that a maximum develops in the steady state response curve of the reduced form of PpsR at intermediate oxygen levels, if PpsR is reduced on a faster time scale than AppA, and if the electron transfer from AppA to PpsR is effectively irreversible. We suggest that the maximum formation could provide a qualitative explanation for the observed blue light repression of PS genes under semi-aerobic conditions. We found that the transition from anaerobic to aerobic growth conditions can also occur via a bistable regime if the copy number of AppA is greater than that of PpsR by at least a factor of two.

To gain further insight into the system, we extended the model for the AppA/PpsR system by incorporating a more detailed mechanism for the

light regulation of the interaction between AppA and PpsR. We identified the kinetic and stoichiometric constraints, which are required for the persistence of the two features of the simple model, namely (i) oxygen-dependent peak formation of reduced PpsR and (ii) bistability, if a detailed mechanism for the light regulation is employed. Our results suggest that the ratio of the two proteins AppA and PpsR must be tightly regulated for a proper light regulation of PS genes under semi-aerobic conditions. We found that the predictions of the extended model can be brought into a good agreement with recent experimental results of the light dependent repression of PS genes under semi-aerobic conditions. In addition, we show that the extended model can also account for the lowered blue light sensitivity observed in an AppA mutant strain. The present study is a first step towards a more qualitative understanding of the regulatory capabilities of the AppA/PpsR system. It will hopefully stimulate new experiments, which may help to validate and improve the current model for the AppA/PpsR system.

# Abstract

Nichtschwefelpurpurbakterien, wie *Rhodobacter sphaeroides* sind bemerkenswert vielseitig bezüglich ihrer Lebensbedingungen, denn sie passen den Mechanismus ihrer Energiegewinnung an die Verfügbarkeit von Sauerstoff und Licht an. Das AppA/PpsR-Regulationssystem ist eines der Systeme die in *R. sphaeroides* den Wechsel zwischen aerober Atmung und Photosynthese auf Transkriptionsebene kontrollieren. PpsR bindet spezifisch an die Promotorregion der Photosynthesegene und unterdrückt ihre Transkription unter aeroben Bedingungen. Das Flavoprotein AppA wirkt der Repressoraktivität von PpsR entgegen. Es verwendet zwei Cofaktoren, FAD und Häm um blaues Licht bzw. Sauerstoff zu detektieren. Es wird angenommen, dass die sauerstoff- und licht-abhängige Interaktion zwischen AppA und PpsR unter semi-aeroben Bedingungen zu einem einzigartigen Phänotyp führt, denn dann können die Photosynthesegene durch Blaulichteinstrahlung reprimiert werden.

Um den molekularen Mechanismus zu verstehen, der zu diesem Phänotyp führt, haben wir ein einfaches mathematisches Modell für das AppA/PpsR-System entwickelt. Es basiert auf zwei experimentellen Erkenntnissen: 1. AppA reduziert die Disulfidbrücke in PpsR und 2. Die Komplexbildung zwischen PpsR und AppA wird durch Licht inhibiert. Eine Analyse der Modellgleichungen im stationären Zustand zeigt, dass sich ein Maximum in der Antwortkurve für reduziertes PpsR entwickelt wenn unter semi-aeroben Bedingungen PpsR schneller von AppA reduziert wird als AppA regeneriert werden kann und der Elektronenfluss von AppA zu PpsR tatsächlich irreversibel ist.

Wir schlagen vor, dass die Bildung dieses Maximums eine qualitative Erklärung für die beobachtete Blaulichtrepression der Photosynthesegene unter semi-aeroben Bedingungen liefern könnte. Ausserdem fanden wir heraus, dass sich das Modell beim Wechsel von anaeroben zu aeroben Wachstumsbedingungen bistabil verhält, wenn die Zahl der AppA-Moleküle mindestens doppelt so groß ist wie die der PpsR-Moleküle.

Um noch tiefere Einblicke in das System zu erlangen, wurde das Modell für das AppA/PpsR-System um einen detaillierteren Mechanismus für die Lichtregulation der Interaktion zwischen AppA und PpsR erweitert. Wir identifizierten die Kinetik und stöchiometrischen Grenzen, die notwendig sind, um die beiden Eigenschaften, sauerstoffabhängige Akkumulation von reduziertem PpsR und Bistabilität, des ursprünglichen Modells zu erhalten, wenn ein detaillierter Lichtregulationsmechanismus zum Einsatz kommt. Unsere Ergebnisse deuten daraufhin, dass das Verhältnis der beiden Proteine AppA und PpsR strikt reguliert werden muss um eine konsistente Regulation der Photosynthesegene unter semi-aeroben Bedingungen zu ermöglichen. Unsere Vorhersagen stimmen gut mit den neuesten Forschungsergebnissen über die lichtabhängige Repression der Photosynthesegene unter semi-aeroben Bedingungen überein.

Zusätzlich zeigen wir, dass das erweiterte Modell auch die geringere Blaulichtsensitivität einer AppA-Mutante wiedergeben kann. Die vorliegende Studie ist ein erster Schritt um die regulatorischen Möglichkeiten des AppA/PpsR-Systems qualitativ besser zu verstehen. Damit ist die Basis für den iterativen Prozess, bestehend aus experimenteller Modellverifikation und anschließender Modellanpassung, gelegt.

# List of Abbreviations

$EC_{50}$	denotes the concentration for half-maximal binding of PpsR to DNA fragment containing the <i>puc</i> promoter
$LI_{50}$	the light irradiance where half-maximal levels of reduced PpsR are reached
AppA	activation of photopigment and <i>puc</i> expression
ATP	adenosine-5'-triphosphate
BLUF	blue light sensing using flavin adenine dinucleotide
CM	cytoplasmic membrane
DNA	deoxyribonucleic acid
ETC	electron transport chain
FAD	flavin adenine dinucleotide
FnrL	fumarate nitrate regulator L
ICM	intracytoplasmic membrane
LHC	light harvesting complex
LI	light irradiance
LP	limit point
$NAD^+$	nicotinamide adenine dinucleotide
NADH	reduced nicotinamide adenine dinucleotide
ODE	ordinary differential equation
PpsR	photopigment suppression in <i>R. sphaeroides</i>

PrrA	photosynthetic response regulator A
PrrB	photosynthetic response regulator B
PS	photosynthesis
Q	ubiquinone
$QH_2$	ubiquinol (reduced ubiquinone)
RC	reaction center
SCHIC	sensor containing <i>heme</i> instead of cobalamin
WT	wild type

# Chapter 1

## Introduction

Nature has given incredible capabilities to organisms, one of them is the ability to sense and respond adequately to changes in their environmental conditions in order to survive in adverse environmental situations. It is a very challenging task to unfold the underlying mechanism through which organisms are able to cope with different environmental stresses. Aiming to understand and unfold such mechanisms, numerous studies have been conducted on facultatively photosynthetic purple bacteria such as *Rhodobacter sphaeroides*, because their physiology is well understood, and they are relatively easy to grow in laboratory cultures (1). Purple bacteria are generally found in diverse environmental conditions such as freshwater, saline, marine soil and hot-springs. Since these bacteria are pigmented with bacteriochlorophyll a or b together with the various carotenoids, they are found in several colours such as purple, red, brown, and orange.

Based on their tolerance and utilization of sulfide, purple bacteria are divided in two groups: Purple sulfur bacteria and purple non-sulfur bacteria (1). Any elemental sulfur formed by the oxidation of sulfide in purple non-sulfur bacteria is not stored intracellularly, instead it is deposited outside the cells (1, 2). In contrast, in purple sulfur bacteria elemental sulfur is stored in globules inside the cells. Purple sulfur bacteria use hydrogen sulfide ( $H_2S$ ) or other reduced sulfur compounds such as thiosulfate ( $S_2O_3^{2-}$ ) as an electron donor (2). Initially, it was thought that purple non-sulfur bacteria are unable to use sulfide as an electron donor. Later it has been observed that they can use sulfide, but the levels of sulfide ideal for purple sulfur bacteria (1-3 mM) are often toxic to most of the non-sulfur bacteria (2). Some of the species of purple non-sulfur bacteria can grow using hydrogen ( $H_2$ ) as a reducing agent (2). Unlike plants, algae, and cyanobacteria, purple bacteria do not produce oxygen as they do not use water as a reducing agent. Purple non-sulfur bacteria come under  $\alpha$  and  $\beta$  class of the phylum proteobacteria

(2), whereas purple sulfur bacteria belong to the  $\gamma$  class of this phylum (3). Purple bacteria are metabolically versatile, and use different strategies to grow depending upon the environmental conditions. These bacteria can grow by aerobic respiration, anaerobic respiration, anoxygenic photosynthesis or fermentation.

*Rhodobacter sphaeroides*, which is a purple non-sulfur bacterium, switches its energy generation mechanism from respiration to photosynthesis depending upon the oxygen tension and light conditions. Under aerobic conditions, they generate energy via respiration (4) using oxygen as the terminal electron acceptor. However, when oxygen tension drops below a certain threshold and the bacteria face the risk of low energy yield via aerobic respiration (5), they convert the available light energy into chemical energy (ATP) via anoxygenic photosynthesis. Therefore, oxygen and light are two major environmental signals for *R. sphaeroides*. Depending upon the amount of dissolved oxygen in the growth medium, three growth regimes are distinguished (6, 7): Aerobic ( $\approx 200 \mu\text{M}$ ), semi-aerobic ( $\approx 100 \mu\text{M}$ ) and anaerobic/low oxygen ( $\leq 3 \mu\text{M}$ ).

A decrease in oxygen level stimulates an intracellular differentiation of the cytoplasmic membrane (CM) leading to the formation of the intracytoplasmic membrane system (ICM) (8, 9). Though the ICM is physically connected to the cytoplasmic membrane, it is functionally distinct from that (9). The specialized intracytoplasmic membrane of *R. sphaeroides* houses the photosynthetic apparatus (9, 10). Photosynthetic apparatus (photosystem) consists of two light harvesting complexes B875 (LHI) and B800-850 (LHII) (6, 8, 10, 11). According to Verméglio et al. (12) the  $bc_1$  complex is also a part of the photosystem. The light harvesting complexes trap the light energy and channel that energy to the reaction center (RC) as excitation energy (6, 12, 13). In the reaction center charge separation and initiation of the electron transport occurs (6, 12, 13). The formation of photosynthetic apparatus is triggered by a decrease in the oxygen levels (8, 10).

Almost all genes required for the formation of the photosynthetic apparatus are located in a region of the chromosome of *R. sphaeroides*, which is known as photosynthesis (PS) gene cluster (11, 14). PS genes such as *puf* and *puhA* (polypeptides of the reaction center and pigment-binding proteins of the light harvesting complex I) (7, 14, 15), *bch* (bacteriochlorophyll), and *crt* (carotenoid synthesis) are part of the PS gene cluster. The *puc* operon (pigment-binding proteins of the light harvesting complex II) is located in a different region on the chromosome (11, 14, 16).

In *R. sphaeroides*, the transition of energy generation mechanism from respiration (aerobic) to photosynthesis (anaerobic) is mediated by three major regulatory transcriptional systems: (i) The PrrB/PrrA two component system which induces the expression of PS genes under anaerobic condi-

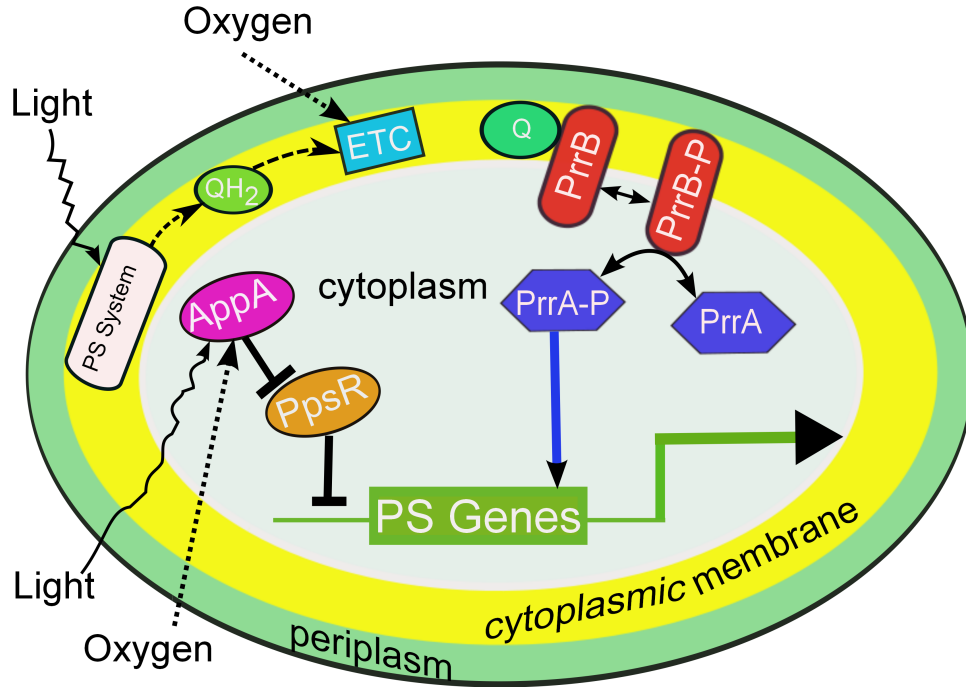


Figure 1.1: A schematic diagram for the light- and redox-dependent signal transduction in *Rhodobacter sphaeroides*. The PrrB-P and PrrA-P denote phosphorylated PrrB and PrrA protein, respectively. The ETC represents the electron transport chain. PS system denotes the photosystem which traps the light energy. Q and QH<sub>2</sub> represent the ubiquinone and ubiquinol (reduced form of ubiquinone), respectively. The lines with a bar end and an arrow with blue colour tail indicate inhibition and activation, respectively. Arrows with dash tail and dot tail denote electron transfer and sensing of oxygen stress, respectively. The arrow with a green colour tail indicates photosynthesis (PS) gene expression. The PpsR protein represses the PS genes under aerobic conditions, and AppA protein inhibits the repressive activity of PpsR. PrrB is a sensor kinase, which under anaerobic conditions, autophosphorylates and transfer its phosphoryl group to cognate response regulator PrrA. Phosphorylated PrrA protein activates the PS gene expression. Under aerobic conditions, ubiquinone binds with PrrB, and inhibits the kinase activity of PrrB. On the other hand, PpsR represses the PS gene expression under these conditions. Consequently, PS genes would be highly repressed under aerobic conditions. Under anaerobic conditions, the concentration of ubiquinone will be low, therefore PrrB will show its kinase activity which leads to the activation of PS genes. At the same time, AppA protein inhibits the repressive activity of PpsR. As a result, PS genes would be induced under anaerobic conditions.

tions (17, 18), (ii) the anaerobic activator FnrI (8, 19), and (iii) the aerobic repressor PpsR (20, 21). PrrB and PrrA are proteins produced from the genes *prrA* (photosynthetic response regulator A) and *prrB* (photosynthetic response regulator B), respectively (8). Also, FnrI and PpsR are proteins produced from the genes *fnrL* (fumarate nitrate regulator L) and *ppsR* (photopigment suppression in *R. sphaeroides*), respectively (8). While the first two are global regulatory systems (PrrB/PrrA and FnrL), the third (PpsR) is specifically involved in the regulation of PS genes.

The PpsR protein is a repressor of PS genes (20, 21), and it exists as a stable tetramer in solution (22). Under aerobic conditions, it binds cooperatively to a pair of palindromic sequences in the target promoters of PS genes (20, 22, 23). DNA-binding of PpsR is stimulated by oxygen through the formation of an intramolecular disulfide bond between two redox-active cysteine residues (21, 24). As the oxygen level drops below a certain threshold ( $\leq 3 \mu\text{M}$ ), the disulfide bonds are reduced to thiol groups, which results in a lower DNA-binding affinity, because the reduced form of PpsR has lower DNA-binding affinity compared to its oxidized state (22).

Experiments conducted by Masuda and Bauer (22) showed that the reduction of PpsR is mediated by AppA which is an oxygen- and blue-light-sensitive flavoprotein (6, 23, 25). The AppA protein is produced by the gene *appA* (activation of photopigment and *puc* expression) (8), and seems to be unique to *R. sphaeroides* as it has no known homolog in *Rhodobacter capsulatus* (the closest purple bacterium to *R. sphaeroides*) (6, 22). The AppA protein utilizes the two cofactors FAD (flavin adenine dinucleotide) and heme to sense blue light and oxygen, respectively. While FAD is noncovalently attached to the N-terminal BLUF (blue light sensing using flavin adenine dinucleotide) domain of AppA (6, 25, 26), the heme cofactor associates to a region in the C-terminal part of that protein (5, 27).

The light dependent regulation of PS gene expression depends on the oxygen tension, the wave length and the number of the incident photons. The light quantities are typically reported in irradiance unit  $\mu\text{molm}^{-2}\text{s}^{-1}$  corresponding to the number of photons in a certain wave length range incident on a unit area per unit time. It has been experimentally observed in *R. sphaeroides* that under semi-aerobic conditions the expression of PS genes such as *puf* and *puc* are highly repressed under blue light (450 nm) illumination (28), which is believed to avoid the accumulation of toxic reactive oxygen species in the simultaneous presence of oxygen and light (13). It has been shown that the FAD cofactor of AppA (therefore AppA) is essential for the blue light-dependent repression of PS gene under semi-aerobic conditions (6). Since the AppA protein only exists in *R. sphaeroides*, the blue light dependent repression of PS genes under semi-aerobic conditions is

unique to *R. sphaeroides* (6).

Molecular genetic analysis conducted by Gomelsky and Kaplan (29), provided first evidence for an interaction between PpsR and AppA in the regulation of photosynthesis genes. This is mainly based on the observation that AppA null mutant is impaired in photosynthetic growth while a secondary PpsR null mutant rescued these PS defects (29). They suggested that AppA can affect photosynthesis gene expression through the PpsR regulatory pathway, and that AppA seems to antagonize PpsR repression. In addition, they showed that *ppsR* gene expression in wild type *R. sphaeroides* is generally unaffected by the growth conditions, which suggests that the regulation of repressor activity of PpsR occurs predominantly at the protein level (post-transcriptional level). This seems necessary since there is only a 2.2-fold change in the DNA binding affinity for oxidized vs. reduced form of PpsR (22) as compared to a factor of 4.5 for the two forms of CrtJ (a homolog of PpsR in *R. capsulatus*) (30). As an effect of that, PS gene expression would only moderately be induced in *R. sphaeroides* under anaerobic/low oxygen conditions. However, in the presence of AppA the difference in the DNA binding affinity between the oxidized and the reduced form of PpsR is increased by a factor of 5 similar to that for CrtJ suggesting that AppA interferes with DNA binding of PpsR and is required for a full induction of PS genes in *R. sphaeroides* (22).

The AppA protein inhibits the DNA-binding activity of oxidized PpsR by two mechanisms (22, 31): (i) By reducing a disulfide bond in PpsR and (ii) by a blue light-dependent sequestration of PpsR protein molecules into transcriptionally inactive complexes. This inhibition leads to the induction of PS genes in the absence of oxygen (31). It is known that in the presence of blue light illumination (450 nm), AppA undergoes a conformational change (32, 33) which presumably leads to the dissociation of the AppA-PpsR complex (5).

Several phenomenological explanations were proposed, based on this core mechanism to explain the effect of oxygen and blue light on the regulatory properties of the AppA/PpsR signal transduction system (5, 6, 22, 34). However, yet, it is unclear whether this two stage interaction between AppA and PpsR is sufficient to generate the experimentally observed behaviours, specifically, the PS gene repression under high light illumination (light irradiance  $\approx 20\mu\text{molm}^{-2}\text{s}^{-1}$ ) at intermediate oxygen levels. Besides that, it is also unknown whether the AppA-mediated anti-repression of PpsR activity has further beneficial effects compared to the simpler regulatory mechanisms in other purple bacteria.

## 1.1 Motivation and Task

The main motivation behind the present study was to investigate whether the known molecular interaction between AppA and PpsR are sufficient to generate the experimentally observed phenotype, where PS genes are suppressed by high light illumination under semi-aerobic conditions.

As a first step towards a quantitative understanding of the regulatory capabilities of the AppA/PpsR system, we develop a simple mathematical model for the light- and redox-dependent interaction of AppA and PpsR, which is the first mathematical model for this system. Since most of the kinetic parameters are unknown, we introduce dimensionless entities to assess the relative importance of individual reaction steps for the steady-state behaviour of the system. We then use standard techniques from nonlinear dynamics such as bifurcation theory and quasi-steady state approximation to analyse the qualitative behavior of the system. This analysis suggests that the high intensity light induced repression of PS genes can indeed occur under semi-aerobic conditions, provided that PpsR is reduced on a much faster time scale than AppA and provide that the reduction of PpsR by AppA occurs in an effectively irreversible manner. In addition, we show that the transition from anaerobic to aerobic growth regime could occur via a bistable regime. We discuss the necessary conditions for the occurrence of the bistability, and suggest possible experiments to verify this prediction.

Subsequently, we describe an extended model for the interaction of AppA and PpsR by incorporating a more detailed light regulation of AppA, as in the simple model we have considered the light-dependent regulation of the interaction between AppA and PpsR only in an effective manner. We investigate the conditions under which the two feature of the simple model persist (oxygen dependent peak formation in the response curve of reduced PpsR and bistability) if a more detailed mechanism for the light regulation is incorporated. Our results suggest that the overexpression of AppA should favor the experimental observation of a bistable induction of PS genes. In addition, we show that the predictions of the extended model can be brought into good agreement with recent results on the light-dependent repression of PS genes under semi-aerobic conditions (35, 36). The extended model can also explain the lowered blue-light sensitivity observed in an AppA mutant strain, which contains a base exchange (tryptophan 104 to phenylalanine) in the FAD binding site of the BLUF domain (36).

## 1.2 Thesis Outline

The present thesis contains five Chapters and seven Appendices. In Chapter 1, a short introduction of the model organism and signal transduction system AppA/PpsR is described. Chapter 2 provides the state of the art. In Chapter 3, construction of a simple mathematical model for the light and oxygen dependent interaction of AppA and PpsR, and the steady state behaviour of the AppA/PpsR system are presented. In Chapter 4, an extension of the simple mathematical model is discussed, and the steady state behaviour of the extended model is presented. Where possible to compare the predictions of the extended model with experimental results on the light dependent repression of PS genes under semi-aerobic conditions. In Chapter 5, conclusions and outlook of the present work are provided. In Appendix A, it is shown that the consideration of a 2:1 stoichiometry, instead of 1:1 in Eq. 3.1 does neither alter our conclusion about the possibility of bistability in the AppA/PpsR system nor the non-monotonic dependence of reduced PpsR as a function of the oxygen concentration under high light conditions. Appendix B, describes the consequences of modeling the complex formation between AppA and PpsR by assuming a multi-step process (Eqs. 3.3, 3.4 and 3.5) instead of a lumped third order process (Eq. 3.6). It is shown that the modeling of complex formation between AppA and PpsR in more detail does not alter our two main conclusions: The possibility of bistability in the AppA/PpsR system and the non-monotonic dependence of reduced PpsR on the oxygen concentration under high light conditions. In addition, it is explained how the effective parameters in Eq. 3.6 can be derived from the kinetic parameters of the multi-step process (Eqs. 3.3, 3.4 and 3.5), through a quasi-equilibrium approximation for the intermediate species. In Appendix C, the Decarte's rule of sign is explained. Appendix D shows a closer analysis, which is used in Section 3.3. In Appendix E, the limit point bifurcation is described. In Appendix F, the principle of detailed balance is discussed. In the last Appendix G, methods are described, which are used to investigate the steady state behavior of the system.

# Chapter 2

## State of the Art

In this chapter, we will discuss the two phenomenological models which were proposed by Masuda et al. (22) and Han et al. (5) to explain the light- and redox-dependent signal transduction in *R. sphaeroides* via AppA/PpsR system.

The first molecular description of the light- and redox-dependent signal transduction through AppA/PpsR is provided by Masuda and Bauer (22). They proposed a model in which the interaction between AppA and PpsR was used to regulate repression of PS gene expression in *R. sphaeroides*. Three stages of control were suggested by them. In what follows we present how they describe the functioning of their model (Fig. 2.1).

Under aerobic conditions, an intramolecular disulfide bond forms between the cysteine (Cys) residues of PpsR, which exists as a tetramer. This disulfide bond formation stimulates DNA binding of PpsR, and inhibits PS gene expression. Under this condition AppA is presumed to exist in its oxidized state, which is the functionally inactive state of AppA (as an antirepressor of PS gene expression). With the decrease in the oxygen level, AppA becomes reduced, and subsequently, facilitates the reduction of the disulfide bond in oxidized form of PpsR. Reduced AppA also effectively prevents PpsR from binding DNA by forming a stable transcriptionally inactive AppA-PpsR complex. Under anaerobic conditions, complex formation between AppA and PpsR is inhibited by a blue light-induced shape change in the AppA protein, which occurs due to the absorption of light by the flavin of AppA. This model is supported by an *in vivo* observation that PpsR is oxidized in aerobically grown cells. It is also supported by genetic studies, which show that AppA null mutants repress PpsR-regulated genes under both aerobic and anaerobic growth regimes (23, 29). The model also takes into account the latter result, which suggests that the reduced form of PpsR containing reduced Cys residues is still capable to repress PS gene expression, however to a weaker

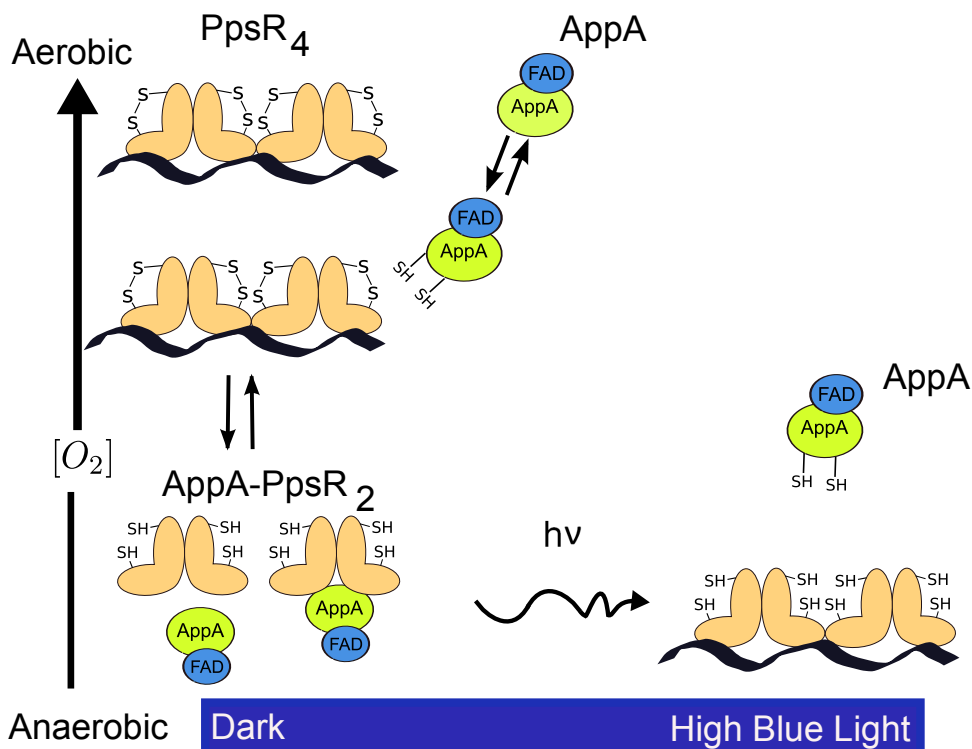


Figure 2.1: *The phenomenological model proposed by Masuda and Bauer (22).*

extent compared to the oxidized form.

Another model for the integration of light and redox signals by the AppA protein, has been suggested by Han et al. (5). According to this model, the C-terminal domain of AppA (*AppA* $\Delta$ N) is only responsive to light when the heme cofactor is in its reduced state (at low oxygen tension). Heme affects the interaction of the C-terminal domain of AppA with PpsR, and also the interaction of the C-terminal domain of AppA with its N-terminal BLUF domain. *In vivo*, the presence of heme increases the association constant of the AppA and PpsR by a factor of 2.4. This model suggests that depending on the redox status, the binding affinity of C-terminal domain with PpsR increases, and simultaneously the C-terminal domain acquires the potential to interact with its BLUF domain. The light signal determines the strength of the interaction between the two domains of AppA. Han et al. suggest that the interference of the BLUF domain in binding between the C-terminal domain of AppA and PpsR is stimulated by light. At low oxygen levels, the redox state of heme keeps the C-terminal domain of AppA in a conformation that

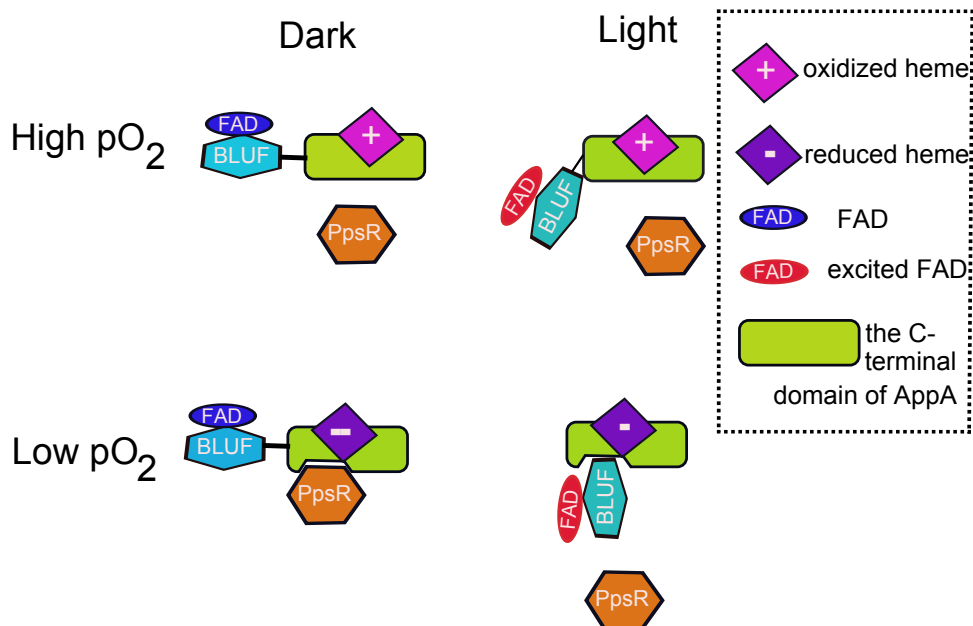


Figure 2.2: *The phenomenological model for the integration of redox and light signals by AppA proposed by Han et al. (5).*

alternatively favours interaction with the BLUF domain or with PpsR. Han et al. further suggested that the reduction of the heme cofactor at low oxygen conditions along with the reduction of the flavin by blue light could cause the electron transfer between AppA and PpsR, in addition to influencing the direct interaction between AppA and PpsR. Therefore, the model proposed by Han et al. suggests that the heme cofactor is essential for redox and light signaling by PpsR.

# Chapter 3

## A Simple Model for the AppA/PpsR System

In this chapter, the construction of a mathematical model for the light- and redox-dependent interaction between PpsR and AppA in *R. sphaeroides* is described. With the help of the model, it is shown how the protein-protein interactions between PpsR and AppA could result in a specific phenotype of this bacteria. In addition, possible experiments to verify the model predictions are discussed.

### 3.1 Model Construction

First evidence for an interaction between AppA and PpsR came from the observation that an AppA null mutant is impaired in photosynthetic growth, whereas a secondary PpsR null mutant relieves this effect (23, 29). Based on a series of experiments it has been shown that AppA antagonizes the repressor activity of PpsR, and AppA is required for a full induction of PS genes (22, 23, 29).

In order to modulate the PpsR repressor activity in a light and redox dependent manner AppA senses and integrates both signals with the help of the cofactors FAD and heme, respectively. AppA is a flavoprotein which contains an FAD-binding domain in its N-terminal region (denoted as BLUF for blue light sensing using flavin adenine dinucleotide). With FAD non-covalently attached to the BLUF domain, AppA can act as a blue-light sensor (22, 25, 26). Moreover, AppA contains a cysteine-rich C-terminal domain which is believed to be involved in the oxidation/reduction of PpsR (22). However, in recent studies two groups independently discovered a heme-binding (SCHIC) domain in the C-terminal part of the AppA protein (5, 27). These findings

suggest that AppA (with heme bound as a cofactor) can act as a redox sensor depending on the redox status of the bound heme. The presence of the cofactors FAD and heme provides AppA a unique capability to integrate both light and redox signals (6).

*In vitro* experiments by Masuda and Bauer (22, 31) showed that the AppA inhibits the DNA binding activity of oxidized PpsR by two mechanisms: First, by reducing a disulphide bond in PpsR, and second by a blue-light-dependent sequestration of PpsR proteins into transcriptionally inactive complexes. Based on these core mechanisms several phenomenological models have been published (5, 22, 34) in order to explain the effect of oxygen and blue light on the regulatory properties of this circuit. Taking into account those models, we develop a simple mathematical model (the first mathematical model) as a first step towards a more quantitative understanding of the regulatory capabilities of the AppA/PpsR system. In what follows we describe the molecular events which are the integral part of our model.

### 3.1.1 Reduction of PpsR by AppA

At the first stage of regulation, the reduced form of AppA ( $A^-$ ) reduces a disulfide bond in the oxidized PpsR ( $P^+$ ) in a light independent manner (22, 31). But the required number of AppA monomers to reduce one PpsR tetramer is yet not known. Though, it is conceivable that four AppA monomers are required to break four disulfide bonds in a PpsR tetramer, for simplicity we assume that the reduction occurs via a standard bimolecular reaction (Eq. 3.1). Considering, for example, a 2:1 stoichiometry in Eq. 3.1 does not alter the main conclusion obtained for 1:1 stoichiometry (*see Appendix A*).

Redox-titration experiments have shown that both PpsR and AppA have two redox-active thiol groups that can form intramolecular disulfide bonds with a similar midpoint potential of approximately -320 mV at pH 7.0 (37). This indicates that the equilibrium constant for the electron transfer from AppA to PpsR is close to 1. However, it is clear from the experiments conducted by Masuda and Bauer (22) that PpsR and AppA do not represent a standard redox couple since they could not observe an inverse electron transfer from reduced PpsR ( $P_4^-$ ) to oxidized AppA ( $A^+$ ).

We model the electron transfer between AppA and PpsR as a reversible reaction (Eq. 3.1) to investigate the effect of both possibilities (reversible and

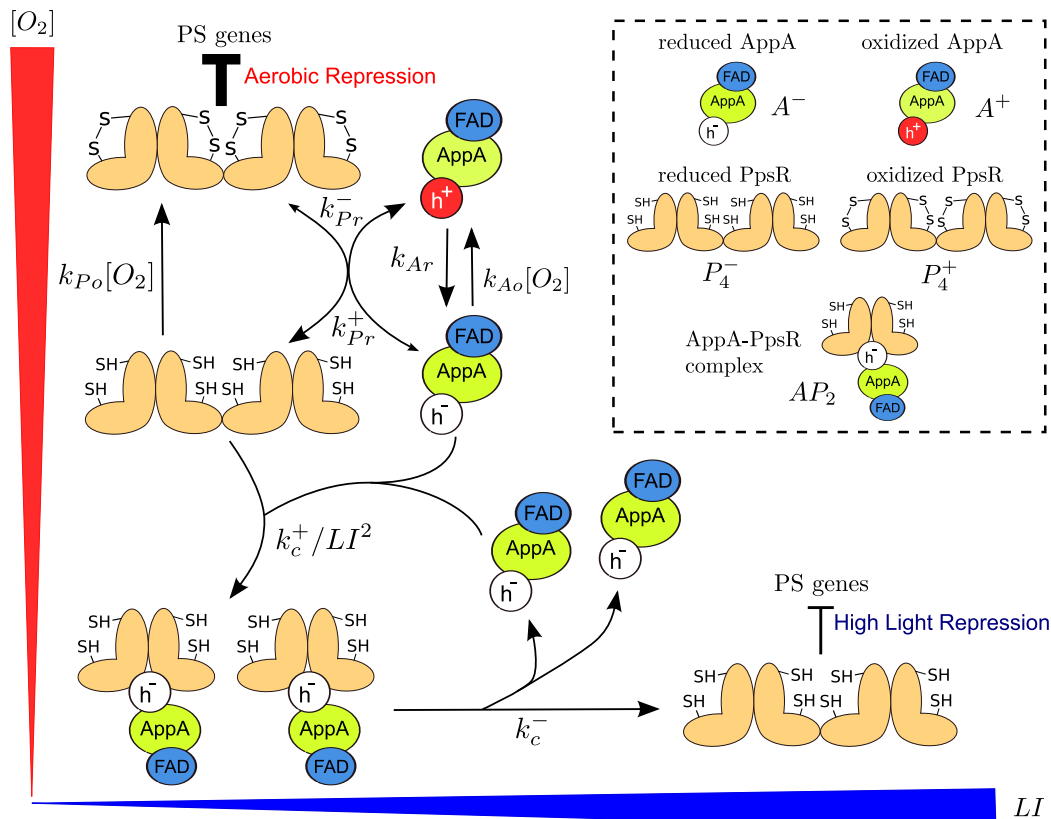
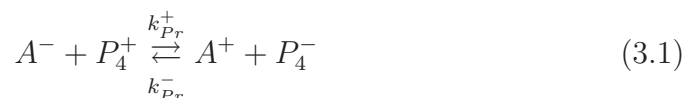


Figure 3.1: Model for the blue-light irradiance and oxygen concentration dependent interaction between AppA and PpsR (based on the experimental knowledge published in (5, 22, 31)). The oxidized and the reduced forms of the PpsR repressor are denoted by the tetramers with intramolecular disulfide bonds (S-S) and thiol groups (SH), respectively (see the legend in the dashed frame). The AppA protein has two cofactors attached, a FAD and a heme cofactor, where  $h^+$  and  $h^-$  represent the oxidized and reduced forms of the heme cofactor, respectively. Both the reduced and the oxidized forms of the PpsR repressor inhibit the expression of photosynthesis genes, but with different strengths as indicated by the line thickness.  $LI$  and  $[O_2]$  denote blue-light irradiance and oxygen concentration, respectively.

irreversible) on the steady state behaviour of the full system



In Eq. 3.1,  $k_{Pr}^+$  and  $k_{Pr}^-$  denote second-order rate constants. The equilibrium

constant  $K_{eq} = k_{pr}^+/k_{pr}^-$  is related to the difference between the midpoint potentials of the dithiol/disulfide couples in PpsR and AppA as

$$\Delta E_m = E_m^{P_4^+/P_4^-} - E_m^{A^+/A^-} = \frac{RT}{2F} \ln K_{eq}. \quad (3.2)$$

At room temperature (T=298 K),  $RT/2F$ , the factor related to the universal constant R and the Faraday constant F has a value of approximately 13 mV ( $RT/2F \approx 13$  mV).

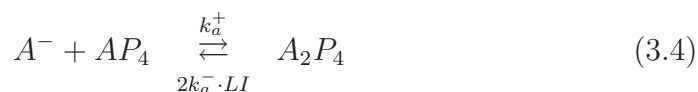
### 3.1.2 Complex Formation between AppA and PpsR

At the second stage of regulation, reduced AppA forms a complex with reduced PpsR under dark conditions (22). Based on size exclusion chromatography experiments and densitometric scanning Masuda and Bauer (22) found that in the complex, one AppA molecule is associated to two monomers of PpsR corresponding to half of a PpsR molecule which exists as a stable tetramer in solution. Further, they reported that the complex formation is inhibited by blue-light irradiance ( $LI=900\mu\text{mol}/m^2\text{s}$ ). However, a recent *in vivo* study (35) showed that, under semi-aerobic conditions, PS genes are inhibited by blue light down to  $0.2\mu\text{mol}/m^2\text{s}$ . It is believed that the light absorption induces a structural change in the BLUF domain of AppA (32), which results in interactions of light-induced FAD domain with its C-terminal part, thereby causing the dissociation of PpsR (5).

To keep the number of state variables and unknown parameters as small as possible, we do not distinguish between light-excited and non-excited forms of AppA. Further, we can model the complex formation between AppA and PpsR in two ways: (i) Considering the complex formation as a multi-step process or (ii) considering the complex formation as a single step process with an effective light dependent association rate.

### Complex Formation as a Two Step Process

We assume that a PpsR tetramer is composed of two identical dimer subunits and firstly, two AppA molecules (monomers) sequentially associate with one PpsR tetramer:



Also, we assume that the dissociation rate in Eq. 3.3 and Eq. 3.4 is proportional to the light irradiance  $LI$ , as blue light illumination is known to inhibit complex formation (22). Therefore,  $k_a^- \cdot LI$  is a pseudo first-order rate constant whereas  $k_a^+$  is a second-order rate constant. These two equations describe the association and dissociation of an AppA molecule to either of the two PpsR dimers. The combinatorial factors 2 in Eq. 3.3 and Eq. 3.4 are the result of the fact that, in the first association event (Eq. 3.3), there are two possibilities for an AppA molecule to bind one of the two PpsR dimers. Similarly, there are two possibilities for an AppA molecule to dissociate from the  $A_2P_4$  complex. For simplicity, we have assumed that the association and dissociation of the second AppA occur independently from the first association and dissociation event such that the rate constants  $k_a^+$  and  $k_a^-$  are the same for both steps.

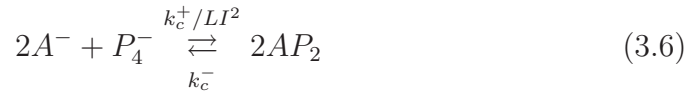
Lastly, the  $A_2P_4$  complex dissociates into two  $AP_2$  complexes where one AppA molecule is associated with one PpsR dimer :



where  $k_d^+$  and  $k_d^-$  are first-order and second-order rate constants, respectively.

## Complex Formation as a Single Step Process

The light-dependent complex formation between AppA and PpsR is modeled in an effective manner as



This effective description takes into account the experimentally observed 2:1 stoichiometry as well as the light-dependent inhibition of the complex ( $AP_2$ ) formation between AppA and PpsR (22). Here in Eq. 3.6,  $k_c^+/LI^2$  and  $k_c^-$  denote an effective third-order rate constant and a second-order rate constant, respectively. The inverse quadratic dependence of the forward rate on light irradiance arises from a more detailed description of the complex formation through an underlying multi-step process (Eq. 3.3 and Eq. 3.4). However, with the help of a quasi-equilibrium approximation we can show how  $k_c^+$  and  $k_c^-$  are related to the kinetic parameters:  $k_a^+$ ,  $k_a^-$ ,  $k_d^+$  and  $k_d^-$  of the multi-step process (Eq. B.16).

In the following, complex formation is assumed as a single step process. In *Appendix B*, we show in details how both assumptions lead to the same conclusion.

### 3.1.3 Redox Regulation of AppA

We follow the model proposed by Han et al. (5) to implement the redox-sensing capabilities of AppA, according to which AppA utilizes heme as a cofactor, bound to its C-terminal domain, to sense the cytosolic redox conditions. Consequently, we assume that AppA exists in two inter-convertible states according to the scheme



where “ $A^+$ ” and “ $A^-$ ” correspond to an oxidized and a reduced heme cofactor, respectively. This is consistent with the light-sensing reaction in Eq. 3.6 since AppA is only responsive to light when the bound heme cofactor is in its reduced state, and heme binding is known to increase the association constant with PpsR by a factor of 2.4 *in vivo* (5). Further, Han et al. (5) suggested that under a low oxygen levels the heme redox state keeps AppA in a conformation which favours the interaction of AppA with its BLUF domain or with PpsR. It was also suggested that the reduction of the heme cofactor could affect the electron flow from AppA to PpsR which is consistent with the reaction in Eq. 3.1. However, it is still unclear how AppA is reduced in the first place because its midpoint potential is probably much more negative than that of the cytosol (37). Note that the electron flow from the more negative to the more positive redox potential. Due to these uncertainties in the molecular redox-sensing mechanism of AppA we simply assume in Eq. 3.7 that, in the absence of oxygen, the heme cofactor in AppA is constitutively reduced by some unknown agent with first-order rate constant  $k_{Ar}$ , whereas the oxidation of the heme occurs proportional to the oxygen concentration. Hence,  $k_{Ao}[O_2]$  is a pseudo first-order rate constant at fixed concentration of oxygen.

### 3.1.4 Reoxidation of PpsR

If the electron transfer from AppA to PpsR in Eq. 3.1 was indeed effectively irreversible ( $k_{Pr}^- \ll k_{Pr}^+$ ), as suggested by the experiments of Masuda and Bauer (22), PpsR would have to be reoxidized through an AppA-independent mechanism. To account for this possibility, we assume that PpsR is reoxidized proportional to the oxygen concentration as



where  $k_{Po}[O_2]$  is a pseudo first-order rate constant.

## 3.2 Model Equations

Assuming mass-action kinetics for the reactions in Eq. 3.1 and Eqs. 3.6 - 3.8 we get the following set of ordinary differential equations

$$\begin{aligned}
 \frac{d}{dt}[A^-] &= k_{Ar}[A^+] - k_{Ao}[O_2][A^-] - k_{Pr}^+[A^-][P_4^+] + k_{Pr}^-[A^+][P_4^-] \\
 &\quad - 2 \left( \frac{k_c^+}{LI^2}[A^-]^2[P_4^-] - k_c^-[AP_2]^2 \right) \\
 \frac{d}{dt}[P_4^-] &= k_{Pr}^+[A^-][P_4^+] - k_{Pr}^-[A^+][P_4^-] - k_{Po}[O_2][P_4^-] \\
 &\quad - \left( \frac{k_c^+}{LI^2}[A^-]^2[P_4^-] - k_c^-[AP_2]^2 \right) \\
 \frac{d}{dt}[AP_2] &= 2 \left( \frac{k_c^+}{LI^2}[A^-]^2[P_4^-] - k_c^-[AP_2]^2 \right)
 \end{aligned} \tag{3.9}$$

In addition, we assume that the total amounts of PpsR and AppA molecules are conserved according to

$$\begin{aligned}
 [P_4^+] + [P_4^-] + \frac{1}{2}[AP_2] &= [P_T] \\
 \text{and } [A^+] + [A^-] + [AP_2] &= [A_T]
 \end{aligned} \tag{3.10}$$

which make Eqs. 3.9 a closed system for the reduced forms of AppA and PpsR as well as for the complex  $AP_2$ . Here,  $A_T$  and  $P_T$  represent the total concentrations of AppA and PpsR, respectively. This assumption seems to be justified for PpsR as its expression levels were found to be largely independent of the growth conditions (29). However, the regulation of AppA expression is unknown, so we will investigate how the steady state behaviour of the system in Eqs. 3.9 depends on the ratio  $[A_T]/[P_T]$ . We neglect dilution terms due to cell growth in the expressions in Eq. 3.9, because we focus on the mechanism of interaction between AppA and PpsR, and to be consistent with the assumption of constant total amounts of AppA and PpsR.

Eqs. 3.9 and 3.10 contain two parameters for the total amounts of AppA and PpsR proteins and six unknown kinetic parameters. Since none of these parameters is known experimentally we will introduce dimensionless quantities which reduce the number of free parameters. In addition, this allows us to assess the relative importance of individual reaction steps for the steady state behaviour of the system. Specifically, if we express concentrations in terms of the total protein concentrations as

$$x_1 = \frac{[A^-]}{[A_T]}, \quad x_2 = \frac{[P_4^-]}{[P_T]}, \quad x_3 = \frac{[AP_2]}{[P_T]}, \quad x_4 = \frac{[P_4^+]}{[P_T]}, \quad x_5 = \frac{[A^+]}{[A_T]} \tag{3.11}$$

the expressions in Eq. 3.9 become

$$\begin{aligned}
 \frac{d}{d\tau}x_1 &= 1 - x_1(1 + O) - \frac{x_3}{\gamma} - \frac{2\delta}{\gamma} \left( x_1^2 x_2 - I^2 \frac{x_3^2}{\gamma^2} \right) \\
 &\quad - \frac{\beta}{\gamma} \left[ x_1 \left( 1 - x_2 - \frac{x_3}{2} \right) - \frac{x_2}{K_{eq}} \left( 1 - x_1 - \frac{x_3}{\gamma} \right) \right] \\
 \frac{d}{d\tau}x_2 &= \beta \left[ x_1 \left( 1 - x_2 - \frac{x_3}{2} \right) - \frac{x_2}{K_{eq}} \left( 1 - x_1 - \frac{x_3}{\gamma} \right) \right] - \alpha O x_2 \\
 &\quad - \delta \left( x_1^2 x_2 - I^2 \frac{x_3^2}{\gamma^2} \right) \\
 \frac{d}{d\tau}x_3 &= 2\delta \left( x_1^2 x_2 - I^2 \frac{x_3^2}{\gamma^2} \right)
 \end{aligned} \tag{3.12}$$

where time ( $\tau$ ) is measured in units of  $1/k_{Ar}$  whereas the other parameters are summarized in Table 3.1. The initial conditions have to be chosen such that the conservation relations

$$x_4 = 1 - x_2 - \frac{x_3}{2} > 0 \quad \text{and} \quad x_5 = 1 - x_1 - \frac{x_3}{\gamma} > 0$$

are obeyed. Note that the factor  $1/2$  in front of  $x_3$  in Eq. 3.12 results from the stoichiometric factor of 2 in Eq. 3.6. Hence,  $x_3$  can vary in the interval  $[0, 2]$  whereas all other variables vary in the interval  $(0, 1]$ .

Table 3.1: **Definition of the parameters in Eq. 3.12.**

$$\begin{array}{cccccc}
 \alpha = \frac{k_{Po}}{k_{Ao}} & \beta = \frac{k_{Pr}^+[A_T]}{k_{Ar}} & \gamma = \frac{[A_T]}{[P_T]} & \delta = \frac{k_c^+ [A_T]^2}{LI^2 k_{Ar}} & K_{eq} = \frac{k_{Pr}^+}{k_{Pr}^-} \\
 O = \frac{[O_2]}{K_O} & I = \frac{LI}{K_L} & K_O = \frac{k_{Ar}}{k_{Ao}} & K_L = \left( \frac{k_c^+ P_T}{k_c^-} \right)^{1/2} & & 
 \end{array}$$

$A_T$  and  $P_T$  denote the total amounts of AppA and PpsR, respectively.

The two main parameters in this study are the oxygen concentration and the light irradiance. They are measured in units of  $K_O := k_{Ar}/k_{Ao}$  and  $K_L := (k_c^+[P_T]/k_c^-)^{1/2}$

$$\text{as } O = \frac{[O_2]}{K_O} \quad \text{and} \quad I = \frac{LI}{K_L}, \quad \text{respectively.}$$

### 3.3 Steady States when $K_{eq} \gg 1$

If the reduction of PpsR by AppA in Eq. 3.1 is effectively irreversible ( $K_{eq} \gg 1$ ) then the steady states of the ODE system in Eq. 3.12 are given by

$$x_3 = \gamma x_1 \frac{\sqrt{x_2}}{I} \quad \text{with} \quad x_1 = \frac{1 - \frac{\alpha}{\gamma} O x_2}{1 + O + \frac{\sqrt{x_2}}{I}} \quad (3.13)$$

and  $x_2$  can be calculated by

$$\beta \left[ \left( \frac{1 - \frac{\alpha}{\gamma} O x_2}{1 + O + \frac{\sqrt{x_2}}{I}} \right) \left( 1 - x_2 - \frac{1}{2} \gamma \left( \frac{1 - \frac{\alpha}{\gamma} O x_2}{1 + O + \frac{\sqrt{x_2}}{I}} \right) \frac{\sqrt{x_2}}{I} \right) \right] - \alpha O x_2 = 0$$

or

$$\begin{aligned} \left( 1 - \frac{\alpha}{\gamma} O x_2 \right) \left( (1 - x_2) \left( 1 + O + \frac{\sqrt{x_2}}{I} \right) - \frac{1}{2} \gamma \left( 1 - \frac{\alpha}{\gamma} O x_2 \right) \frac{\sqrt{x_2}}{I} \right) \\ - \frac{\alpha}{\beta} O x_2 \left( 1 + O + \frac{\sqrt{x_2}}{I} \right)^2 = 0 \end{aligned}$$

i.e.  $x_2$  is determined by the non-negative roots of the fifth-order polynomial

$$p_5(y) = f_\infty(y) - f_\beta(y) = 0, \quad y \equiv \sqrt{x_2}. \quad (3.14)$$

Here,  $f_\infty$  and  $f_\beta$  are given by

$$f_\infty(y) = \left( 1 - \frac{\alpha O}{\gamma} y^2 \right) p_3(y) \quad (3.15)$$

$$f_\beta(y) = \frac{\alpha O}{I \beta} y^2 (I(1 + O) + y)^2. \quad (3.16)$$

In Eq. 3.15  $p_3(y)$  denotes the third-order polynomial

$$p_3(y) = (1 - y^2) (I(1 + O) + y) - \frac{\gamma y}{2} \left( 1 - \frac{\alpha O}{\gamma} y^2 \right) \quad (3.17)$$

$$= I(1 + O) (1 - y^2) + y \left( 1 - \frac{\gamma}{2} \right) - y^3 \left( 1 - \frac{\alpha O}{2} \right). \quad (3.18)$$

Note that  $f_\infty$  is independent of  $\beta$  while  $f_\beta$  is inversely proportional to it, hence

$$\lim_{\beta \rightarrow \infty} p_5(y) = f_\infty(y).$$

The fifth-order polynomial  $p_5(y)$  in Eq. 3.14, in general, can admit at most five real roots corresponding to five possible stationary states of Eqs. 3.12 and 3.13. However, they should fall within the interval  $(0, 1)$  to be biologically meaningful (due to the scaling in Eqs. 3.11). One can derive some simple conclusions about the possible number of positive steady states of Eqs. 3.12 and 3.13 from the structure of the polynomials  $p_5$  and  $p_3$ . For example, from Eqs. 3.14-3.17 it is obvious that  $p_5(0) > 0$  and  $p_5(1) < 0$ . Therefore, by continuity,  $p_5$  must have at least one positive root in the interval  $(0, 1)$ , independent of all other parameter values.

In what follows, we are mostly interested in the case when  $\beta \gg 1$ . In that case the roots of  $p_3$  closely approximate those of  $p_5$  because  $f_\beta$  in Eq. 3.14 can be neglected. By Descartes' sign rule (*explained in Appendix C*)  $p_3$  has precisely one positive root if  $\alpha O \leq 2$  because the coefficients in  $p_3$  (Eq. 3.18) exhibit only one sign change (counted in consecutive order in  $y$ ). On the other hand,  $p_3$  shows two sign changes if  $\alpha O > 2$ . In that case  $p_3$  can have either two or none positive roots. Hence,  $\alpha O > 2$  is necessary for  $p_5$  to have three positive roots altogether. By a closer analysis (*see Appendix D*), we found that  $\alpha O > \gamma > 2$  is an additional necessary condition for all three roots to fall within  $(0, 1)$  when  $\beta \gg 1$ .

For the later interpretation of the results it is also important to note that the steady state values of Eqs. 3.12, as defined by Eqs. 3.14-3.18, only depend on  $\gamma$  and the three parameter combinations

$$b_1 = \alpha O, \quad b_2 = \beta I, \quad b_3 = I(1 + O). \quad (3.19)$$

Hence, if we report a certain behaviour of the system for a particular set of the four parameters  $\alpha$ ,  $\beta$ ,  $O$  and  $I$  it is clear from Eqs. 3.19 that the same behaviour also exists for any other set of (positive) parameters  $\alpha'$ ,  $\beta'$ ,  $O'$  and  $I'$ , as long as the constants  $b_1$ ,  $b_2$  and  $b_3$  retain their numerical values.

### 3.4 Meaning of the Parameters

The definitions of the parameters are collectively presented in Table 3.1. The parameter  $\gamma$  compares the ratio between total amounts of AppA and PpsR proteins. The parameters  $\alpha$  and  $\beta$  can be interpreted in terms of the relative time scales for the oxidation and reduction of PpsR and AppA, respectively. For example,  $\alpha$  compares the time scale for the oxidation of reduced PpsR (Eq. 3.8) with that for the oxidation of reduced AppA (Eq. 3.7) at a given oxygen concentration. Large values of  $\alpha$  mean that reduced form of PpsR is oxidized faster than the reduced form of AppA. Similarly,  $\beta$  compares the time scale for the reduction of oxidized PpsR (Eq. 3.1) with that for the

reduction of oxidized AppA (Eq. 3.7). As a result, large values of  $\beta$  indicate that PpsR is reduced on a faster time scale than AppA.

## 3.5 Results

In most of the later presentation of results and their interpretation, we will assume that the electron transfer from AppA to PpsR in Eq. 3.1 is effectively irreversible ( $k_{Pr}^- \ll k_{Pr}^+$ ), which was suggested by the observations of Masuda and Bauer (22). Note that this corresponds to the limit  $K_{eq} \rightarrow \infty$  in Eqs. 3.12. In selected cases we will show how a finite value of the equilibrium constant would affect the steady-state behaviour of the system.

Since the steady state behaviour of the ODE system in Eqs. 3.12 qualitatively differs depending on the ratio between total copy numbers of AppA and PpsR ( $[A_T]/[P_T] < 2$  or  $[A_T]/[P_T] \geq 2$ ) we will consider both cases separately. If possible, the results will be related to the behaviour of the system expected from current experimental knowledge.

### 3.5.1 When $[A_T]/[P_T] < 2$

For convenience, we first assume that the total amounts of AppA and PpsR proteins are equal ( $\gamma = [A_T]/[P_T] = 1$ ). If, in addition, the time scales for reduction and oxidation of both molecules are equal ( $\alpha = \beta = 1$ , compare to Table 3.1), the steady state levels of reduced PpsR ( $P_4^-$ ), oxidized PpsR ( $P_4^+$ ) and the AppA-PpsR complex ( $AP_2$ ) change monotonously with oxygen concentration (Fig. 3.2).

Under aerobic conditions ( $O = [O_2]/K_O \gg 1$ ), set by  $K_O$ , the PpsR protein is mostly oxidized, and the levels of reduced PpsR and the AppA-PpsR complex are low (Fig. 3.2A, 3.2B). This behaviour is in agreement with the idea that PpsR is a repressor of PS genes under aerobic conditions (20–22, 29, 38). In fact, under these conditions PS genes would be strongly repressed as most of the PpsR protein molecules are in oxidized state, which is a 2.2 fold stronger repressor in comparison with its reduced form (22).

Under low oxygen levels ( $O \ll 1$ ) and, particularly, under anaerobic conditions ( $O = 0$ ), it depends on the light irradiance whether PpsR is mostly in its reduced form or associated with AppA in a complex (Fig. 3.2C). This behaviour is in agreement with the general idea that, under high light conditions ( $I = LI/K_L \gg 1$ ), the induction of photosynthesis (PS) genes is inhibited due to the repressive action of reduced PpsR while under low light conditions ( $I \ll 1$ ) PS genes are induced since AppA sequesters PpsR molecules into transcriptionally inactive complexes (22, 31). However, from Fig. 3.2 C it

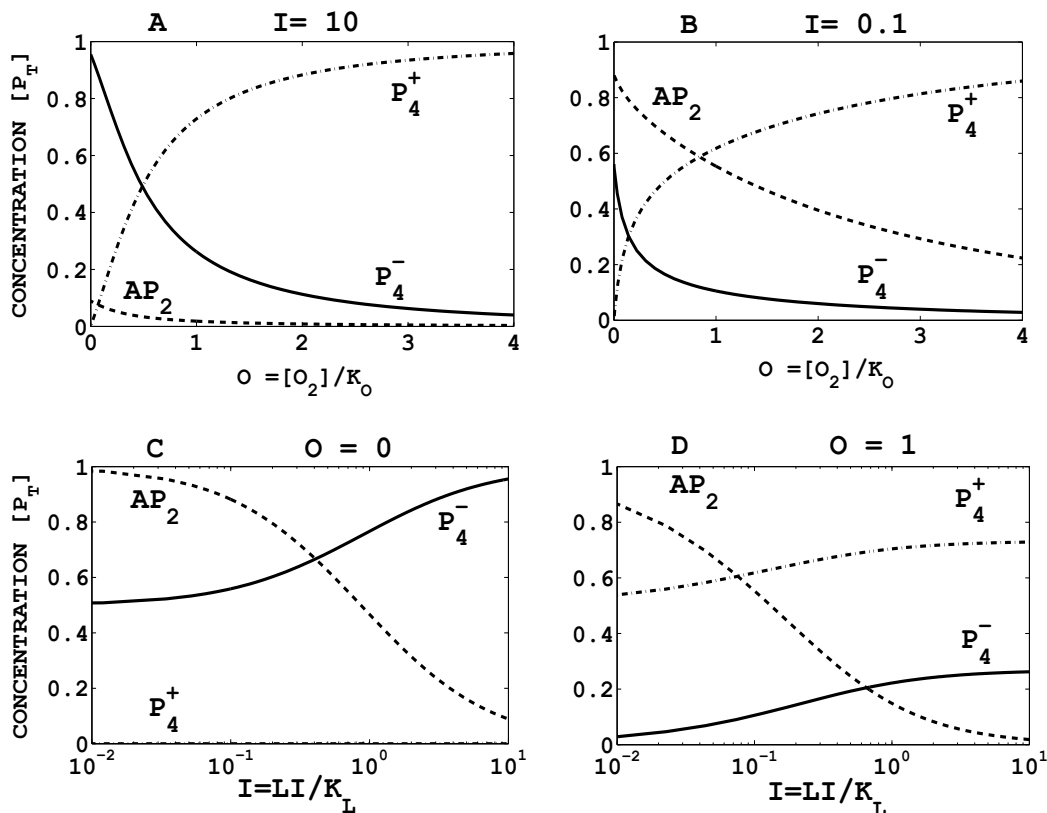


Figure 3.2: Monotonic change in the steady-state levels of reduced PpsR ( $P_4^-$ ), oxidized PpsR ( $P_4^+$ ) and the AppA-PpsR complex ( $AP_2$ ) as a function of: (A and B) the oxygen concentration  $O = [O_2]/K_O$  for different values of the light irradiance ( $I = LI/K_L$ ) and (C and D) the light irradiance for different oxygen concentrations. Note that the concentration of  $P_4^+$  under anaerobic conditions ( $O = 0$ ) is zero (C). Used parameters are:  $K_{eq} = \infty$ ,  $\alpha = \beta = \gamma = 1$  (compare to Table 3.1).

is obvious that not all PpsR molecules can be sequestered by AppA if both proteins are present in equal amounts ( $\gamma = 1$ ), because two AppA molecules are required to bind one PpsR molecule. Therefore, even under low light conditions half of the PpsR molecules were still free to bind DNA which would preclude an efficient induction of PS genes.

Under semi-aerobic conditions ( $O \sim 1$ ), there is a significant amount of free oxidized PpsR ( $P_4^+$ ) under both, low light ( $I \ll 1$ ) and high light ( $I \gg 1$ ) conditions (Fig. 3.2D). Consequently, the induction of PS genes would be suppressed largely independent of the light irradiation—in contrast

to the specific repression of PS genes observed experimentally under high light conditions (28, 35). This suggests that the phenomenon of high light repression of PS genes at intermediate oxygen levels cannot be explained, if the rates for oxidation and reduction of PpsR and AppA are all equal ( $\alpha = \beta = 1$ ).

### Specific High Light PS Gene Repression at Intermediate $O_2$ Levels

If the light irradiance  $I$  is sufficiently large (Fig. 3.3), and the rate of PpsR reduction is significantly increased compared to the rate of AppA reduction ( $\beta \gg 1$ ) then a maximum in the steady state response curve of the reduced form of PpsR ( $P_4^-$ ) develops at intermediate oxygen levels ( $O \sim 1$ ).

The exact position of this peak depends on the parameter  $\alpha$  (Fig. 3.4). Small values of  $\alpha$  shift the peak in  $P_4^-$  to higher oxygen concentrations, whereas large values of  $\alpha$  do the opposite. When the concentration of reduced PpsR ( $P_4^-$ ) reaches a maximum, the concentration of the AppA-PpsR complex ( $AP_2$ ) is low (Fig. 3.3 D) and, consequently, PS genes would be effectively repressed at intermediate oxygen levels by the reduced form of PpsR. This suggests that the non-monotonic dependence of reduced PpsR ( $P_4^-$ ) on the oxygen concentration could provide a rationale for the specific repression of PS genes in *R. sphaeroides* at intermediate oxygen levels ( $O \sim 1$ ) under high light conditions. In fact, as the light irradiation decreases the maximum of reduced PpsR ( $P_4^-$ ) at intermediate oxygen concentrations disappears (Fig. 3.5).

### High Light PS Gene Repression under Anaerobic Regime

Under high light conditions, the concentration of reduced PpsR ( $P_4^-$ ) at completely anaerobic conditions ( $O = 0$ ) is only slightly lower compared to the maximum at intermediate oxygen concentrations (Fig. 3.3 D). Consequently, PS genes would still be largely repressed in that regime by reduced PpsR. A similar phenotype has recently been observed in PrrB knock-out experiments (7). Compared to wild-type cultures, where the repressive action of the AppA/PpsR system is normally counteracted by the PrrB/PrrA two-component system, these experiments revealed that in the absence of the sensor kinase PrrB, photosynthesis genes are repressed by blue light to almost the same extent as under semi-aerobic conditions, suggesting that the non monotonic dependence of  $P_4^-$  on the oxygen concentration can also account for this particular phenotype.

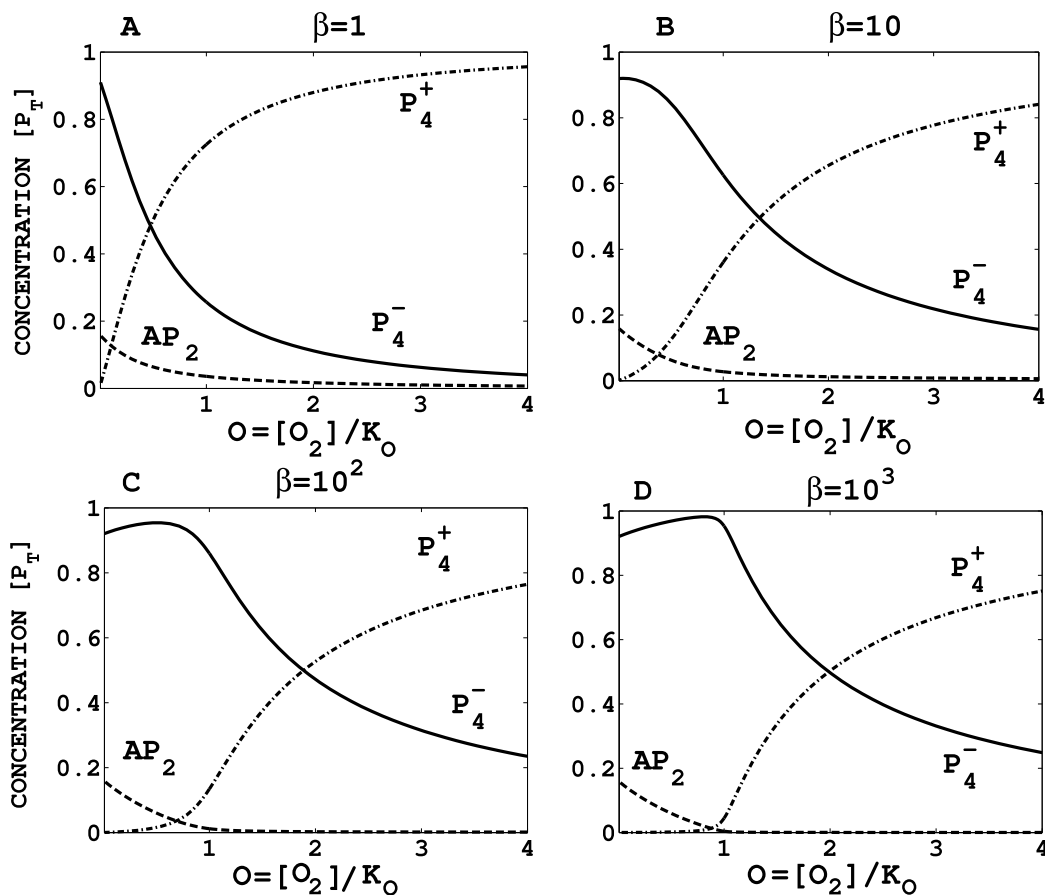


Figure 3.3: A maximum develops in the oxygen-dependent steady state curve of reduced form of PpsR ( $P_4^-$ ) as the relative rate ( $\beta = k_{Pr}^+[A_T]/k_{Ar}$ ) between the reduction of PpsR and that of AppA increases. (A)  $\beta = 1$ . (B)  $\beta = 10$ . (C)  $\beta = 10^2$ . (D)  $\beta = 10^3$ . Used parameters are:  $I = 5$ ,  $K_{eq} = \infty$ ,  $\alpha = \gamma = 1$ .

### When $K_{eq} = 1$

Now, we investigate how a finite value of the equilibrium constant ( $K_{eq}$ ) modifies the steady state behaviour of the system (Eq. 3.12). Particularly, we investigate how the peak formation in the steady state curve of reduced PpsR ( $P_4^-$ ) depends on the reversibility of the electron transfer from AppA to PpsR in Eq. 3.1. Apparently, as the rate  $k_{Pr}^-$  for the reduction of PpsR by AppA increases ( $K_{eq}$  decreases) the maximum in the steady state response curve of reduced PpsR ( $P_4^-$ ) becomes smaller and eventually disappears (Fig. 3.6) when the forward ( $k_{Pr}^+$ ) and the backward rates ( $k_{Pr}^-$ ) become equal ( $K_{eq} =$

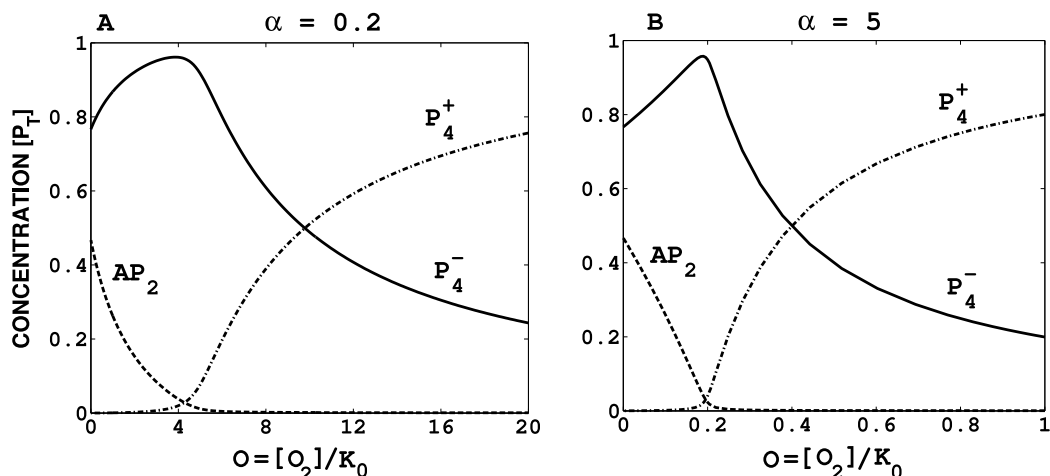


Figure 3.4: The parameter  $\alpha = k_{P_0}/k_{A_0}$  determines the position of the maximum in the steady state curve of reduced PpsR ( $P_4^-$ ) at intermediate oxygen concentrations. Small values of  $\alpha$  shift the peak to higher oxygen concentrations, whereas large values of  $\alpha$  do the opposite. In (A) the peak occurs at  $O \approx 4$  while in (B) it occurs at  $O \approx 0.2$ . For comparison: Figure 3.5 A shows the case when  $\alpha = 1$ . Used parameters are:  $\beta = 10^3$ ,  $K_{eq} = \infty$ ,  $I = LI/[K_L] = 1$ ,  $\gamma = 1$ . Note that the  $O = [O_2]/K_0$  are presented in different scales.

1). This suggests that the observed phenotype of high light repression of PS genes at intermediate oxygen levels is not compatible with an equilibrium constant close to 1. It also supports the view that AppA and PpsR are not in redox equilibrium *in vivo* (37), in agreement with the observation that the electron transfer between AppA and PpsR is effectively irreversible (22).

### 3.5.2 When $[A_T]/[P_T] \geq 2$

An efficient sequestration of PpsR molecules into AppA-PpsR complexes can occur only if the protein copy numbers of AppA exceed those of PpsR by at least a factor of two ( $\gamma \geq 2$ ), which is a simple consequence of the stoichiometry of the reaction in Eq. 3.6. Under these conditions, almost all PpsR molecules are complexed by AppA molecules under low light irradiation in the anaerobic regime (Fig. 3.7). Consequently, the concentration of free reduced PpsR ( $P_4^-$ ) drops significantly, which would result in an effective PS gene induction under low light conditions. Note that  $([P_4^-] + [P_4^+] + [AP_2]/2)/[P_T] = 1$  such that  $[P_4^-]/[P_T] < 1$  and  $[P_4^+]/[P_T] < 1$  while the

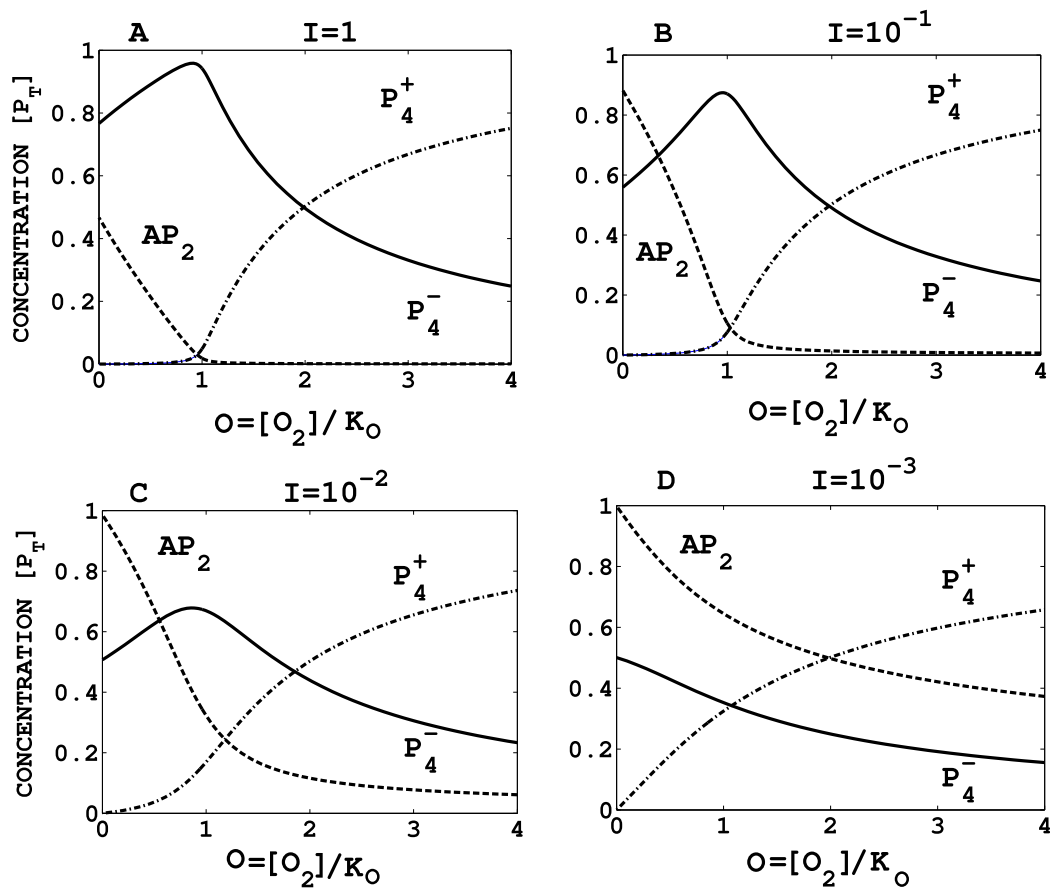


Figure 3.5: The maximum in the steady state curve of reduced PpsR ( $P_4^-$ ) at intermediate oxygen levels ( $O = [O_2]/K_O \approx 1$ ) disappears as the light irradiation ( $I = LI/K_L$ ) decreases. Used parameters are:  $\beta = 10^3$ ,  $K_{eq} = \infty$ ,  $\alpha = \gamma = 1$ .

upper bound for  $[AP_2]/[P_T]$  is 2. If, in addition to  $\gamma > 2$  and  $\beta \gg 1$ , the ratio between the rate of re-oxidation of PpsR and that of AppA is sufficiently large ( $\alpha O > 2$ ) then another interesting phenomenon becomes possible: Under these conditions the transition from the anaerobic to the aerobic growth regime can occur via a bistable switch at intermediate oxygen levels (Fig. 3.8 A). In the region ( $0.6 \leq O \leq 1$ ), two stable stationary states (solid lines) coexist. The coexistence region is bounded by two limit points (LP) (LP is explained in Appendix E). Almost all PpsR is complexed by AppA at low values of the oxygen concentration while the concentration of both reduced and oxidized PpsR is low (Fig. 3.8 B). As a result, in that regime, PS genes would be effectively transcribed. However, there would be

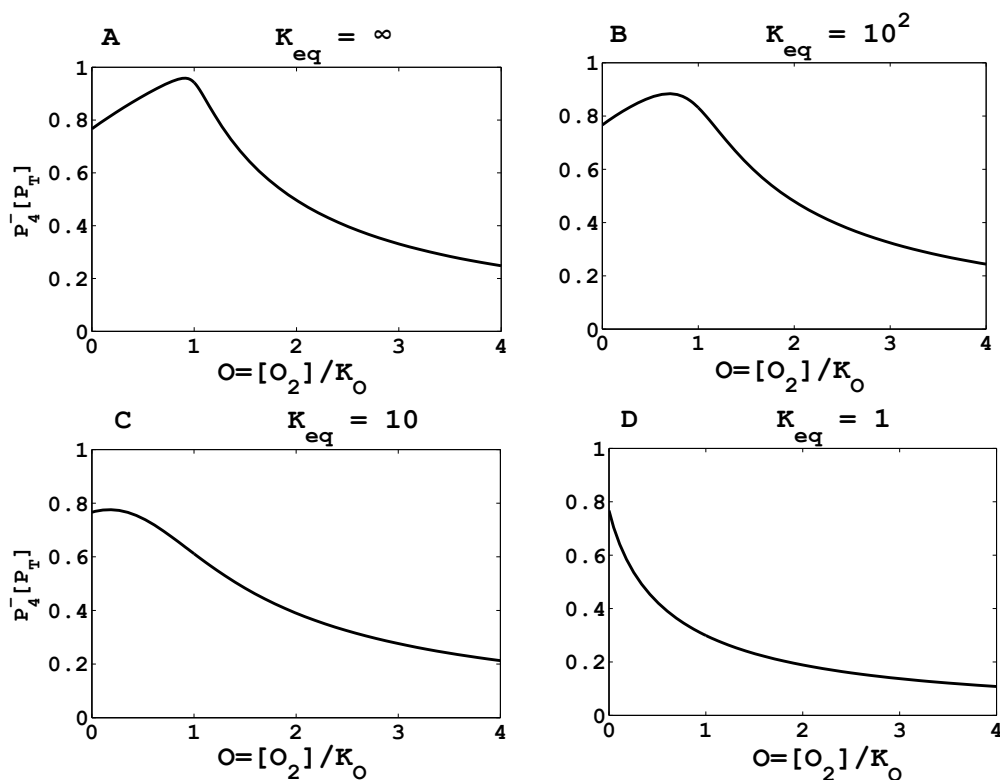


Figure 3.6: *The peak of reduced PpsR ( $P_4^-$ ) at intermediate oxygen levels ( $O = [O_2]/K_O \sim 1$ ) disappears as the rate  $k_{P_r}^-$  in Eq. 3.1 increases such that the equilibrium constant  $K_{eq} = k_{P_r}^+/k_{P_r}^-$  approaches unity. Used parameters are:  $\beta = 10^3$ ,  $K_{eq} = \infty$ ,  $\alpha = 1 = \gamma$ ,  $I = 1$ .*

an abrupt change in the expression levels of PS genes upon increasing the oxygen concentration beyond the saddle-node bifurcation at  $O \approx 1$ , as the concentration of free PpsR molecules ( $P_4^-$  and  $P_4^+$ ) jumps to large values while  $AP_2$  levels significantly decrease. In the other direction, when coming from high oxygen concentrations, PS genes would remain repressed until  $O_2$  levels decrease beyond the second saddle-node bifurcation at  $O \approx 0.6$ , where almost all PpsR is again sequestered into inactive complexes leading to hysteresis.

### Regions and Conditions for Bistability

As it is mentioned in section 3.3, the steady states of Eqs. 3.12 depend on the parameter  $\gamma$  and the parameter combinations  $\alpha O$ ,  $\beta I$  and  $I(1 + O)$  (See

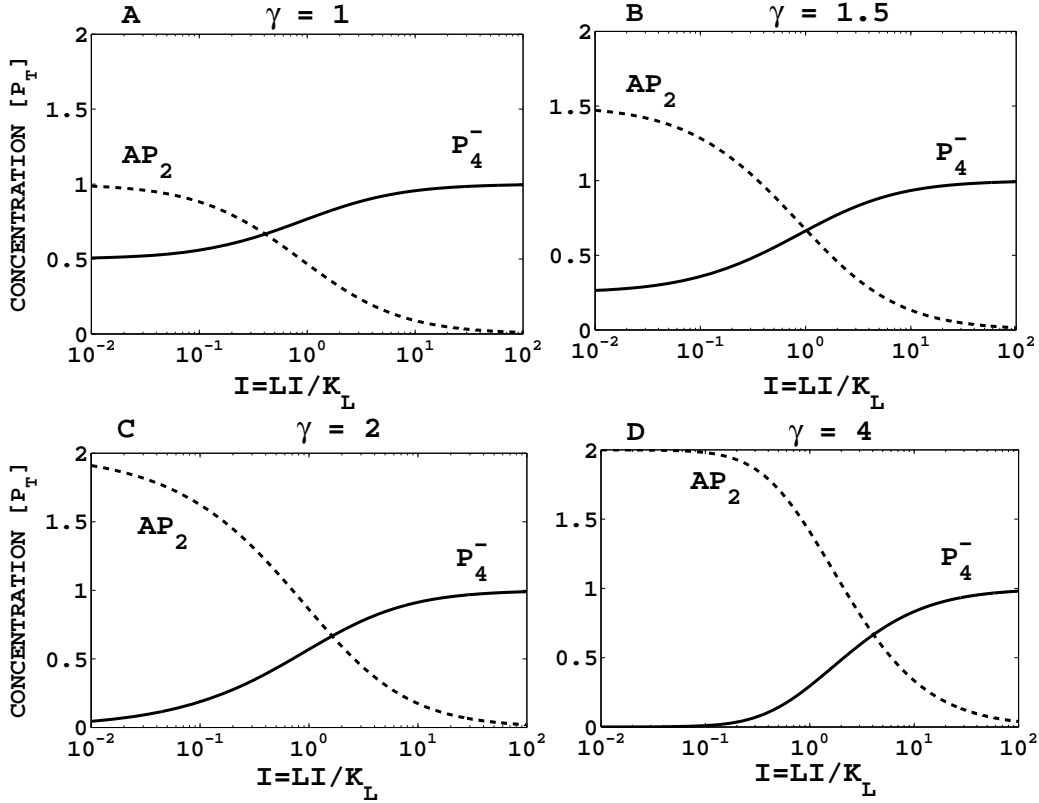


Figure 3.7: An increase in the ratio between total amounts of AppA and PpsR proteins ( $\gamma = [A_T]/[P_T]$ ) increases the amount of reduced PpsR ( $P_4^-$ ) that can be sequestered into complexes ( $AP_2$ ) under low light ( $I \ll 1$ ) conditions. Note that  $([P_4^-] + [P_4^+] + [AP_2]/2)/[P_T] = 1$  such that  $[P_4^-]/[P_T] < 1$  and  $[P_4^+]/[P_T] < 1$  while the upper bound for  $[AP_2]/[P_T]$  is 2. Used parameters are:  $O = [O_2]/K_O = 0$ ,  $\beta = 10^3$ ,  $K_{eq} = \infty$ ,  $\alpha = 1$ .

expressions in Eq. 3.19). Consequently, as long as the constants  $b_1$ ,  $b_2$  and  $b_3$  retain their numerical values, a change in  $\alpha$  and  $\beta$  can always be compensated by an appropriate change in  $O$  and  $I$  without compromising the ability to generate bistability. For example, when the oxygen concentration and the light irradiance are fixed at the values used in Fig. 3.8, there is a whole region in the two-parameter plane spanned by  $\alpha$  and  $\gamma$  (Fig. 3.9 A) or  $\alpha$  and  $\beta$  (Fig. 3.9 B) where bistability (gray shaded region) can occur. Together, the figures Fig. 3.9 A and Fig. 3.9 B suggest that for  $\gamma > 2$ , bistability can only emerge if there is a sufficiently large time scale separation between the oxidation of PpsR and AppA ( $\alpha \gg 1$ ) as well as between the reduction of

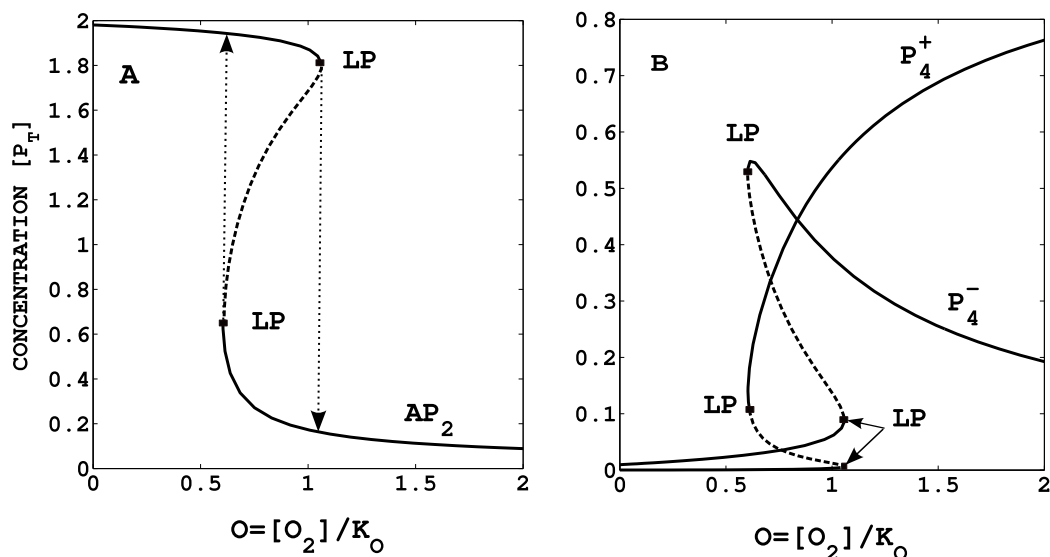


Figure 3.8: *Signal-response curve (one-parameter bifurcation diagram) showing how the number of steady states changes as a function of the oxygen concentration. (A) AppA-PpsR complex ( $AP_2$ ) (B) reduced PpsR ( $P_4^-$ ) and oxidized PpsR ( $P_4^+$ ). In the region between the two limit points (LP) three stationary states coexist and the system exhibits hysteresis (indicated by dotted lines). Here, upper and lower branches denote stable steady states (solid lines) while the middle branch (dashed line) corresponds to an unstable steady state. Used parameters are:  $\beta = 10^3$ ,  $K_{eq} = \infty$ ,  $\alpha = 10$ ,  $\gamma = 4$ ,  $I = 0.1$ .*

PpsR and AppA ( $\beta \gg 1$ ).

Interestingly, similar to the peak formation in Fig. 3.6, we find that the bistable region at intermediate oxygen levels ( $O \approx 1$ ) disappears as the rate of the backward reaction ( $k_{Pr}^-$ ) in Eq. 3.1 increases such that the equilibrium constant ( $K_{eq} = k_{Pr}^+/k_{Pr}^-$ ) approaches unity (Fig. 3.10). It suggests that decreasing the equilibrium constant for the electron transfer from AppA to PpsR (Eq. 3.1) compromises the ability of the system to generate a bistable response.

The presence of a sufficiently strong positive feedback mechanism is a necessary condition for a reaction network to exhibit bistability (39), although such a feedback mechanism might be difficult to identify by merely visual inspections of the network (40). In the case of the AppA/PpsR network shown in Fig. 3.1, the situation is quite similar, as it does not contain any apparent positive feedback loops. However, it is well known that sequestration of signalling molecules (41) and dead-end complex formation (42) can result in a

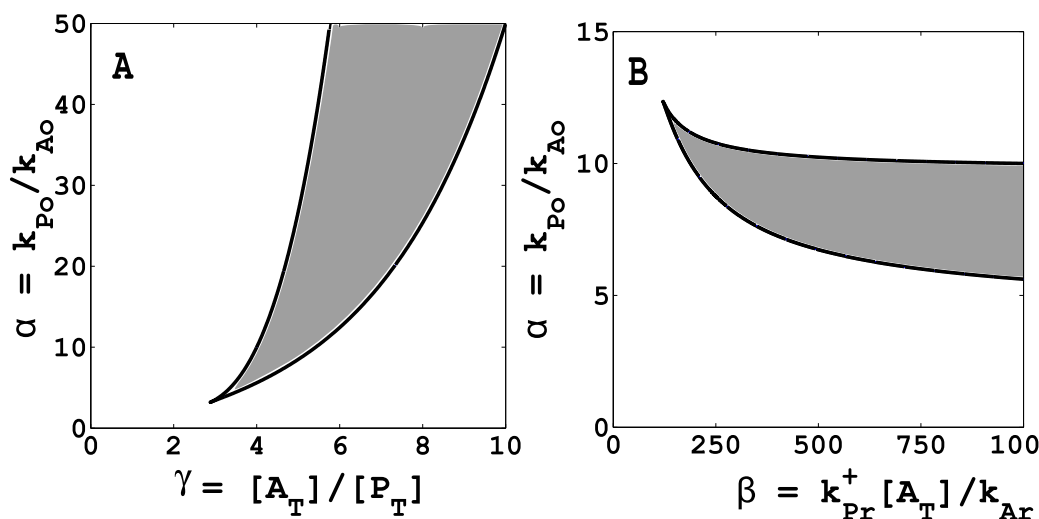


Figure 3.9: *Bistable regions projected on different two-parameter planes: (A)  $\alpha$  vs.  $\gamma$  for  $\beta = 10^3$  (B)  $\alpha$  vs.  $\beta$  for  $\gamma = 4$ . In the gray shaded region, two stable steady states and one unstable steady state coexist, which is bounded by two limit points (solid lines). Used parameters are:  $O = 1$ ,  $I = 0.1$ ,  $K_{eq} = \infty$ .*

bistable system response. Therefore, the light-dependent complex formation between AppA and PpsR could represent a potential source of bistability in the AppA/PpsR system. Indeed, a strong positive feedback becomes apparent when we plot the dissociation rate ( $v_c^-$ ) of the  $AP_2$  complex against the steady state concentration of reduced AppA (Fig. 3.11), since increasing amounts of reduced AppA lead to an even higher production of reduced AppA through the dissociation of the  $AP_2$  complex.

### 3.6 Discussion and Summary

In the photosynthetic bacterium, *Rhodobacter sphaeroides*, the AppA-PpsR system is an important signal transduction system which regulates the genes encoding the components of the photosynthetic apparatus. This system helps the bacterium to survive under adverse environment conditions such as sudden increase/depletion of oxygen tension and production of reactive oxygen species (ROS) in the simultaneous presence of light and oxygen.

AppA is a flavoprotein which is exclusive to *R. sphaeroides*, and it has the remarkable feature to sense and integrate both oxygen and light signals

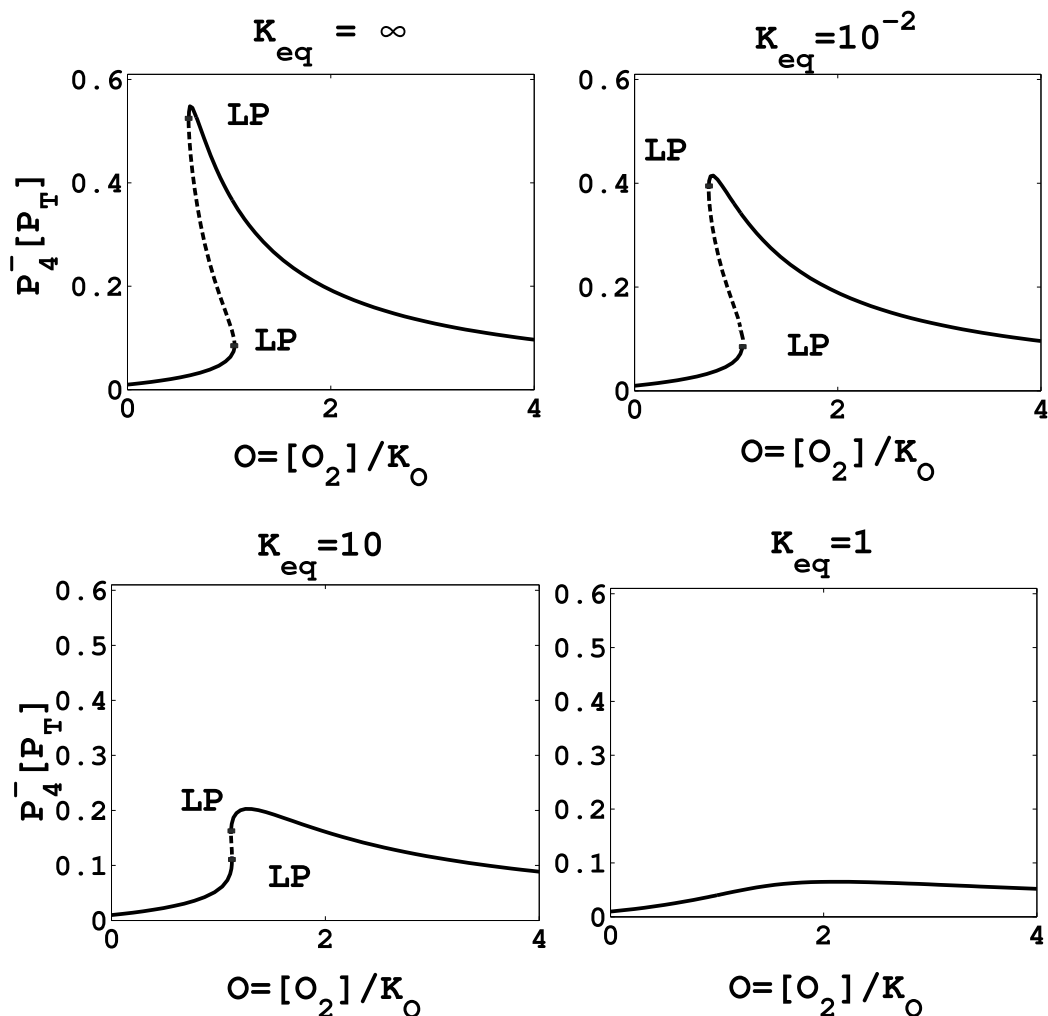


Figure 3.10: The bistable region at intermediate oxygen levels ( $O \approx 1$ ) disappears as the rate of the backward reaction ( $k_{P_r}^-$ ) in Eq. 3.1 increases such that the equilibrium constant  $K_{eq} = k_{P_r}^+/k_{P_r}^-$  for the electron transfer between AppA and PpsR approaches unity. Used parameters are:  $\beta = 10^3$ ,  $\alpha = 10$ ,  $\gamma = 4$ ,  $I = LI/[K_L] = 0.1$ .

(5, 6, 22). AppA antagonizes the repressor activity of PpsR (29), which is an aerobic transcriptional repressor of photosynthesis (PS) genes (21, 38). As a result of the protein-protein interaction between AppA and PpsR, *R. sphaeroides* exhibits a unique phenotype: The blue light-dependent repression of PS genes under semi-aerobic conditions (28). In the present chapter, we have investigated how this phenotype arises from the molecular interac-

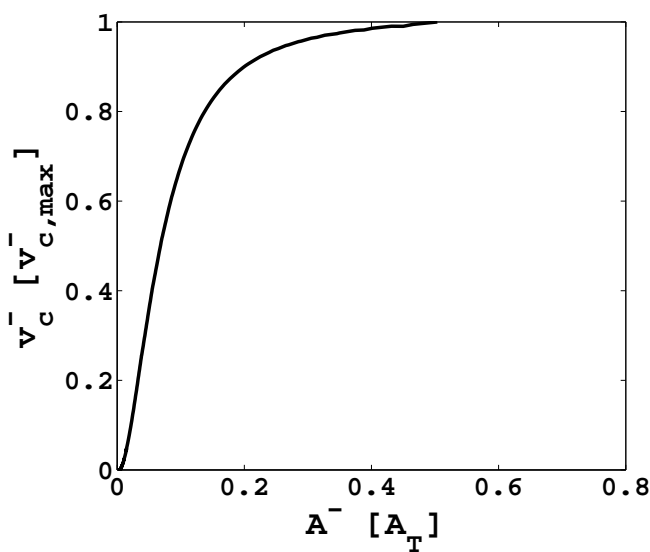


Figure 3.11: *Positive feedback becomes apparent when the dissociation rate ( $v_c^-$ ) of the  $AP_2$  complex is plotted against the steady state concentration of reduced AppA ( $A^-$ ). Apparently, increasing the concentration of reduced AppA ( $A^-$ ) leads to a strong increase in its own production rate (positive feedback) via the dissociation of the AppA-PpsR complex (Eq. 3.6). Here,  $v_c^- = k_c^- [AP_2]^2$  denotes the rate of the backward reaction for the complex formation which is plotted relative to its maximal value  $v_{c,max}^-$ . Used parameters are:  $\beta = 10^3$ ,  $\alpha = 10$ ,  $\gamma = 4$ ,  $K_{eq} = \infty$ ,  $I = LI/[K_L] = 0.1$ .*

tions between AppA and PpsR. For that, we developed a simple mathematical model based on the structural knowledge of the AppA/PpsR interactions (Fig. 3.1), in particular, the AppA-mediated reduction of PpsR (Eq. 3.1) and the light-dependent complex formation between the reduced forms of AppA and PpsR (Eq. 3.6). This core mechanism was augmented by a redox-sensing reaction for AppA (Eq. 3.7) and an oxygen-dependent re-oxidation of PpsR (Eq. 3.8). However, in present model we have assumed the light regulation of the interaction between AppA and PpsR in an effective manner. The aim was to analyse the kinetic requirements for these processes that could lead to a PS gene repression at intermediate oxygen concentrations and, thereby, provide a mechanistic basis for the understanding of the AppA/PpsR system in *R. sphaeroides*.

### 3.6.1 PS Gene Repression under Semi-Aerobic Conditions

Based on our results, we suggest that the phenomenon of high light repression of PS genes under semi-aerobic conditions can be related to the development of a maximum in the concentration of reduced PpsR at intermediate oxygen levels (Fig. 3.3), which occurs only if the light irradiance is sufficiently large (Fig. 3.5). Our numerical investigations indicate two additional requirements for the peak formation in the steady state response curve of reduced PpsR to occur: First, the rate of reduction of PpsR has to be significantly larger than that for the reduction of AppA ( $\beta \gg 1$ ), and, second, the equilibrium constant for the reaction describing electron transfer from AppA to PpsR must be sufficiently large ( $K_{eq} \gg 1$ ).

The requirement that  $K_{eq} \gg 1$  agrees with the observation of Masuda and Bauer (22), according to which the electron transfer from AppA to PpsR is effectively irreversible. However, this requirement seems to contradict experiments by Kim et al. (37) which suggest that the midpoint redox potentials of AppA and PpsR are equal ( $K_{eq} = 1$ ). Kim et al. argued that the protein-protein interactions between AppA and PpsR could be responsible for a shift in the midpoint potential of one or both proteins which could favor the electron transfer from AppA to PpsR under *in vivo* conditions. We can estimate from Fig. 3.6 that a significant peak formation in the steady state response curve of reduced PpsR requires an equilibrium constant of  $K_{eq} \gg 10$ . Using Eq. 3.2 we estimate that this would result in a shift of the midpoint potential difference between PpsR and AppA of at least  $\Delta E_m = 30 \text{ mV}$  (at  $T = 298\text{K}$ ). Based on the observation that heme binding to AppA increases the association rate between AppA and PpsR (5), it is conceivable that the heme is also involved in mediating protein-protein interactions between AppA and PpsR, which could explain such a shift in the midpoint potential.

### 3.6.2 PS Gene Repression under Anaerobic Conditions

Our simulation results suggest that under high light irradiance ( $I \gg 1$ ), PS genes would be repressed under anaerobic ( $O = 0$ ) to almost the same extent as under semi-aerobic conditions. This suggestion is based on our simulation result that under high light conditions, the concentration of reduced PpsR ( $P_4^-$ ) is only slightly lower compared to the maximum at intermediate oxygen concentrations (Fig. 3.3D). Such a phenotype has recently been observed in PrrB knock-out experiments (7). This suggests that the non-monotonic dependence of  $P_4^-$  on the oxygen concentration can also explain such a phenotype.

### 3.6.3 Bistability in the AppA/PpsR System

We found that the AppA/PpsR system can potentially exhibit bistable behaviour, which would result in a hysteretic switch-like induction of PS genes as a response to changing redox conditions in the environment (Fig. 3.8). In addition, the steady state analysis of Eqs. 3.12 shows that the experimentally observed interactions between AppA and PpsR (22) are sufficient to explain the high light repression of PS genes under semi-aerobic conditions. Also, through an analysis of the root structure of the 5<sup>th</sup>-order polynomial in Eq. 3.14, we have derived necessary conditions for the emergence of multiple steady states, they can be summarized as  $\beta \gg 1$  and  $\alpha O > \gamma > 2$ . Further, we show that the bistability, similar to the peak formation at intermediate oxygen concentrations, requires a time scale separation between the reduction rates of PpsR and AppA ( $\beta \gg 1$ ), and an effectively irreversible transfer of electrons from AppA to PpsR. However, in addition to that, bistability also requires that PpsR can be efficiently sequestered by AppA molecules ( $\gamma > 2$ ) and that re-oxidation of PpsR occurs on a faster time scale than re-oxidation of AppA corresponding to the shaded region in Fig. 3.9 A.

The prediction of bistability in the AppA/PpsR system is somewhat surprising, as to our knowledge, no hysteretic behaviour has been reported for PS gene expression in *R. sphaeroides* yet. However, we believe that the likelihood for the parameters are such that the bistability can occur. For example, given that the kinetic requirement  $\beta \gg 1$  is also essential for the specific PS gene repression in the semi-aerobic regime, we expect this condition to be generally valid. The condition  $\gamma > 2$  should also be fulfilled because otherwise an efficient sequestration of PpsR molecules, as it is necessary for the induction of PS genes under anaerobic conditions, would not be possible (Fig. 3.2C, Fig. 3.7). Hence, measurement of the remaining kinetic parameter  $\alpha = k_{Po}/k_{Ao}$  would give a first indication whether bistability could be observable in the AppA/PpsR system. Alternatively, the measurement of the relative rates of reduction and oxidation of AppA ( $K_O = k_{Ar}/k_{Ao}$ ) could be used to estimate  $\alpha$  since both parameters determine the semi-aerobic regime in our model. For example, a value of  $K_O = 500\mu M$  means

$$O = [O_2]/[K_O] = 100/500 = 0.2$$

which would correspond to a value of  $\alpha = 5$  according to Fig. 3.4B.

Recently, in arabinose/lactose utilizing system (43, 44), it has been reported that in the bistable regime, the transition from the non-induced (not utilizing arabinose/lactose) to the induced state (utilizing arabinose/lactose at a high rate) is often driven by random molecular fluctuations leading to a coexistence of induced and non-induced cells. Similarly, in our case in the

bistable regime, a fraction of the cell population would already derive energy from photosynthesis while the remaining fraction still performed respiration. Recent studies on other bacteria, suggest that such heterogeneity in gene expression patterns could be an advantageous survival strategy for a population in the face of unforeseeable environmental fluctuations (45–47).

### 3.6.4 Possible Experiments to Verify Bistability

Bistability has become a recurring theme in biology (39, 48). It has, for example, been observed in sugar uptake systems of *E. coli* using single-cell measurements (43, 44). However, to our knowledge, all experiments concerning the regulation of PS genes in *R. sphaeroides* were done with whole cell populations which might be one reason why bistability in that system has not been observed experimentally yet. Indeed, if the involved regulatory proteins were present in only low copy numbers then the stochastic nature of protein-binding events to the DNA could become important. As a result, each cell would respond in an all-or-none fashion to an applied stimulus in the bistable regime while measurements of the global response (averaged over the population) changed only gradually. Recent experiments have clearly demonstrated the need to observe gene expression patterns at the single cell level in order to visualize bistable behaviour which is typically derived based on ODE models for cell populations (43, 44, 49). Hence, on the basis of single cell level measurements of PS gene expression patterns, one could provide an independent indication for the existence of bistability in the AppA/PpsR system.

As mentioned in the section 3.6.3, the measurement of the kinetic parameter  $\alpha = k_{P_o}/k_{A_o}$  would give a first indication for occurrence of the bistability in the AppA/PpsR system. Additionally, the measurement of the ratio between total amounts of AppA and PpsR proteins under different growth conditions would also provide an indication whether bistability could happen in principle. Since the expression levels of PpsR were found to be largely independent of growth conditions (29) it is conceivable that the total amount of AppA or the amount of redox-active AppA molecules is actively regulated, e.g. through the availability of the heme cofactor which is required for redox signalling of AppA (5). By increasing total amounts of AppA the system could be driven in a regime where bistability can occur.

### 3.6.5 Model Limitations

In the present model (Fig. 3.1 and Eqs. 3.12), the light-dependent complex formation between AppA and PpsR has been implemented in a very simple

way (Eq. 3.6). In particular, Eqs. 3.12 does not explicitly account for possible conformational changes of AppA induced by light excitation of its bound FAD cofactor, which would require to introduce two additional AppA states (one for oxidized AppA and one for reduced AppA each with an excited FAD cofactor)—similar as in the model proposed by Han et al. (5). Therefore, this model can be extended by incorporating a detailed mechanism for the effect of light on the interplay between AppA and PpsR. For the extended version of the model, it would also be desirable to incorporate the redox- and light-dependent binding of PpsR to DNA explicitly. In that way, one could compare the model results directly with measurements of mRNA levels of PS genes such as *puc*, *bch* and *crt*, whose promoters contain the PpsR binding consensus sequence (14). However, the mechanism through which PpsR binds the DNA is still debated (21). While there is consensus that PpsR has to bind two adjacent sites containing the palindromic consensus sequence for an effective repression of PS genes (15), it is still unclear whether it binds as two dimers (30), one tetramer (22) or two tetramers (50).

## Chapter 4

# An Extended Model for the AppA/PpsR System

In this Chapter, an extension of the simple mathematical model developed in Chapter 3 for the light- and redox-dependent interaction between PpsR and AppA in *R. sphaeroides* is discussed. In the simple model, we focused mainly on the effect of oxygen on the interaction between AppA and PpsR while light regulation was considered in an effective manner. In the extended version of the model, we incorporate a more detailed and realistic mechanism for the effect of light on the interaction between AppA and PpsR. The extended model allows a comparison of the model predictions with experimental results. In addition, we discuss potential kinetic and stoichiometric constraints which are imposed on the functionality of the AppA/PpsR system by the interplay between light and redox regulation, especially for the emergence of a possible bistable response.

### 4.1 Development of the Extended Model

In the extended version of the model, some of the reaction steps of the simple model are kept as it is, and to show a clear distinction between the simple and the extended model, those reaction steps are described together in the following section. Subsequently, we explain the detailed mechanism which is incorporated for the effect of light on AppA and on the complex formation between AppA and PpsR. The full set of oxygen- and light-dependent reaction steps is summarized in Fig. 4.1.

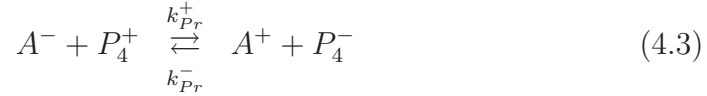
### 4.1.1 Reaction Steps from the Simple Model

We consider the simple first-order kinetics to implement the regulation of the redox states of AppA and PpsR by the ambient oxygen concentration



In Eq. (4.1) we followed the model proposed by Han et al. (5) which suggests that AppA utilizes heme as a cofactor, bound to its C-terminal domain, to sense the cytosolic redox conditions. Accordingly,  $A^+$  and  $A^-$  correspond to an oxidized and a reduced heme cofactor, respectively. Also, in Eqs. 4.1 and 4.2 we assumed that the reoxidation of AppA and PpsR occurs in proportion to the concentration of dissolved oxygen ( $[O_2]$ ) such that  $k_{Ao}[O_2]$  and  $k_{Po}[O_2]$  correspond to pseudo first-order rate constants (for fixed  $[O_2]$ ), whereas  $k_{Ar}$  denotes a first order rate constant describing the reduction of AppA by an, as yet, unknown mechanism.

The light-independent reduction of a disulfide bond in oxidized PpsR ( $P_4^+$ ) by the reduced form of AppA is modelled as



In Eq. 4.3,  $k_{Pr}^+$  and  $k_{Pr}^-$  denote second-order rate constants. Their ratio  $K_{eq} = k_{Pr}^+/k_{Pr}^-$  defines the equilibrium constant, which is related to the difference between the midpoint potentials of the dithiol/disulfide couples in PpsR and AppA via

$$\Delta E_m = E_m^{P_4^+/P_4^-} - E_m^{A^+/A^-} = \frac{RT}{2F} \ln K_{eq} .$$

Note that based on *in vitro* studies, Masuda and Bauer suggested that the electron transfer from AppA to PpsR is effectively irreversible (i.e.  $K_{eq} \gg 1$ ), as under a wide range of conditions, they could not observe an inverse electron flow from reduced PpsR to oxidized AppA ( $A^+$ ) (22). This finding is also supported by our simulations in Chapter 3, which show that particular regulatory features, which we believe are associated with the phenotype of high light repression of photosynthesis genes under semi-aerobic conditions, disappear as  $K_{eq} \rightarrow 1$ . However, for the sake of generality, we prefer to model the electron transfer from AppA to PpsR as a reversible process.

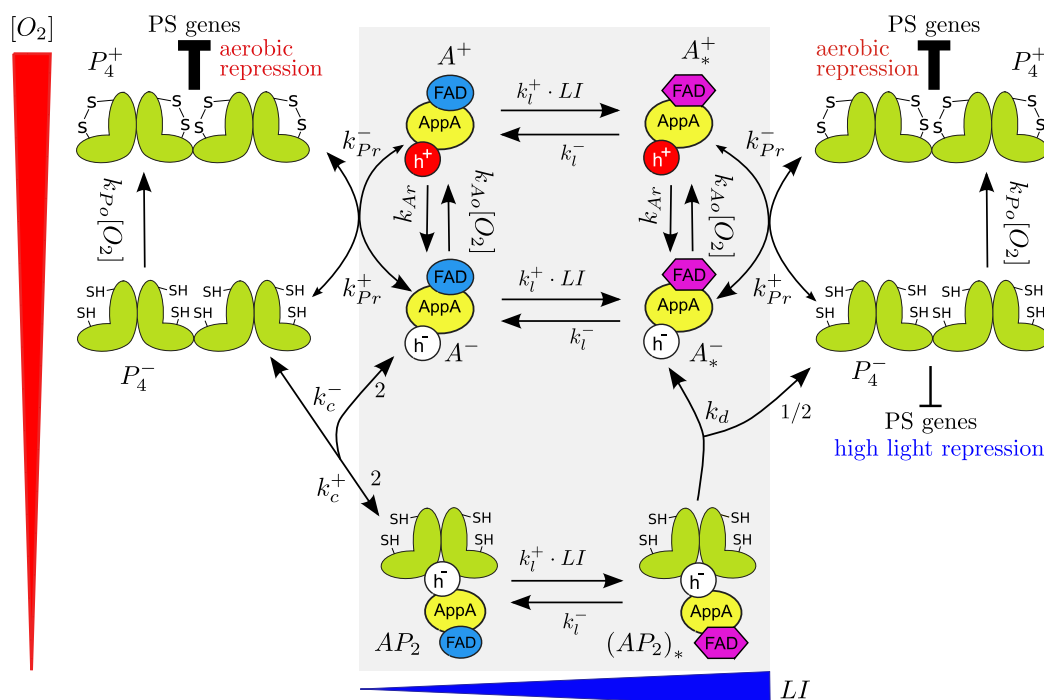


Figure 4.1: A schematic diagram of the extended model for the blue-light- and oxygen-dependent interactions between AppA and PpsR as described by Eqs. 4.3-4.9.  $P_4^+$  and  $P_4^-$  denote PpsR tetramers in an oxidized or in a reduced state, respectively. Here S-S and SH denote intramolecular disulfide bonds and thiol groups, respectively. AppA can be reversibly inter-converted between four states, corresponding to a reduced ( $A^-$ ) or an oxidized ( $A^+$ ) heme cofactor and depending on whether the FAD cofactor is light-excited ( $A_*^-$  and  $A_*^+$ ). As shown, AppA and PpsR can reversibly associate in a complex ( $AP_2$ ). Additionally, upon blue-light excitation the light-excited complex ( $AP_2$ )<sub>\*</sub> irreversibly dissociates into  $A_*^-$  and half of a PpsR tetramer. Numbers denote stoichiometric coefficients. Note that under aerobic conditions photosynthesis (PS) genes are mainly repressed by the oxidized form of PpsR, whereas the reduced form is the predominant repressor of PS genes under semi-aerobic conditions. The grey-shaded region encompasses the light-dependent reactions.  $LI$  and  $[O_2]$  represent the light irradiance and the oxygen concentration, respectively.

#### 4.1.2 A Detailed Mechanism for the Light Regulation

AppA is a flavoprotein (apart from being redox-active) which enables it to act as a blue-light sensor by means of a FAD cofactor bound to its N-terminal

BLUF domain (22, 25, 26). Han et al. (5) suggested that the C-terminal domain of AppA is only responsive to light when the attached heme cofactor is in the reduced state. They also suggested that the redox state of heme keeps C-terminal domain in a conformation that alternatively favors the binding of C-terminal domain with the BLUF domain or with PpsR protein under low oxygen levels.

The flavin of AppA undergoes a photocycle upon blue light excitation in the course of which a long-lived signalling state is formed (22, 51, 52). This transition to the signalling state is accompanied by a conformational change in the AppA protein (32, 33) which is believed to result in interactions of the N-terminal BLUF domain with its C-terminal part (5, 32). Therefore, under anaerobic condition and in presence of the light the C-terminal domain of AppA binds with the BLUF-domain of AppA instead of PpsR which leads to the repression of PS genes by PpsR (5, 32).

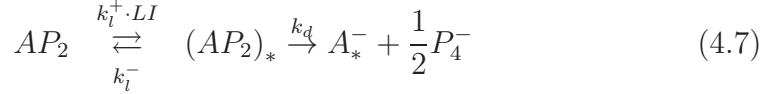
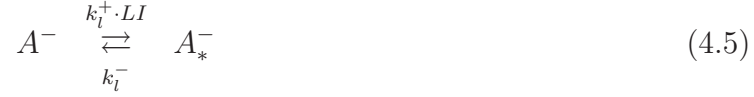
Considering these experimental results, it seems unlikely that light irradiation directly affects the association rate between AppA and PpsR as assumed in Eq. 3.6. Therefore, in the extended model we assume that reversible complex formation occurs independently of the light irradiance ( $LI$ ) as



where  $k_c^+$  and  $k_c^-$  represent an effective third- and a second-order rate constant, respectively. Here, we only account for the overall stoichiometry of this process although it is likely that it occurs in multiple steps. However, using a quasi-steady state approximation it can be shown (see Appendix B) how the effective parameters  $k_c^+$  and  $k_c^-$  in Eq. 4.4 can be related to the kinetic parameters of an underlying multi-step process (53).

In addition, we follow the model proposed by Han et al. (5) to implement a more realistic model for the light-dependent interaction between AppA and PpsR. This model suggests that the light-induced structural changes of AppA mediate the dissociation of the AppA-PpsR complex and prevent the re-binding of PpsR to light-excited AppA when the C-terminally bound heme is in its reduced state (Fig. 4.1). Taking this into account, we introduce three new states  $A_*^+$ ,  $A_*^-$  and  $(AP_2)_*$  corresponding to the light-excited forms of oxidized and reduced AppA, respectively, as well as to the light-excited form of AppA when bound in a complex with PpsR. Now, light regulation is modeled as a simple two state process where the excitation rate is proportional to the light irradiance ( $LI$ ), and the thermal recovery to the ground state is

described by a first-order rate constant as



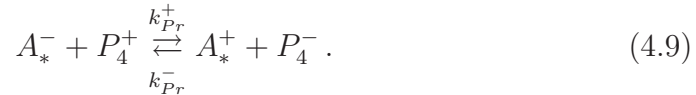
where  $k_d$  in Eq. (4.7) denotes a first-order rate constant that describes the light-induced dissociation of the AppA-PpsR complex in an effective, yet stoichiometrically correct, manner.

In order to complement the transitions between the four AppA species, as defined in Eqs. (4.1), (4.5), and (4.6), we assume that redox regulation of AppA occurs independently of the light excitation.



Note that we choose the rate constants in the cyclic reactions (4.1), (4.5), (4.6) and (4.8) in such a way that “the principle of detailed balance” (explained in the Appendix F) holds.

At last, we have to account for the observation that the reduced form of AppA can reduce the disulfide bond in oxidized PpsR irrespective of the light excitation of the flavin (22) which leads to



Here, we have assumed that the rates of reduction and re-oxidation are the same as for the non-excited forms of AppA (cf. Eq. 4.3) to keep the number of unknown parameters as low as possible.

## 4.2 System Equations and Parameters

Mass action kinetics is assumed to get the dynamics of the reaction network formed by Eqs. 4.1-4.9, which results in the following ordinary differential

equations (ODEs) system:

$$\begin{aligned}
 \frac{d[P_4^-]}{dt} &= -k_{Po}[O_2][P_4^-] + k_{Pr}^+([A^-] + [A_*^-])[P_4^+] + \frac{k_d}{2}[(AP_2)_*] \\
 &\quad - \left(k_c^+[A^-]^2[P_4^-] - k_c^-[AP_2]^2\right) - k_{Pr}^-([A^+] + [A_*^+])[P_4^-] \\
 \frac{d[P_4^+]}{dt} &= k_{Po}[O_2][P_4^-] - k_{Pr}^+([A^-] + [A_*^-])[P_4^+] \\
 &\quad + k_{Pr}^-([A^+] + [A_*^+])[P_4^-] \\
 \frac{d[AP_2]}{dt} &= 2 \left(k_c^+[A^-]^2[P_4^-] - k_c^-[AP_2]^2\right) - k_l^+[LI][AP_2] + k_l^-[(AP_2)_*] \\
 \frac{d[(AP_2)_*]}{dt} &= k_l^+[LI][AP_2] - (k_l^- + k_d)[(AP_2)_*] \\
 \frac{d[A^-]}{dt} &= k_{Ar}[A^+] - k_{Ao}[O_2][A^-] - k_l^+[LI][A^-] + k_l^-[A_*^-] \quad (4.10) \\
 &\quad - 2 \left(k_c^+[A^-]^2[P_4^-] - k_c^-[AP_2]^2\right) \\
 &\quad - k_{Pr}^+[A^-][P_4^+] + k_{Pr}^-[A^+][P_4^-] \\
 \frac{d[A_*^-]}{dt} &= k_l^+[LI][A^-] - k_l^-[A_*^-] + (k_{Ar}[A_*^+] - k_{Ao}[O_2][A_*^-]) \\
 &\quad - k_{Pr}^+[A_*^-][P_4^+] + k_{Pr}^-[A_*^+][P_4^-] + k_d[(AP_2)_*] \\
 \frac{d[A_*^+]}{dt} &= - (k_{Ar}[A_*^+] - k_{Ao}[O_2][A_*^-]) + k_l^+[LI][A^+] - k_l^-[A_*^+] \\
 &\quad + k_{Pr}^+[A_*^-][P_4^+] - k_{Pr}^-[A_*^+][P_4^-] \\
 \frac{d[A^+]}{dt} &= -k_{Ar}[A^+] + k_{Ao}[O_2][A^-] - k_l^+[LI][A^+] + k_l^-[A_*^+] \\
 &\quad + k_{Pr}^+[A^-][P_4^+] - k_{Pr}^-[A^+][P_4^-]
 \end{aligned}$$

Here, we have assumed that the total amounts of the proteins PpsR and AppA are conserved

$$[P_4^+] + [P_4^-] + \frac{1}{2}[AP_2] + \frac{1}{2}[(AP_2)_*] = [P_T] \quad \text{and} \quad (4.11)$$

$$[A^+] + [A^-] + [A_*^+] + [A_*^-] + [AP_2] + [(AP_2)_*] = [A_T]$$

where  $P_T$  and  $A_T$  denote the total concentrations of PpsR and AppA, respectively. This assumption is in agreement with the fact that the expression level of PpsR were found to be largely independent of the growth conditions (29). However, the regulation of AppA is not known. Hence, we will treat the ratio  $\gamma = [A_T]/[P_T]$  as a free parameter in our study. We also neglect dilution terms due to cell growth in the expressions in Eqs. 4.10 to be consistent with

Table 4.1: **Definition of dimensionless parameters.**

$\alpha = \frac{k_{Po}}{k_{Ao}}$	$\beta = \frac{k_{Pr}^+[AT]}{k_{Ar}}$	$\gamma = \frac{[AT]}{[PT]}$	$\delta = \frac{k_c^+[AT]^2}{k_{Ar}}$
$O = \frac{[O_2]}{K_O}$	$I = \frac{LI}{K_L}$	$K_O = \frac{k_{Ar}}{k_{Ao}}$	$K_L = \frac{k_i^-}{k_i^+}$
$\eta = \frac{k_i^-}{k_{Ar}}$	$\lambda = \frac{k_d}{k_i^-}$	$K_{eq} = \frac{k_{Pr}^+}{k_{Pr}^-}$	$K_c = \frac{k_c^-}{k_c^+[PT]}$

our assumptions.

The steady state behaviour of the ODE system in Eqs. 4.10 is analysed by introducing dimensionless parameters (cf. Table 4.1). This facilitates to assess the relative significance of individual reaction steps for a certain type of behaviour while keeping the number of free parameters as small as possible. In addition, concentrations are measured in terms of the total protein concentrations as defined in Table 4.2. Thus, in dimensionless units the ODE system reads

$$\begin{aligned}
 \frac{d}{d\tau}x_1 &= x_5 - Ox_1 - \frac{2\delta}{\gamma} \left( x_1^2x_2 - K_c \frac{x_3^2}{\gamma^2} \right) - \eta(Ix_1 - x_6) \\
 &\quad - \frac{\beta}{\gamma} \left( x_1x_4 - \frac{x_2x_5}{K_{eq}} \right) \\
 \frac{d}{d\tau}x_2 &= \beta \left( x_4(x_1 + x_6) - \frac{x_2(x_5 + x_7)}{K_{eq}} \right) - \delta \left( x_1^2x_2 - K_c \frac{x_3^2}{\gamma^2} \right) \\
 &\quad - \alpha Ox_2 + \frac{\lambda\eta}{2}x_8 \\
 \frac{d}{d\tau}x_3 &= 2\delta \left( x_1^2x_2 - K_c \frac{x_3^2}{\gamma^2} \right) - \eta(Ix_3 - x_8) \\
 \frac{d}{d\tau}x_6 &= x_7 - Ox_6 - \frac{\beta}{\gamma} \left( x_4x_6 - \frac{x_2x_7}{K_{eq}} \right) + \eta \left( Ix_1 - x_6 + \frac{\lambda}{\gamma}x_8 \right) \\
 \frac{d}{d\tau}x_7 &= \eta(Ix_5 - x_7) - x_7 + Ox_6 + \frac{\beta}{\gamma} \left( x_4x_6 - \frac{x_2x_7}{K_{eq}} \right) \\
 \frac{d}{d\tau}x_8 &= \eta(Ix_3 - x_8 - \lambda x_8)
 \end{aligned} \tag{4.12}$$

where  $x_4$  and  $x_5$  are given by the dimensionless form of the conservation relations (cf. Eqs. 4.11)

$$\begin{aligned}
 x_4 &= 1 - x_2 - \frac{x_3}{2} - \frac{x_8}{2} \quad \text{and} \\
 x_5 &= 1 - x_1 - x_6 - x_7 - \frac{x_3}{\gamma} - \frac{x_8}{\gamma}.
 \end{aligned} \tag{4.13}$$

Table 4.2: Definition of dimensionless state variables.

$x_1 = \frac{[A^-]}{[A_T]}$	$x_2 = \frac{[P_4^-]}{[P_T]}$	$x_3 = \frac{[AP_2]}{[P_T]}$	$x_4 = \frac{[P_4^+]}{[P_T]}$
$x_5 = \frac{[A^+]}{[A_T]}$	$x_6 = \frac{[A_*^-]}{[A_T]}$	$x_7 = \frac{[A_*^+]}{[A_T]}$	$x_8 = \frac{[(AP_2)_*]}{[P_T]}$

Table 4.3: Comparison of the parameters of the extended and simple model.

Extended Model	Simple model
$K_O = \frac{k_{Ar}}{k_{Ao}}$	$K_O = \frac{k_{Ar}}{k_{Ao}}$
$K_L = \frac{k_l^-}{k_l^+}$	$K_L = \left( \frac{k_c^+[P_T]}{k_c^-} \right)^{1/2}$
$K_{eq} = \frac{k_{Pr}^+}{k_{Pr}^-}$	$K_{eq} = \frac{k_{Pr}^+}{k_{Pr}^-}$
$O = \frac{[O_2]}{K_O}$	$O = \frac{[O_2]}{K_O}$
$I = \frac{LI}{K_L}$	$I = \frac{LI}{K_L}$
$\alpha = \frac{k_{Po}}{k_{Ao}}$	$\alpha = \frac{k_{Po}}{k_{Ao}}$
$\beta = \frac{k_{Pr}^+[A_T]}{k_{Ar}}$	$\beta = \frac{k_{Pr}^+[A_T]}{k_{Ar}}$
$\gamma = \frac{[A_T]}{[P_T]}$	$\gamma = \frac{[A_T]}{[P_T]}$
$\delta = \frac{k_c^+[A_T]^2}{k_{Ar}}$	$\delta = \frac{k_c^+[A_T]^2}{LI^2 k_{Ar}}$
$\eta = \frac{k_l^-}{k_{Ar}}$	no such parameter
$\lambda = \frac{k_d}{k_l^-}$	no such parameter
$K_c = \frac{k_c^-}{k_c^+[P_T]}$	no such parameter

Note that, in Eqs. 4.12, time ( $\tau$ ) is measured in units of  $1/k_{Ar}$ . The oxygen concentration ( $[O_2]$ ), which is measured in units of  $K_0 = k_{Ar}/k_{Ao}$ , and the

light irradiance ( $LI$ ), which is measured in units of  $K_L = k_l^-/k_l^+$  (typically  $\mu\text{mol}/\text{m}^2\text{s}$ ) are the two main parameters of the present model. The parameters  $\alpha$ ,  $\beta$ ,  $\gamma$  and  $K_{eq}$  are defined in the same way as in Chapter 3, (and in Ref. (53)) whereas  $\delta$  is now independent of the light irradiance ( $LI$ ) due to the redefinition of  $k_c^+$  in Eq. 4.4. A comparison of the parameters of the extended and simple model is shown in Table 4.3.

While doing a direct comparison with the results of the simple model (examined in Chapter 3), it is important to keep in mind that the definitions of  $K_L$  and  $\delta$  are different from those of the simple model. Another consequence of this redefinition is that the effective dissociation constant  $K_c$  now plays the same role as the square of the dimensionless light irradiance ( $I^2$ ) plays in the simple model.

In the end, there are two new parameters (see Table 4.3):

$$\eta = \frac{k_l^-}{k_{Ar}} \quad \text{and} \quad \lambda = \frac{k_d}{k_l^-}$$

which have a direct effect on light regulation. Particularly,  $\eta$  represents the ratio between the rates of the thermal recovery of light-excited AppA species and that of AppA reduction, whereas  $\lambda$  compares the dissociation rate of the light-excited complex with the thermal recovery rate.

### 4.3 Steady State Expressions

Although a detailed analytical steady state analysis of Eqs. (4.12) is not feasible without simplifying assumptions, it is straightforward to deduce some relations which show how the oxygen concentration and the light irradiance determine the fraction of oxidized to reduced and light excited to non-excited states, respectively under steady state conditions.

$$\begin{aligned} x_5 - Ox_1 - \frac{2\delta}{\gamma} \left( x_1^2 x_2 - K_c \frac{x_3^2}{\gamma^2} \right) - \eta (Ix_1 - x_6) \\ - \frac{\beta}{\gamma} \left( x_1 x_4 - \frac{x_2 x_5}{K_{eq}} \right) = 0 \end{aligned} \quad (4.14)$$

$$\begin{aligned} \beta \left( x_4 (x_1 + x_6) - \frac{x_2 (x_5 + x_7)}{K_{eq}} \right) - \delta \left( x_1^2 x_2 - K_c \frac{x_3^2}{\gamma^2} \right) \\ - \alpha Ox_2 + \frac{\lambda\eta}{2} x_8 = 0 \end{aligned} \quad (4.15)$$

$$x_7 - Ox_6 - \frac{\beta}{\gamma} \left( x_4x_6 - \frac{x_2x_7}{K_{eq}} \right) + \eta \left( Ix_1 - x_6 + \frac{\lambda}{\gamma}x_8 \right) = 0 \quad (4.16)$$

$$\eta(Ix_5 - x_7) - x_7 + Ox_6 + \frac{\beta}{\gamma} \left( x_4x_6 - \frac{x_2x_7}{K_{eq}} \right) = 0 \quad (4.17)$$

$$2\delta \left( x_1^2x_2 - K_c \frac{x_3^2}{\gamma^2} \right) = \eta(Ix_3 - x_8) \quad (4.18)$$

$$Ix_3 - x_8 - \lambda x_8 = 0 \quad (4.19)$$

Addition of Eq. 4.16 with Eq. 4.17 and use of Eq. 4.19 results in

$$I \left( x_1 + x_5 + \frac{x_3}{\gamma} \right) - \left( x_6 + x_7 + \frac{x_8}{\gamma} \right) = 0 \quad (4.20)$$

Using this relation in Eq. 4.13, we get

$$x_1 + x_5 + \frac{x_3}{\gamma} = \frac{1}{1+I} \quad (4.21)$$

$$x_6 + x_7 + \frac{x_8}{\gamma} = \frac{I}{1+I} \quad (4.22)$$

These two equations (Eqs. 4.21- 4.22) describe how the light irradiance determines the relative concentration of light-excited (Eq. 4.22) and non-excited (Eq. 4.21) states .

Addition of Eq. 4.14 and Eq. 4.16 results in

$$\begin{aligned} x_5 + x_7 - O(x_1 + x_6) - \frac{2\delta}{\gamma} \left( x_1^2x_2 - K_c \frac{x_3^2}{\gamma^2} \right) + \eta \frac{\lambda}{\gamma} x_8 \\ - \frac{\beta}{\gamma} \left( x_4(x_1 + x_6) - \frac{x_2(x_5 + x_7)}{K_{eq}} \right) = 0 \end{aligned} \quad (4.23)$$

After adding Eq. 4.15 with Eq. 4.23, and using Eq. 4.18 and Eq. 4.19 we obtain

$$\frac{x_5 + x_7}{x_1 + x_6 + \frac{\alpha}{\gamma}x_2} = O \quad (4.24)$$

Eq. 4.24 shows that how the oxygen concentration determines the ratio between oxidized and reduced states.

## 4.4 Results

In most of the simulations, the electron transfer from AppA to PpsR in Eq. 4.3 is assumed effectively irreversible, as suggested by the experimental

results of Masuda and Bauer (22). This assumption corresponds to the limit  $K_{eq} \rightarrow \infty$  in Eqs. 4.12 or  $k_{Pr}^- = 0$  in Eq. 4.3. We first present the effect of new parameters in absence of light regulation. Afterwards, we estimate the some of the parameters and show the role of new parameters in the full model (in presence of redox and light regulation) along with the comparison of model prediction with experimental results. In the end we will discuss how extended model also account for the lowered blue light sensitivity observed in the AppA mutant strain (36).

#### 4.4.1 Effect of the New Parameters in the Absence of Light

It is straight forward to see that the total amount of light-excited species is conserved, if we set  $\eta=0$  in the Eqs. 4.12, i.e.  $d(x_5 + x_6 + x_7)/dt = 0$ , and if we set the initial concentrations of these species to zero they will remain zero in time. Hence, under these conditions we recover the structure of the simple model (Chapter 3) (53). Particularly, the maximum of reduced PpsR at intermediate oxygen concentrations ( $O \approx 2$ ) is lowered, as  $K_c$  is decreased (Figs. 4.2A, 4.2B). Since decreasing the value of  $K_c$  increases the effective binding affinity for complex formation between AppA and PpsR, the amount of free reduced PpsR molecules is lower under anaerobic conditions ( $O = 0$ )(Figs. 4.2A, 4.2B). Similar to the simple model, when  $\alpha$  and  $\gamma$  are chosen such that the condition  $\alpha O > \gamma > 2$  is fulfilled, lowering  $K_c$  can also induce a bistable response in the transition from the anaerobic to the aerobic growth regime (Figs. 4.2C, 4.2D).

#### 4.4.2 Parameter Estimation for the Extended Model

There is a total of 12 parameters (Table 4.1) in the model (defined by Eqs. 4.12), two of which ( $K_O$  and  $K_L$ ) can be ‘absorbed’ into the definition of the dimensionless oxygen concentration ( $O = [O_2]/K_O$ ) and the dimensionless light irradiance ( $I = LI/K_L$ ), respectively. Reasonable ranges for the parameters  $\alpha$ ,  $\beta$ ,  $\gamma$  and  $K_{eq}$  are suggested by the analysis of the simple model (cf. Fig. 4.2). A biologically plausible range for the two parameters,  $\eta = k_l^-/k_{Ar}$  and  $\lambda = k_d/k_l^-$ , can be estimated as follows:  $k_l^-$  describes the thermal relaxation of light-excited AppA back to the ground state. Experiments have shown that, upon blue light excitation, AppA undergoes a photocycle in the course of which a long-lived signaling state is formed (22, 51, 52). The half-life of the signaling state was found to be 15 min (22) corresponding to  $k_l^- \approx 10^{-3}/s$ . On the other hand,  $k_{Ar}$  characterizes the rate of reduction of AppA while  $k_d$  is related to the light-induced conformational change of

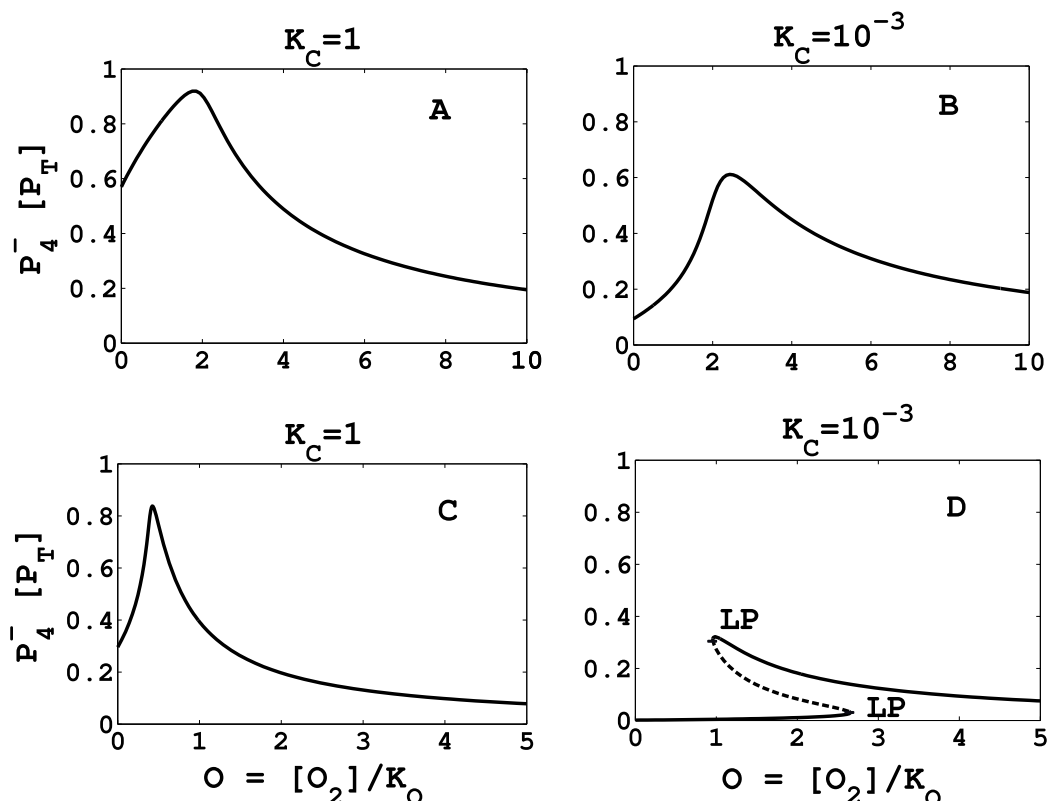


Figure 4.2: Effect of the new parameters in the absence of light regulation ( $\eta = 0$ ): (A and B) When  $\alpha = 1$  and  $\gamma = 2$ , decreasing  $K_c$  lowers the maximum of reduced PpsR ( $P_4^-$ ) at intermediate oxygen concentrations ( $O \approx 2$ ) as well as the amount of free reduced PpsR ( $P_4^-$ ) under anaerobic conditions ( $O = 0$ ). (C and D) When  $\alpha = 10$  and  $\gamma = 4$ , decreasing  $K_c$  results in a bistable response. In the region between the two limit points (LP), two stable steady states (solid lines) coexist with one unstable steady state (dashed line). Other used parameters are:  $K_{eq} = \infty$  and  $\beta = 10^3$ .

AppA. It can be expected that both processes occur on a significantly faster time scale compared to  $1/k_l^-$ . For example, conformational changes of proteins typically occur on a time scale of milliseconds (54) such that we expect  $\lambda \gg 1$  and  $\eta \ll 1$ .

The parameters  $K_L$ ,  $K_c$  and  $\delta$  can be estimated by combining results from experimental measurements with general mechanistic reasoning. This will be attempted in the following sections

### (a) Estimation of $K_L$

We have modeled the light-dependent excitation of the FAD domain in the AppA protein as a simple two-state process (Eqs. 4.5-4.7), where the rate of the forward reaction  $k_l^+ \cdot LI$  is assumed to be proportional to the light irradiance  $LI$ , whereas the rate of the backward reaction is modeled as a thermal recovery process characterized by a first order rate constant  $k_l^-$ . Therefore, the quantity  $K_L = k_l^-/k_l^+$  defines a unit scale with respect to which we measure the light irradiance as  $LI = I \cdot K_L$ , i.e.  $K_L$  has the same dimension as  $LI$  (typically  $\mu\text{mol}/\text{m}^2\text{s}$ ), whereas  $I$  is dimensionless.

Recently Metz et al., estimated both the parameters  $k_l^+$  and  $k_l^-$  by fitting *in vivo* measurements of the AppA-mediated repression of the *puc* operon over a broad range of light irradiation to models of different complexity for the photocycle of AppA (36). They approximated the rate constant  $k_l^+$  for light excitation from the photochemical quantum yield ( $Q \approx 0.3$ ) and the extinction coefficient of AppA in the dark state ( $\varepsilon = 6764 \text{ M}^{-1} \cdot \text{cm}^{-1}$  in the wavelength range of 400 – 700 nm) as (36)

$$\begin{aligned} k_l^+ &= Q \cdot \varepsilon \cdot \ln 10 \\ &\approx 4.7 \cdot 10^3 \frac{l}{\text{mol} \cdot \text{cm}} \\ &= 0.00047 \frac{\text{m}^2}{\mu\text{mol}}. \end{aligned} \quad (4.25)$$

The thermal recovery rate was estimated to be in the range (36):

$$k_l^- = 0.00012/\text{s}, \dots, 0.0013/\text{s} \quad (4.26)$$

which is compatible with an independent estimate for the half-life of the AppA-excited state of  $T_{1/2} = 15 \text{ min}$  (22) i.e. decay rate =  $\frac{\ln 2}{t_{1/2}} = 0.0008/\text{s}$ . Combining Eqs. (4.25) and (4.26) we can estimate the unit of light irradiation as

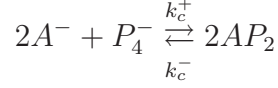
$$K_L = \frac{k_l^-}{k_l^+} = 0.26, \dots, 2.8 \frac{\mu\text{mol}}{\text{m}^2\text{s}}. \quad (4.27)$$

We will use a value of  $K_L = 1 \mu\text{mol}/\text{m}^2\text{s}$  to compare the results of our simulations with experimental measurements over the range of light irradiation between  $0.1, \dots, 20 \mu\text{mol}/\text{m}^2\text{s}$ .

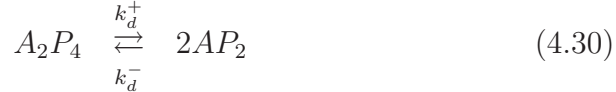
### (b) Estimation of $K_c$

Through Eq. 4.4, we have modeled the complex formation between the reduced forms of AppA ( $A^-$ ) and PpsR ( $P_4^-$ ) as an effective third order process

according to the scheme



where  $AP_2$  denotes the complex between an AppA monomer and half of a PpsR tetramer. In Eq. 4.4,  $k_c^+$  and  $k_c^-$  denote effective third and second order rate constants, respectively. In Ref. (53) we have shown that these effective rate constants can be derived from the kinetic parameters of an underlying multi-step process of the form



In the above scheme, we have assumed that PpsR tetramer is composed of two identical dimer subunits. The first two equations of this scheme describe the association of an AppA molecule to either of the two PpsR dimers. In Eqs. 4.28 and 4.29, the combinatorial factors of 2 result from the fact that in the first association event (Eq. 4.28), there are two possibilities for an AppA molecule to bind one of the two PpsR dimers. Similarly, there are two possibilities for an AppA molecule to dissociate from the  $A_2P_4$  complex. To make it simple, we have assumed that binding of the second AppA molecule occurs independently from the first binding event such that the rate constants  $k_a^+$  and  $k_a^-$  are the same for both binding steps. The last equation, Eq. 4.30, represents the formation of the experimentally observed AppA-PpsR complex ( $AP_2$ ). In Ref. (53) using a quasi-steady state approximation for the intermediate association steps we have shown that the effective parameters  $k_c^+$  and  $k_c^-$  are related to the kinetic parameters of the underlying multi-step process (Eqs. 4.28-4.30) as

$$k_c^+ = \frac{k_d^+}{K_a^2} \quad \text{and} \quad k_c^- = k_d^- \quad (4.31)$$

where  $K_a = k_a^-/k_a^+$  denotes the dissociation constant for the association between AppA and PpsR. We also define the dissociation constant  $K_d = k_d^+/k_d^-$  for the dissociation of  $A_2P_4$  into two  $AP_2$  complexes (Eq. 4.30).

To estimate the numerical value of the parameter  $K_c$  as defined in Table 4.1 we express  $K_c$  in terms of  $K_a$ ,  $K_d$  and the total PpsR concentration ( $P_T$ ) as

$$K_c \equiv \frac{k_c^-}{k_c^+ P_T} = \frac{K_a^2}{K_d P_T}. \quad (4.32)$$

Since *in vivo* data is not available, we estimate the parameters  $K_a$  and  $P_T$  from the binding experiments between PpsR and DNA fragments containing the *puc* promoter with the palindromic consensus sequence for PpsR-binding (22). The  $EC_{50}$ -value of PpsR ranges between 20  $nM$  and 50  $nM$  for oxidized and reduced PpsR, respectively, under dark conditions. In the presence of AppA, the  $EC_{50}$ -value is shifted towards higher values of around 100  $nM$  due to the formation of AppA-PpsR complexes. In the presence of light, the  $EC_{50}$ -value is lowered to around 70  $nM$  due to the dissociation of these complexes which releases more PpsR for DNA-binding.

Based on these findings, one can expect the dissociation constant for AppA-PpsR binding to be lower than 100  $nM$  because otherwise complex formation would not be effective. Also, to reach saturating levels of DNA-binding under all conditions the PpsR concentration should be larger than 100  $nM$ . On the other hand, for an effective sequestration of PpsR molecules into AppA-PpsR complexes the total AppA concentration should exceed that of PpsR by at least a factor of 2 because two AppA molecules are required to sequester one PpsR tetramer. Hence, it seems reasonable to assume that the total PpsR concentration in the cell is larger than 100  $nM$ , but not too large in order to allow for an effective sequestration by AppA. As a conservative estimate we assume that  $K_a = 0.1 \mu M$  and  $P_T = 0.2 \mu M$  which leads to

$$K_c = \frac{0.1^2 \mu M^2}{0.2 \mu M \cdot K_d} = \frac{0.05 \mu M}{K_d}. \quad (4.33)$$

A reasonable value for  $K_d$  can be estimated by the following argument: For complex formation, as described by Eqs. 4.28-4.30, to be effective one would expect that the rate of dissociation of the intermediate  $A_2P_4$  complex into  $AP_2$  complexes (Eq. 4.30) is much higher than the rate for the formation of  $A_2P_4$  from two  $AP_2$  complexes. Hence, one expects that the dissociation constant  $K_d$  is large compared to the total concentrations of PpsR and AppA. For example, a value of  $K_d = 50 \mu M$  would result in a value of 0.001 for the parameter  $K_c$ .

Together, this shows that when the dissociation of the intermediate  $A_2P_4$  complex is effectively irreversible ( $K_d \gg P_T, A_T$ ) and when the binding between AppA and PpsR is tight ( $K_a \ll P_T$ ) the dimensionless parameter  $K_c$  assumes values in the range  $K_c \ll 0.1$ . For the simulations we have mostly used for  $K_c$  a value of  $10^{-4}$ .

**(c) Estimation of  $\delta$** 

Recall that in formulation of the model in Chapter 3,  $\delta$  was light-dependent although the steady state behaviour did not depend on  $\delta$ . Here, the parameter  $\delta = k_c^+[A_T]^2/k_{Ar}$  compares the time scale for the reduction of AppA ( $1/k_{Ar}$ ) with that for the association between AppA and PpsR ( $1/k_c^+[A_T]^2$ ).

The value of  $\delta$  can be estimated by following arguments: The simple model (Chapter 3), indicates that for an efficient sequestration of PpsR by AppA the total amounts of AppA should exceed those of PpsR by at least a factor of 2. Therefore, if total amounts of PpsR were in the range between  $0.1 \mu M$  and  $0.2 \mu M$  (see Section: *Estimation of  $K_c$* ) we would expect  $[A_T]$  to be in the range between  $0.2 \mu M$ - $0.4 \mu M$ . The rate of AppA reduction ( $k_{Ar}$ ) can be estimated from the requirement  $\eta = k_l^-/k_{Ar} \ll 1$  as discussed in the Section *Estimation of the Parameters for the Extended Model*. Since the recovery rate of light-excited AppA,  $k_l^- \approx 0.0013/s$ , is small we can expect that  $k_{Ar}$  is larger or much larger than  $0.01/s$ . For specificity, we assume that  $k_{Ar} = 0.01/s, \dots, 0.1/s$ .

Finally, to estimate the value of  $k_c^+ = k_d^+/K_a^2$  (Eq. 4.31) we use the previous estimate for  $K_a = 0.1 \mu M$  (see Section *Estimation of  $K_c$* ). A reasonable value for  $k_d^+$  can be obtained from our estimate of the dissociation constant  $K_d = k_d^+/k_d^-$  which was based on the requirement that the final reaction step in the formation of the AppA-PpsR complex (Eq. 4.30) is effectively irreversible. Hence, we expect the re-association rate  $k_d^-$  between two  $AP_2$  molecules to be much smaller than the association rate  $k_a^+$  between AppA and PpsR in Eqs. (4.28) and (4.29) which has been measured in Ref. (5) as  $0.04/\mu Ms$ . For specificity we assume that  $k_d^- = 0.001/\mu Ms$ . To be consistent with our previous estimate (see Section *Estimation of  $K_c$* ) we further assume that  $K_d = 50 \mu M$  which leads to  $k_d^+ = 0.05/s$  and  $k_c^+ = 5/\mu M^2s$ . Putting everything together we find that  $\delta$  lies in the range between 2 and 80. For the simulations we have used a value of  $\delta = 10$ .

We find that  $K_L \approx 1 \mu mol/m^2s$ ,  $K_c \ll 0.1$  and  $\delta = 2, \dots, 80$ . The reasonable or estimated value of the all the parameters are summarized in the Table 4.4.

**4.4.3 Peak Development in the Extended Model**

The *in vivo* study by Metz et al. (35) showed that the AppA/PpsR system responds to blue light signals down to a light irradiance of  $0.2 \mu mol/m^2s$  where half maximal repression of the *puc* gene was observed. They observed that saturating levels of *puc* gene repression were reached at  $LI \approx 1 \mu mol/m^2s$  and they remained constant up to  $LI = 20 \mu mol/m^2s$ . These observations

Table 4.4: **Estimated/Reasonable or Used Value of Parameters**

Parameters	Estimated/Reasonable Value
$K_L = \frac{k_i^-}{k_i^+}$	$1 \frac{\mu\text{mol}}{\text{m}^2\text{s}}$ (0.26, ..., 2.8 $\frac{\mu\text{mol}}{\text{m}^2\text{s}}$ )
$K_{eq} = \frac{k_{Pr}^+}{k_{Pr}^-}$	1, ..., $\infty$
$\alpha = \frac{k_{Po}}{k_{Ao}}$	1, ..., 10
$\beta = \frac{k_{Pr}^+[A_T]}{k_{Ar}}$	1, ..., 1000
$\gamma = \frac{[A_T]}{[P_T]}$	1, ..., 4
$\delta = \frac{k_c^+[A_T]^2}{k_{Ar}}$	2, ..., 80
$\eta = \frac{k_i^-}{k_{Ar}}$	$10^{-2}$ ( $\ll 1$ )
$\lambda = \frac{k_d}{k_i^-}$	$10^2$ ( $\gg 1$ )
$K_C = \frac{k_c^-}{k_c^+[P_T]}$	$10^{-4}$ ( $\ll 0.1$ )

suggest that, *in vivo*, the range  $LI \geq 1 \mu\text{mol}/\text{m}^2\text{s}$  can already be regarded as ‘high light’ conditions although *in vitro* studies often used a light irradiance that was up to two orders of magnitude larger (22, 28, 29). No repression of PS genes was observed at a light irradiance of  $LI \leq 0.1 \mu\text{mol}/\text{m}^2\text{s}$  which, thus, marks the lower bound for the sensitivity range with respect to light.

As it is shown in Fig. 4.3, the extended model predicts the formation of a light-dependent maximum in the concentration of reduced PpsR at intermediate oxygen concentrations for a reasonable set of parameters (see Section 4.4.2). This peak formation requires a sufficiently large time scale separation between the reduction rate of PpsR and that of AppA ( $\beta \gg 1$ ) similar to the simple model discussed in Chapter 3 and Ref. (53). Additionally, two trends are apparent: First, at a fixed value of  $\beta$  the difference between the maximum under low light conditions ( $0.1 \mu\text{mol}/\text{m}^2\text{s}$ , no gene repression) and that under high light conditions ( $1 \mu\text{mol}/\text{m}^2\text{s}$ , maximal gene repression) is determined by the binding affinity ( $K_c$ ) of the AppA-PpsR complex. For smaller values of  $K_c$ , when complex formation between AppA

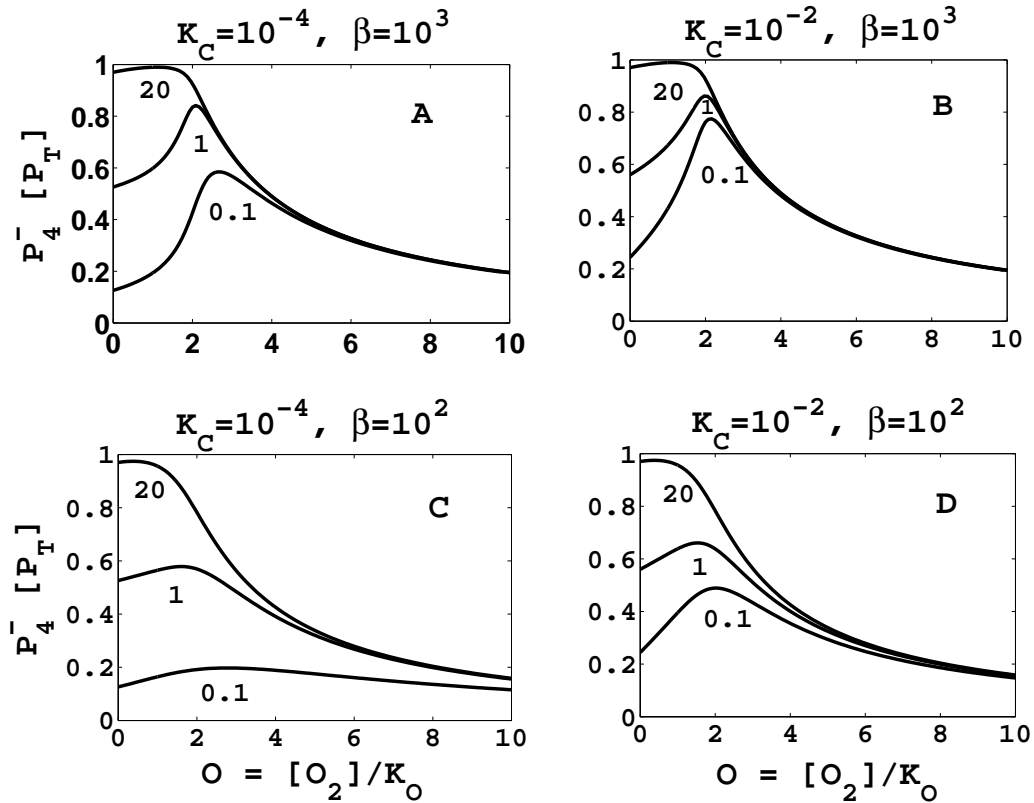


Figure 4.3: *Light-dependent development of the peak in the steady state response curve of reduced PpsR in the extended model (Eqs. 4.12). It shows the steady state response curves of reduced PpsR ( $P_4^-$ ) as functions of the oxygen concentration ( $O$ ) for different values of  $K_c$  and  $\beta$ . The light irradiance  $LI$  in  $\mu\text{mol}/\text{m}^2\text{s}$  is denoted by small numbers. As  $K_c$  increases (from left to right) the maximum of reduced PpsR ( $[P_4^-]$ ) at intermediate oxygen levels ( $O \approx 2$ ) increases under low light conditions ( $LI = 0.1 \mu\text{mol}/\text{m}^2\text{s}$ ). As  $\beta$  decreases (from top to bottom) the maximum of reduced PpsR at intermediate oxygen levels decreases significantly under low light conditions. Used parameters are:  $K_{eq} = \infty$ ,  $\eta = 10^{-2}$ ,  $\lambda = 10^2$ ,  $\delta = 10$ ,  $\alpha = 1$ ,  $\gamma = 2$ .*

and PpsR occurs with higher affinity, the difference between the maxima in the concentration of reduced PpsR gets larger. Second, peak formation is more pronounced when the time scale separation between AppA and PpsR reduction is large ( $\beta = 10^3$ ) although it does not vanish under low light conditions ( $LI = 0.1$ , Figs. 4.3A, 4.3B). In contrast, when  $\beta = 10^2$  (corresponding to an intermediate time scale separation) the response curve of reduced PpsR

still develops a maximum at intermediate oxygen concentrations, but peak formation under low light conditions is significantly suppressed, especially when  $K_c = 10^{-4}$  (Figs. 4.3C, 4.3D).

At present, the response curves in Fig. 4.3 can not be directly compared with experiments since measurements of reduced PpsR under different light conditions are not available. However, under the hypothesis that the specific repression of PS genes under semi-aerobic conditions is associated with the occurrence of a maximum in the response curve of reduced PpsR, we expect the parameters  $\beta$  and  $K_c$  to be constrained by two antagonistic goals: Peak formation, apparently, requires a sufficiently large time scale separation between AppA and PpsR reduction ( $\beta \gg 1$ ). On the other hand, increasing  $\beta$  decreases the difference between the maxima of reduced PpsR under high and low light conditions. As a consequence, the range of PpsR concentrations over which PS gene transcription would have to respond becomes smaller requiring a higher sensitivity of these systems. Therefore, to guarantee a proper functionality of the AppA/PpsR system with respect to both light and redox regulation, we expect  $\beta$  and  $K_c$  to be constrained such that the peak formation at intermediate oxygen levels becomes possible ( $\beta$  sufficiently large) while maintaining a sufficiently large difference of the maximal PpsR concentrations between high and low light conditions ( $\beta$  not ‘too large’ and  $K_c$  sufficiently small).

#### 4.4.4 Repression of PS genes Under Semi-Aerobic Conditions

*In vivo* blue light dependent regulation of PS genes by the AppA/PpsR system under semi-aerobic conditions has been recently investigated by Metz et al. (35, 36). Their studies showed that the most substantial changes in the expression level of the *puc* gene occurred over only one order of magnitude in the range of light irradiance between  $0.1 \mu\text{mol}/\text{m}^2\text{s}$  (no repression) and  $1 \mu\text{mol}/\text{m}^2\text{s}$  (maximal repression). Note that, when *puc* gene repression reached maximal levels the relative repression level was only around 70% indicating a residual transcriptional activity even under high light conditions.

The extended model can reproduce both features of the simple model, the peak formation and bistable response, for the parameter set used in Fig. 4.3A. To compare the response curve of reduced PpsR as a function of the light irradiance (Fig. 4.5 A, solid curve) with experimental measurements of *puc* gene inhibition (Fig. 4.5 B, filled circles) we have assumed that the extent of *puc* inhibition is proportional to the amount of reduced PpsR that is bound to

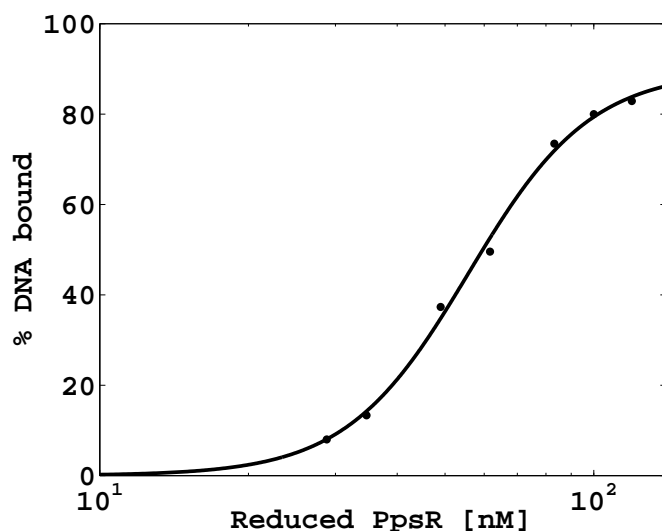


Figure 4.4: Estimation of the effective Hill coefficient from the experimental data of DNA-binding measurements. Black filled circles represent measurements (taken from Masuda and Bauer (22)) of the percentage of reduced PpsR bound to DNA containing the *puc* promoter with the palindromic consensus sequence of PpsR. The solid line represents a non-linear least square fit using a Hill function of the form:  $A \times [PpsR]^n / (EC_{50}^n + [PpsR]^n)$  where  $A = 89.6 \pm 10$ ,  $EC_{50} = (55.8 \pm 6)nM$  and  $n = 3.5 \pm 0.88$ .

DNA. Using the results of DNA-binding experiments by Masuda and Bauer (22) the relationship between *puc* inhibition and the fraction of DNA-bound PpsR ( $x_2 = [P_4^-]/[P_T]$ ) can be described by a simple Hill function of the form (cf. Fig. 4.5 B, dashed line):

$$puc \text{ inhibition} = 100 \frac{x_2^n}{K^n + x_2^n},$$

where  $K = EC_{50}/[P_T]$  and  $n$  denote a relative DNA-binding affinity and an effective Hill coefficient, respectively. The  $EC_{50}$  was found to be  $69 nM$  (22), while the effective Hill coefficient was estimated from DNA-binding measurements as  $n \approx 3.5$  (Fig. 4.4). In Fig. 4.5, no attempt was made to find a set of parameters that fits the experimental data points optimally. The conclusion that can be drawn at this stage is that there exists a biologically reasonable set of parameters which leads to a response curve that is in agreement with experimental measurements.

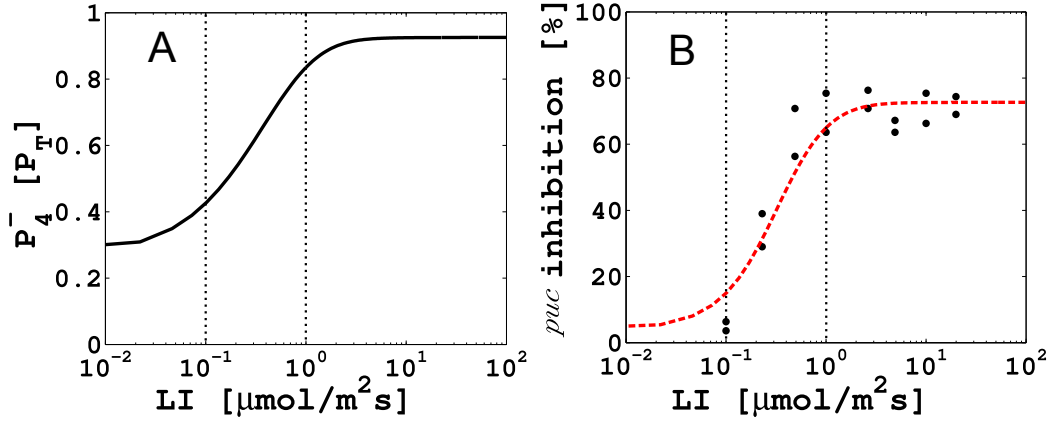


Figure 4.5: The prediction of the extended model for the light response, and comparison with experiments. (A) The response curve of reduced PpsR ( $P_4^-$ ) (solid line) for the parameter set  $K_{eq} = \infty$ ,  $K_c = 10^{-4}$ ,  $\alpha = 1$ ,  $\beta = 10^3$ ,  $\gamma = 2$ ,  $\delta = 10$ ,  $\eta = 10^{-2}$ ,  $\lambda = 10^2$ ,  $O = 2$  (cf. Fig. 4.3 A). (B) The dashed curve denotes the percentage of *puc* gene inhibition as calculated from:  $puc\ inhibition = 100 \times x_2^n / (K^n + x_2^n)$  with  $x_2 = [P_4^-]/[P_T]$  (cf. Table 4.1),  $n = 3.5$  (effective Hill coefficient) and  $K = EC_{50}/[P_T] = 0.7$  where  $EC_{50}$  denotes the concentration for half-maximal saturation. Filled circles represent experimental measurements (2 repetitions) of *puc* inhibition taken from Ref. (36).

To demonstrate how parameter changes affect the shape of the response curve shown in Fig. 4.5 A (solid line) we have generated a set of response curves for different combinations of the parameters  $\delta$ ,  $\lambda$  and  $\eta$  (Figs. 4.6A, 4.6B, 4.6C). Observe that, in general, changing any of these parameters affects the steepness of the response curve and/or the  $LI_{50}$  value, i.e. the light irradiance where half-maximal levels of reduced PpsR are reached. Particularly, increasing the parameter  $\delta = k_c^+[A_T]^2/k_{Ar}$ , which describes the time scale separation between complex formation and AppA reduction, increases the  $LI_{50}$  while leaving the steepness almost unchanged (Fig. 4.6A). However, decreasing  $\delta$  does not only lead to a smaller  $LI_{50}$ , but also significantly decreases the steepness of the response curve. Therefore, we conclude that the time scales for complex formation and AppA reduction have to be appropriately balanced to generate a light response as observed experimentally.

Similar conclusions can be drawn with respect to changes of the parameters  $\lambda = k_d/k_l^-$  and  $\eta = k_l^-/k_{Ar}$ , both of which have a direct effect on light regulation (cf. Eqs. 4.5-4.7). Recall that in Section 4.4.2 we have argued that, due to the small relaxation rate of the AppA signaling state ( $k_l^- \approx 10^{-3}/s$ ), we expect that  $\lambda \gg 1$  and  $\eta \ll 1$ . Increasing the value of  $\eta$

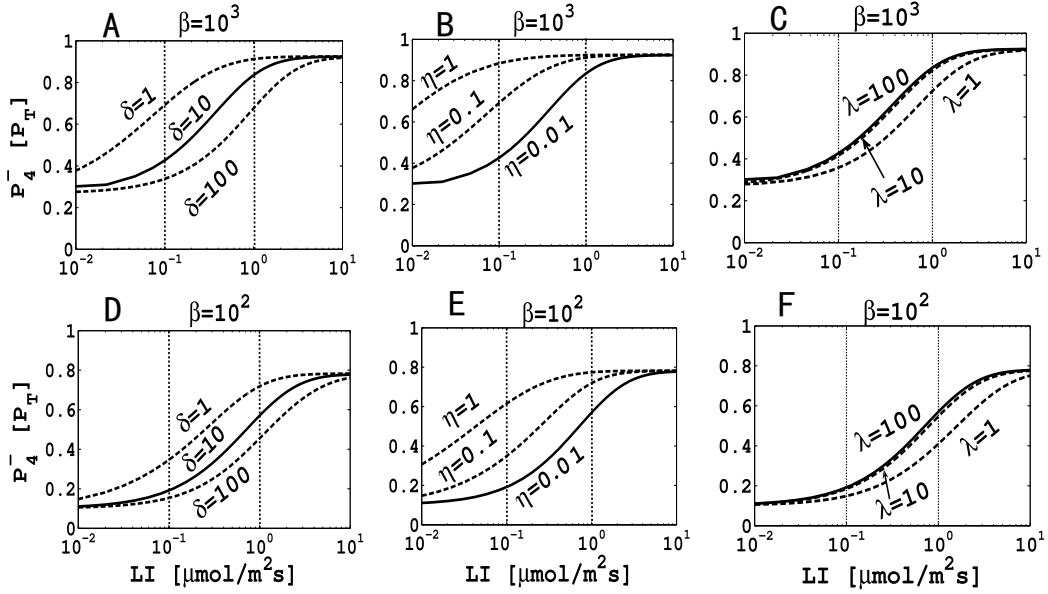


Figure 4.6: A demonstration of how changes in  $\delta$ ,  $\lambda$  and  $\eta$  affect the light response under semi-aerobic conditions ( $O = 2$ ). Solid lines denote the steady state response curves of reduced PpsR ( $P_4^-$ ) as functions of the light irradiance (LI) for  $\beta = 10^3$  (A,B,C) and  $\beta = 10^2$  (D,E,F) for the parameter set used in Fig. 4.5:  $\alpha = 1$ ,  $\gamma = 2$ ,  $\delta = 10$ ,  $\lambda = 10^2$ ,  $\eta = 10^{-2}$ ,  $K_C = 10^{-4}$ ,  $K_{eq} = \infty$ . Dashed lines show how the shape and/or the position of the reference response curve would be affected by changing independently one of the parameters  $\delta$  (A,D),  $\eta$  (B,E) or  $\lambda$  (C,F) as indicated. Dotted lines mark the region of light irradiance over which repression of the *puc* gene changes from its minimal value ( $LI = 0.1 \mu\text{mol}/\text{m}^2\text{s}$ ) to its maximal value ( $LI = 1 \mu\text{mol}/\text{m}^2\text{s}$ ) as observed experimentally (35, 36).

significantly affects the steepness of the response curve as well as the  $LI_{50}$ , both of which are lowered (Fig. 4.6 B). In contrast, a 10-fold decrease of  $\lambda$  to a value of 10 has virtually no effect on the response curve (Fig. 4.6 C). We see a modest increase in the  $LI_{50}$  only when the relaxation rate  $k_l^-$  becomes comparable with the dissociation rate of AppA-PpsR complexes ( $\lambda = 1$ ). Briefly, these results suggest that a proper response to light signals in the experimentally observed range requires a clear time scale separation between redox- and light-dependent processes ( $\eta \ll 1$ ) while the precise value of  $\lambda$  seems to be less important as long as  $\lambda \geq 1$ .

Notice that the conclusions drawn in this Section are independent of the particular value of  $\beta$  which only causes a ‘vertical’ shift of the response curves

while the effect of  $\delta$ ,  $\lambda$  and  $\eta$  on the response behaviour remains qualitatively same (Figs. 4.6D, 4.6E, 4.6F). These results all together indicate that the qualitative behaviour of the system remains robust within an extended region of the parameter space.

#### 4.4.5 Role of $\gamma$ on the Peak-Position and Bistability

In Chapter 3 and Ref. (53), it has been shown that the ratio between total copy numbers of AppA and PpsR ( $\gamma = [A_T]/[P_T]$ ) does not only determine how many PpsR molecules can be sequestered by AppA under anaerobic conditions, but also whether or not bistability is possible. In fact, in Chapter 3 it has been shown that an efficient sequestration requires  $\gamma \geq 2$  while bistability can occur for  $\alpha O > \gamma > 2$ .

The extended model shows that  $\gamma$  also affects the position of the maximum in the steady state response curve of reduced PpsR (Fig. 4.7). Particularly, for  $\gamma = 1$  the maximum occurs at a fixed oxygen concentration which depends on the parameter  $\alpha = k_{Po}/k_{Ao}$ , but not on the light irradiance (Figs. 4.7A, 4.7B). In contrast, as  $\gamma$  is increased the position of the PpsR maximum is shifted towards larger oxygen concentrations and a bistable response becomes possible (Figs. 4.7C, 4.7D). This result suggests that if a well-defined semi-aerobic regime is to exist (i.e. light-dependent peak formation occurs in a narrow region of oxygen concentrations) then there should exist a stoichiometric constraint for the ratio between total amounts of AppA and PpsR ( $\gamma = [A_T]/[P_T]$  must not become too large). As PpsR expression levels ( $[P_T]$ ) were found to be largely independent of the growth conditions (29) therefore this means that AppA expression levels ( $[A_T]$ ) would have to be regulated in such a way that  $\gamma \leq 2$  (Fig. 4.3). This indicates that  $\gamma \approx 2$  might be an optimal value in the sense that it allows for an efficient sequestration of PpsR while minimizing the light-dependent shift of the semi-aerobic regime (Fig. 4.7).

We observed that the occurrence of bistability is restricted to low light conditions ( $I \leq 1$  corresponding to  $LI \leq 1 \mu\text{mol}/\text{m}^2\text{s}$ ) and intermediate oxygen levels (Fig. 4.8A). Like the model in Chapter 3 and Ref. (53), the existence of bistability seems to require that  $\alpha$  and  $\beta$  assume sufficiently large values (Figs. 4.8B, 4.8C), which implies that there must be a sufficiently large time scale separation between processes that modulate the redox states of AppA and PpsR. Contrary to that, the requirements for the parameters  $\lambda$  and  $\eta$ , both of which have a direct effect on light regulation, seem to be much less stringent. In fact, both parameters can vary over several orders of magnitude within a broad band without leaving the bistability region (Fig. 4.8D). Although a bistable response is, as yet, not experimentally validated in the

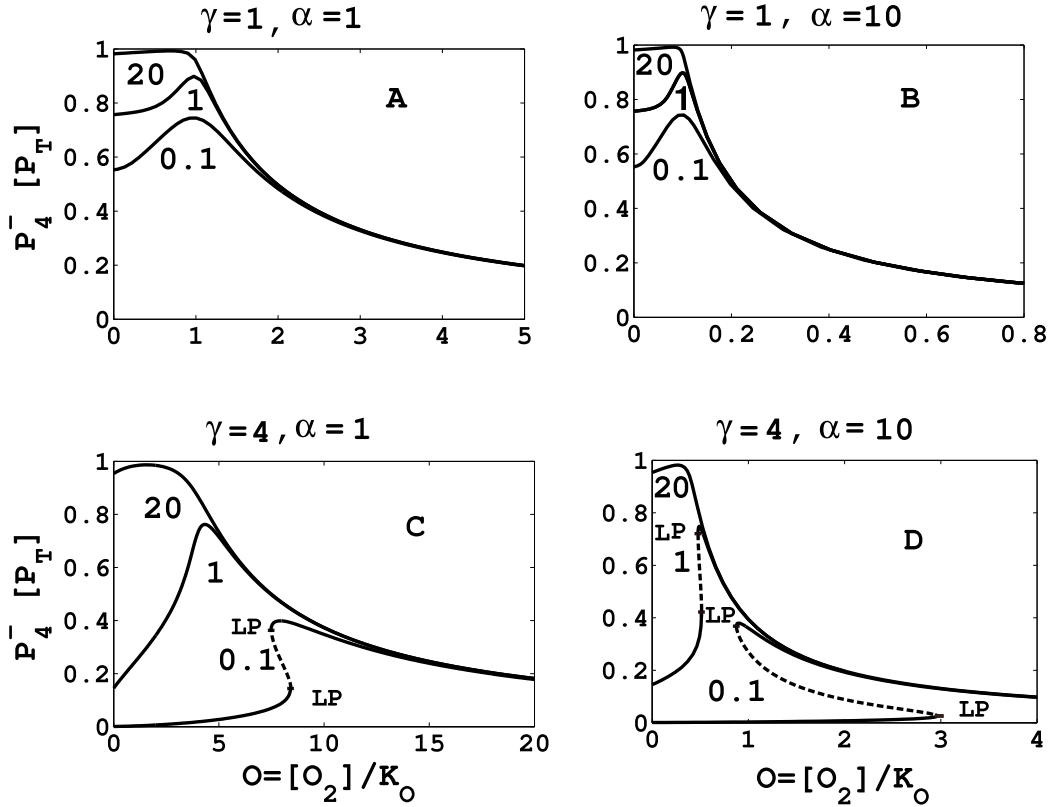


Figure 4.7: Shift of the peak position (light,  $\alpha$  and  $\gamma$  dependent) and bistability (light and  $\alpha$  dependent). Shown are the steady state curves of reduced PpsR ( $P_4^-$ ) as functions of the oxygen concentration ( $O$ ) for different combinations of  $\alpha = k_{P_O}/k_{A_O}$  and  $\gamma = [A_T]/[P_T]$ . The light irradiance  $LI$  in  $\mu\text{mol}/\text{m}^2\text{s}$  is denoted by small numbers. (A and B) If  $\gamma = 1$ , the maximum of reduced PpsR at intermediate oxygen levels occurs at a fixed oxygen concentration which depends on the value of  $\alpha$ . (C and D) When  $\gamma$  is increased, the position of the maximum is shifted towards larger oxygen concentrations in a light-dependent manner, and the response becomes bistable. In the region between the two limit points (LP), two stable steady states (solid lines) coexist with one unstable steady state (dashed line). Other used parameters are:  $K_{eq} = \infty$ ,  $K_c = 10^{-4}$ ,  $\beta = 10^3$ ,  $\eta = 10^{-2}$ ,  $\lambda = 10^2$ ,  $\delta = 10$ .

AppA/PpsR system, our results suggest that a straightforward way to test this possibility would be to overexpress AppA by providing some extra copies of the *appA* gene (29). Notice that an increase of the total AppA concentration ( $A_T$ ) would lead to an increase in the parameters  $\beta$ ,  $\gamma$  and  $\delta$  (cf. Table 4.1). As it is clear from Fig. 4.8, the region of bistability increases

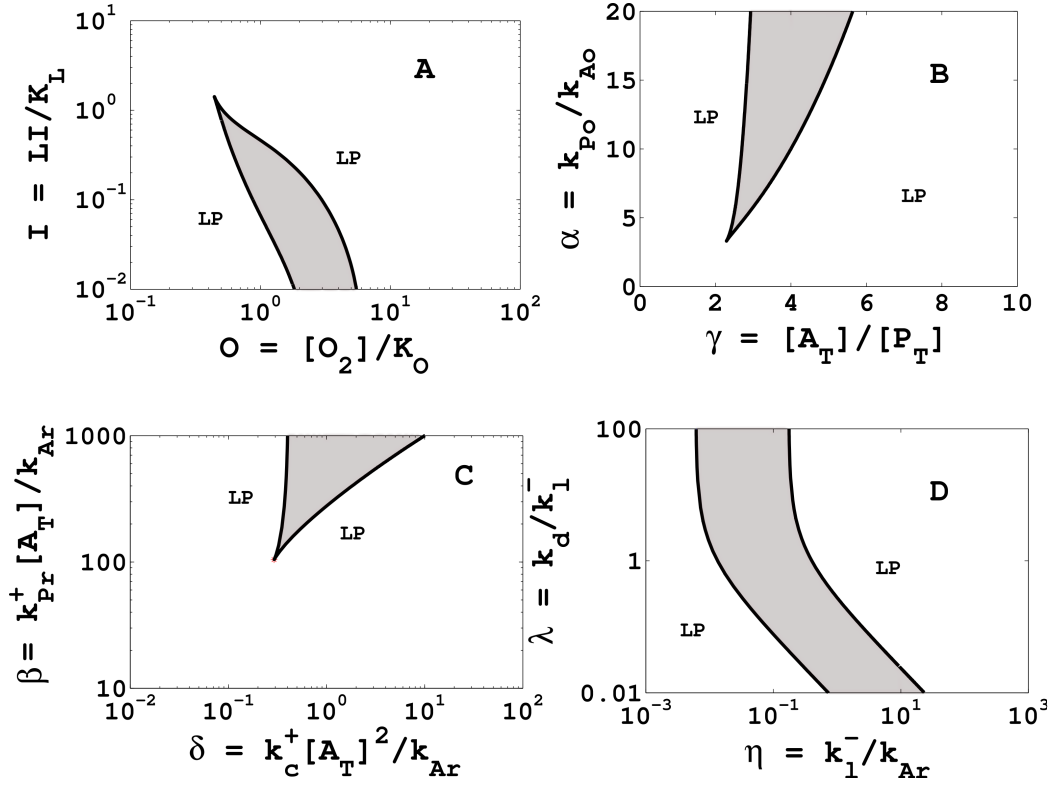


Figure 4.8: Regions of bistability (gray-shaded regions) projected on different two-parameter planes. In the gray-shaded regions two stable steady states coexist with one unstable steady state. These regions are bounded by two limit points (LP). Used parameters other than shown in the respective panel have the values:  $K_{eq} = \infty$ ,  $K_c = 10^{-4}$ ,  $\alpha = 10$ ,  $\beta = 10^3$ ,  $\gamma = 4$ ,  $\delta = 10$ ,  $\eta = 10^{-2}$ ,  $\lambda = 10^2$ ,  $O = 1$ ,  $I = 0.1$ .

as these parameters become larger, hence, increasing  $A_T$  should facilitate the observability of a bistable response. It is advantageous to perform such experiments with a PrrB knock-out strain to prevent interference with the PrrB/PrrA two-component system, which specifically induces PS gene expression under anaerobic conditions (7). A heterogeneous response in the expression level of PS genes could be an advantageous survival strategy for a population of photosynthetic bacteria to cope with fluctuations in oxygen and light availability, especially under semi-aerobic and low light conditions.

#### 4.4.6 Role of $K_{eq}$ for the Peak of Reduced PpsR

The peak formation at intermediate oxygen levels is completely suppressed as the equilibrium constant  $K_{eq}$  for the electron transfer between AppA and PpsR (Eq. 4.3) approaches 1 (Fig. 4.9). A similar result is obtained for the simple model in Chapter 3. Thereby, we expect that, *in vivo*,  $K_{eq}$  is sufficiently large ( $K_{eq} \gg 10$ ) which is in agreement with the experimental observation by Masuda and Bauer according to which this electron transfer is effectively irreversible (22).

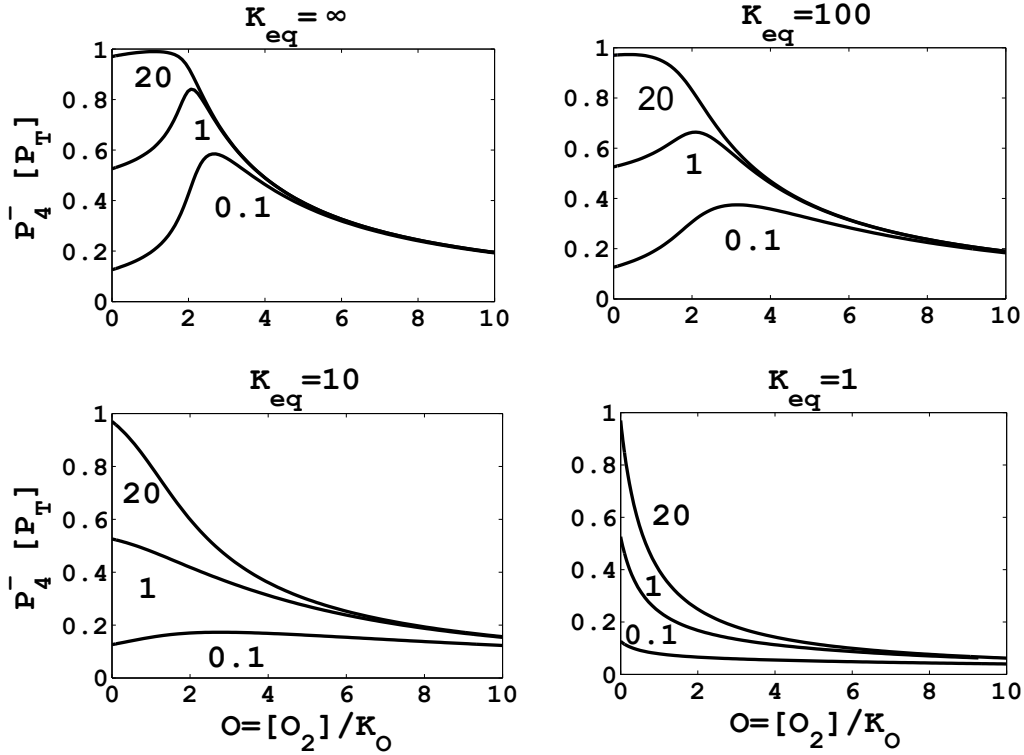


Figure 4.9: A demonstration of how the reversibility of the electron transfer from AppA to PpsR (Eq. 4.3) affects the formation of the peak in the steady state response curve of PpsR. As shown, when the equilibrium constant  $K_{eq}$  approaches unity the maximum in the concentration of reduced PpsR ( $P_4^-$ ) at intermediate oxygen concentrations ( $O \approx 2$ ) vanishes. Numbers denote light irradiance  $LI$  in  $\mu\text{mol}/\text{m}^2\text{s}$ . Parameters are the same as in Fig. 4.3A:  $K_c = 10^{-4}$ ,  $\alpha = 1$ ,  $\beta = 10^3$ ,  $\gamma = 2$ ,  $\delta = 10$ ,  $\eta = 10^{-2}$ ,  $\lambda = 10^2$ .

### 4.4.7 Light Response Curve of an AppA Mutant

A central role of several amino acid residues (Gln63, Trp104 and Tyr21) in the FAD binding site of the AppA protein for a proper functioning of its photocycle has been shown by *in vitro* studies (55–57). More specifically, it has been suggested that tryptophan 104 is involved in mediating light-induced structural changes in the AppA protein (32, 33). A recent experimental study showed that a base exchange from tryptophan 104 to phenylalanine yields an AppA protein (W104F) with substantially lowered (10 to 20-fold) blue-light sensitivity under semi-aerobic conditions (36), i.e. the required light irradiance for maximal inhibition of the *puc* gene is increased 10 to 20-fold (Fig. 4.10B, red circles). Metz et al. (36) suggested that this change in blue-light sensitivity would be attributed to a 10-fold increase of the thermal recovery rate of the AppA signaling state.

The thermal recovery rate is represented by  $k_l^-$  in the present model, and a 10-fold increase in this parameter will cause a change in the value of 3 dimensionless parameters ( $K_L$ ,  $\eta$  and  $\lambda$ ; cf. Table 4.1) relative to the parameter values that were used to model the wild type (WT) strain (Fig. 4.10, black lines). Particularly,  $K_L$  and  $\eta$  will be 10-fold larger compared to the values used for the WT strain while  $\lambda$  will be 10-fold lower. If we use the new parameter values we find, indeed, a shift of the WT response curve (Fig. 4.10, black lines) towards higher light irradiance (Fig. 4.10, blue lines) in agreement with a lower sensitivity. Nevertheless, the shift is far less pronounced as the shift observed in experiments (Fig. 4.10B red circles). To achieve better agreement with the experimentally observed shift in the light response curve, we had to take into account that the W104F AppA protein also exhibits a lowered ability to release PpsR when bound in a complex with AppA (36). In the model, we can account for this effect by increasing the association rate between AppA and PpsR or lowering the dissociation rate of the AppA-PpsR complex ( $k_d$ ) or both. A good agreement of the light response curve obtained by simulation with the experimentally observed curve was obtained by a simultaneous decrease (increase) of  $k_d$  ( $k_c^+$ ) by a factor of 10 (Fig. 4.10, red lines), which suggests that the base exchange from tryptophan 104 to phenylalanine does not only affect the thermal recovery rate of AppA, but also the interaction strength between AppA and PpsR.

## 4.5 Discussion and Summary

In this Chapter an extended model for the oxygen- and light-dependent interaction between AppA and PpsR proteins has been proposed and the steady

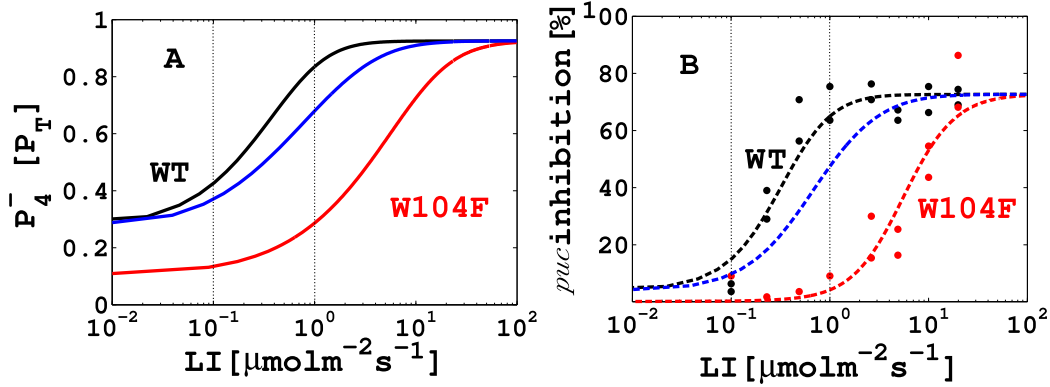


Figure 4.10: *Response curves of the AppA W104F mutant strain to changes in light irradiance, and comparison of the model predictions (light response curves) with experiments (36). (A) Shown are the steady state response curves of reduced PpsR ( $P_4^-$ ) for different parameter sets. Black line:  $K_L = 1$ ,  $K_c = 10^{-4}$ ,  $\delta = 10$ ,  $\eta = 10^{-2}$ ,  $\lambda = 10^2$  (cf. Fig. 4.5), blue line:  $K_L = 10$ ,  $K_c = 10^{-4}$ ,  $\delta = 10$ ,  $\eta = 0.1$ ,  $\lambda = 10$  corresponding to a 10-fold increase of the thermal recovery rate  $k_l^-$  and red line:  $K_L = 10$ ,  $K_c = 10^{-5}$ ,  $\delta = 100$ ,  $\eta = 0.1$ ,  $\lambda = 1$  corresponding to a 10-fold increase of  $k_l^-$  and  $k_c^+$ , and a 10-fold decrease of  $k_d$ . Other used parameters are:  $\alpha = 1$ ,  $\beta = 10^3$ ,  $\gamma = 2$ ,  $K_{eq} = \infty$ ,  $O = 2$ . (B) Filled circles are experimental measurements of *puc* inhibition (taken from Ref. (36)): black circles (wild-type), red circles (W104F). Dashed lines represent the percentage of *puc* gene inhibition that was calculated using the corresponding curve from panel A:  $puc\ inhibition = 100 \times x_2^n / (K^n + x_2^n)$  with  $x_2 = [P_4^-]/[P_T]$ ,  $K = 0.7$  and  $n = 3.5$  (cf. Fig. 4.5). Dotted lines indicate the range of light irradiance over which *puc* inhibition changes from its minimal to its maximal level in the wild-type strain.*

state behaviour of the extended model has been analysed. These proteins (AppA and PpsR) are part of a signal transduction system, which is specifically involved in the regulation of photosynthesis genes in the facultative photosynthetic bacterium *Rhodobacter sphaeroides*. This model is based on our simple model (Chapter 3), and in it a detailed mechanism for the light-dependent interactions between AppA and PpsR is incorporated, as proposed by Han et al. (5). In contrast with the PrrB/PrrA system, which is involved in PS gene induction under anaerobic conditions (17, 31), the AppA/PpsR system does not represent a standard two-component system (58), though it also consists of a sensory protein (AppA) that modulates the activity of an associated effector protein (PpsR) in response to environmental signals. Due

to the presence of the AppA protein, which integrates both blue light and redox signals, the *R. sphaeroides* bacterium exhibits a specific phenotype at intermediate oxygen levels, where PS genes are repressed by sufficiently strong blue light illumination (28, 35, 59). This phenotype seems to be unique to *R. sphaeroides* (6), as an AppA-homolog does not seem to exist in other purple bacteria.

The potential kinetic and stoichiometric requirements for the regulatory processes between AppA and PpsR, that could explain the emergence of such phenotype, are analysed with the help of mathematical modeling. It is shown that, using biologically plausible parameter values, the model predictions can be brought in congruence with experimental measurements of light-dependent PS gene repression under semi-aerobic conditions. Additionally, the model can qualitatively account for the reduced light sensitivity observed in an AppA mutant strain (36). Simulation results suggest that the specific light-dependent repression of PS genes under semi-aerobic conditions is caused by two time scale separations in the AppA/PpsR interaction network: The first time scale separation arises when the rate of PpsR reduction is much larger than that of AppA (i.e if  $\beta$  is sufficiently large). As a result, the steady state curve for reduced PpsR exhibits a pronounced maximum at intermediate oxygen levels and the height of this maximum decreases in a light-dependent manner (Fig. 4.3). We expect  $\beta$  to lie in the range between 100 and 1000, depending on the sensitivity of signal transduction systems downstream of PpsR. The second time scale separation arises from the fact that the AppA signaling state has a comparably long half-life of approximately 15 minutes (22, 36). Our simulation results indicate that, in order to ensure a proper response to light signals under semi-aerobic conditions (Fig. 4.5, Fig. 4.6) the corresponding relaxation rate ( $k_l^-$ ) has to be much smaller than the rate of AppA reduction ( $k_{Ar}$ ).

Further, our simulation results suggest that constraining the ratio between total amounts of AppA and PpsR ( $\gamma = [A_T]/[P_T]$ ), to the range between 1 and 2 could help to prevent the occurrence of a significant light-dependent shift of the semi-aerobic regime (Fig. 4.7) while still allowing for an efficient sequestration of PpsR by AppA. However, this constrain for  $\gamma$  would preclude the possibility of a bistable response (Fig. 4.8). We suggest that a simple way to induce or favor a bistable response is to increase the total concentration of AppA relative to that of PpsR, e.g. by overexpressing the *appA* gene.

# Chapter 5

## Conclusions and Outlook

In *Rhodobacter sphaeroides*, the AppA/PpsR signal transduction system is part of the switching mechanism for the generation of energy from photosynthesis to respiration, and vice versa, as a response to changing oxygen levels and light conditions. The molecular mechanism underlying this switching behaviour is theoretically poorly understood, yet. It is also unclear why these bacteria use the additional protein AppA along with PpsR compared to simple systems like CrtJ in *Rhodobacter capsulatus* (the closest purple bacteria to *R. sphaeroides*).

In a broader context, we were addressing the question, how photosynthetic bacteria sense, integrate and respond adequately to oxygen and light signals. We tried to find out what are the extra features and regulatory capabilities the AppA/PpsR system of *R. sphaeroides* has, due to the presence of additional protein AppA, which other purple bacteria such as *R. capsulatus* do not have. Another aim was to explain how the light and redox-dependent interaction between AppA and PpsR leads to the PS gene repression under semi-aerobic conditions under high blue light irradiance ( $LI \approx 20 \mu\text{molm}^{-2}\text{s}^{-1}$ ).

To obtain a better quantitative understanding of the regulatory features of the AppA/PpsR system, we first developed a simple mathematical model of the AppA/PpsR system taking into account mainly redox regulation, which is the first mathematical model for this system (discussed in Chapter 3). Subsequently, we extended the simple model by incorporating a more detailed light regulation of the interaction between AppA and PpsR (discussed in Chapter 4), as in the simple model we modeled the light regulation only in an effective manner. We then employed well established techniques from nonlinear dynamics to analyse the model equations, and to explore the steady state behaviour of the system.

With the help of the steady state analysis, we successfully explained the

potential kinetic and stoichiometric requirements for the regulatory processes between AppA and PpsR that could result in the emergence of the phenotype in which PS genes are repressed under blue light illumination at intermediate oxygen levels. We suggested that a peak formation in the steady state response curve of reduced PpsR could account for this phenotype. The peak formation is caused by two time scale separations in the AppA/PpsR interaction network. The first time scale separation arises when the rate of reduction of PpsR is much larger than that of AppA (i.e. if  $\beta$  is sufficiently large). The second time scale separation originates due to the fact that the AppA signaling state has a comparably long half-life of approximately 15 minutes (22, 36). Our results suggest that the corresponding relaxation rate ( $k_l^-$ ) has to be much smaller than the rate of AppA reduction ( $k_{Ar}$ ) to ensure a proper response to light signals under semi-aerobic conditions (Fig. 4.5, Fig. 4.6). The peak formation also requires that the electron transfer from AppA to PpsR should be effectively irreversible. Also, the extended model can qualitatively account for the observed lowered light sensitivity in an AppA mutant strain (36).

In addition, we found that the network structure of the AppA/PpsR system is such that it can potentially exhibit bistable behaviour, which would lead to a hysteretic switch-like induction of PS genes as a response to changing redox conditions in the environment (Fig. 3.8). For the simple model discussed in Chapter 3, we provided necessary conditions for bistability which can be summarized as follows: The rate of reduction of PpsR should be larger than that of AppA ( $\beta \gg 1$ ), and the total amounts of AppA proteins should be larger than that of PpsR by at least a factor of 2 ( $\gamma > 2$ ). Bistability also requires that PpsR should be efficiently sequestered by AppA molecules (i.e.  $\gamma > 2$ ). However, the extended model discussed in Chapter 4 suggests that the ratio between the total amounts of AppA and PpsR ( $\gamma$ ) should lie in the range 1, . . . , 2 to prevent the occurrence of a significant light-dependent shift of the semi-aerobic regime (Fig. 4.7) as well as to allow an efficient sequestration of PpsR molecules by AppA. Therefore, it seems that most likely  $\gamma \approx 2$ .

A necessary condition for a reaction network to exhibit bistability is the presence of a sufficiently strong positive feedback mechanism (39). We found that the light-dependent complex formation between AppA and PpsR can provide an implicit positive feedback loop, which can lead to a bistable response as a result of changing light and oxygen conditions. Bistability is not a new phenomenon in biology. It has been observed and thoroughly investigated in artificial gene circuits (39, 60), natural signal transduction systems (39, 48), and in other biological systems such as, sugar uptake system of *Escherichia coli* using single cell measurements (43, 44). We suggest that

a simple way to induce or favor a bistable response in *R. sphaeroides* is to increase the copy number of the AppA protein relative to that of PpsR.

As an extension of the present work, we suggest to perform single cell measurements of PS gene expression in a *prpB* and *prpA* mutant strain of *R. sphaeroides* to test for bistability in the AppA/PpsR system. The *prpB* and *prpA* mutant strain should be used to avoid interference of the PrrB/PrrA system with the AppA/PpsR system. In the bistable region, which is predicted to occur under semi-aerobic conditions, we expect a heterogeneous population of *R. sphaeroides* bacteria. It means, in a transition from anaerobic to aerobic conditions one should observe a regime under semi-aerobic conditions in which a fraction of the population of bacteria are performing photosynthesis whereas the rest of the bacteria have already started generating energy via respiration.

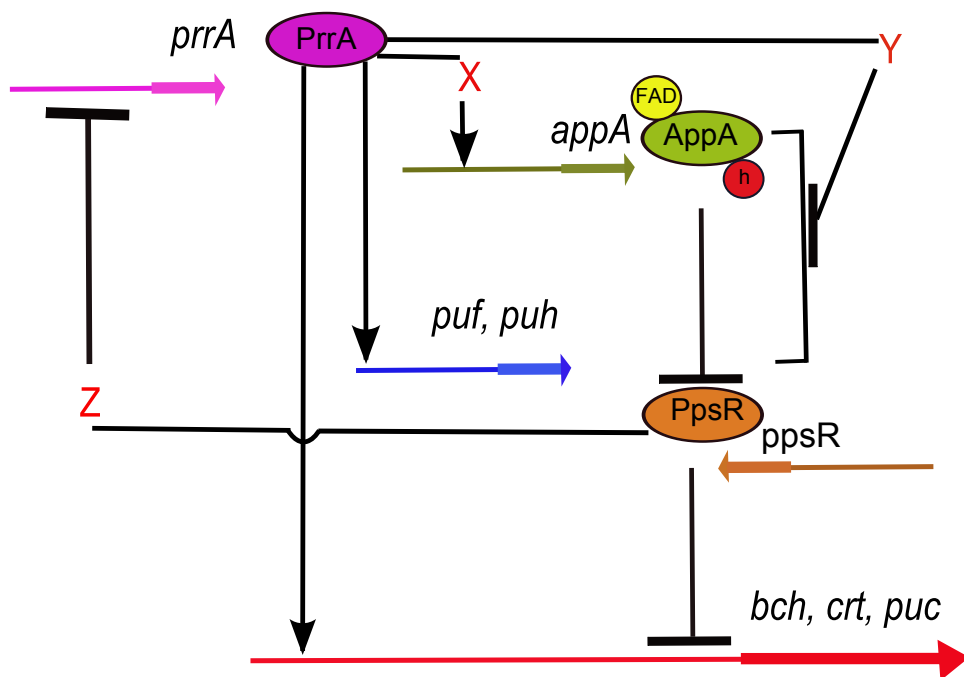


Figure 5.1: A scheme for the coupling between the AppA/PpsR and the PrrB/PrrA system (proposed by Gomelsky et. al (11)). Thick arrows represent regulatory genes (*prpA*, *appA*, *ppsR*), or PS genes/operons (*bch*, *crt*, *puc*, *puf*, and *puh*). Thin arrows denote activating interactions, and arrows with a bar end represent the inhibitory interactions. X, Y, and Z are putative, as they are, yet, unidentified regulatory components.

Another interesting extension of the present model would be to model

the regulatory pathways via which the AppA/PpsR system (that represses PS genes under aerobic conditions) interacts with PrrB/PrrA system (that activates the PS genes under anaerobic conditions) as they do not work independently of each other; rather a hierarchical relationship is found between them (11). In this hierarchy, the PrrB/PrrA system is positioned above the AppA/PpsR system (Fig. 5.1), and the PrrB/PrrA system exerts its dominance over the AppA/PpsR system at two levels: One level of dominance involves transcriptional regulation of *appA* gene expression (encoding AppA) by PrrA via a, yet, unidentified regulatory component (X in Fig. 5.1). The second level of dominance involves the post-transcriptional level control of AppA and/or PpsR activity by the PrrB/PrrA system via another unknown regulatory component (Y in Fig. 5.1). In addition, the AppA/PpsR system exhibits a feedback regulation on the PrrB/PrrA system but the mechanism remains unclear (Z in Fig. 5.1). Therefore, it would be interesting to characterize the three unknown regulatory components X, Y, and Z (Fig. 5.1). If more experimental data become available, one could modify the present model accordingly. The present model will start the iterating process of experiment and model validation.

*This page is intentionally left blank*

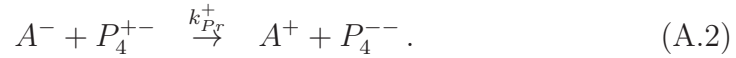
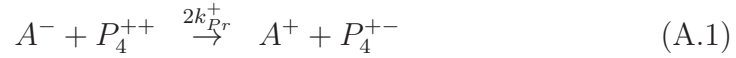
*This page is intentionally left blank*

# Appendix A

## Reduction of PpsR with a 2:1 Stoichiometry

In Section 3.1.1, a 1:1 stoichiometry is assumed in Eq. 3.1 to model the reduction of oxidized PpsR by reduced AppA. Here, we show that considering a 2:1, instead of 1:1 stoichiometry does neither alter our conclusion about the possibility of bistability in the AppA/PpsR system nor the non-monotonic dependence of reduced PpsR as a function of the oxygen concentration under sufficiently high light conditions.

In place of Eq. 3.1, we now consider the following reaction mechanism



Here, we have assumed that the electron transfer from reduced AppA to oxidized PpsR proceeds in an effectively irreversible manner, which is consistent with the observation of Masuda and Bauer (22). Additionally, it is assumed that two (instead of one) encounters between AppA and PpsR are required to achieve a full reduction of a PpsR tetramer. In this case, PpsR tetramers can exist in three forms instead of two. The fully oxidized and reduced forms of PpsR are denoted as  $P_4^{++}$  and  $P_4^{--}$ , respectively, while the partially oxidized (or reduced) form is denoted as  $P_4^{+-}$ . For the sake of simplicity, we consider the two PpsR dimer subunits as indistinguishable, hence  $P_4^{+-} \equiv P_4^{-+}$ . The combinatorial factor of 2 in Eq. (A.1) accounts for the fact that, during the first encounter, AppA can reduce either of the two PpsR dimer subunits. Replacement of Eq. 3.1 with Eqs. A.1 and A.2 leads to the following ODE

system

$$\begin{aligned}
 \frac{d}{dt} [A^-] &= k_{Ar} [A^+] - k_{Ao} [O_2] [A^-] - 2k_{Pr}^+ [A^-] [P_4^{++}] \\
 &\quad - k_{Pr}^+ [A^-] [P_4^{+-}] - 2 \left( \frac{k_c^+}{LI^2} [A^-]^2 [P_4^{--}] - k_c^- [AP_2]^2 \right) \\
 \frac{d}{dt} [P_4^{--}] &= -k_{Po} [O_2] [P_4^{--}] + k_{Pr}^+ [A^-] [P_4^{+-}] \\
 &\quad - \left( \frac{k_c^+}{LI^2} [A^-]^2 [P_4^{--}] - k_c^- [AP_2]^2 \right) \\
 \frac{d}{dt} [P_4^{+-}] &= 2k_{Pr}^+ [A^-] [P_4^{++}] - k_{Pr}^+ [A^-] [P_4^{+-}] \\
 \frac{d}{dt} [AP_2] &= 2 \left( \frac{k_c^+}{LI^2} [A^-]^2 [P_4^{--}] - k_c^- [AP_2]^2 \right)
 \end{aligned} \tag{A.3}$$

together with the conservation relations

$$\begin{aligned}
 A_T &= [A^+] + [A^-] + [AP_2] \\
 P_T &= [P_4^{++}] + [P_4^{--}] + [P_4^{+-}] + \frac{1}{2} [AP_2].
 \end{aligned}$$

In Eq. A.3, we have assumed that only the fully reduced form of PpsR ( $P_4^{--}$ ) is capable of forming a complex ( $AP_2$ ) with reduced AppA.

If we measure concentrations in terms of the total protein concentrations as

$$\begin{aligned}
 x_1 &= \frac{[A^-]}{[A_T]}, & x_2 &= \frac{[P_4^{--}]}{[P_T]}, & x_3 &= \frac{[AP_2]}{[P_T]} \\
 x_4 &= \frac{[P_4^{++}]}{[P_T]}, & x_5 &= \frac{[A^+] + [AP_2]}{[A_T]}, & x_6 &= \frac{[P_4^{+-}]}{[P_T]}
 \end{aligned} \tag{A.4}$$

the ODE system in Eq. A.3 becomes

$$\begin{aligned}
 \frac{d}{d\tau} x_1 &= 1 - x_1(1 + O) - \frac{x_3}{\gamma} - \frac{2\delta}{\gamma} \left( x_1^2 x_2 - I^2 \frac{x_3^2}{\gamma^2} \right) \\
 &\quad - \frac{\beta}{\gamma} x_1 \left[ 2 \left( 1 - x_2 - x_6 - \frac{x_3}{2} \right) + x_6 \right] \\
 \frac{d}{d\tau} x_2 &= \beta x_1 x_6 - \alpha O x_2 - \delta \left( x_1^2 x_2 - I^2 \frac{x_3^2}{\gamma^2} \right) \\
 \frac{d}{d\tau} x_3 &= 2\delta \left( x_1^2 x_2 - I^2 \frac{x_3^2}{\gamma^2} \right) \\
 \frac{d}{d\tau} x_6 &= \beta x_1 \left[ 2 \left( 1 - x_2 - x_6 - \frac{x_3}{2} \right) - x_6 \right]
 \end{aligned} \tag{A.5}$$

where time ( $\tau$ ) is measured in units of  $1/k_{Ar}$  and the dimensionless parameters  $\alpha$ ,  $\beta$ ,  $\gamma$ ,  $I$ ,  $O$  and  $K_{eq}$  are defined in the table A.1.

Table A.1: **Definition of the parameters in Eqs. A.5.**

$$\begin{array}{l} \alpha = \frac{k_{Po}}{k_{Ao}} \quad \beta = \frac{k_{Pr}^+[A_T]}{k_{Ar}} \quad \gamma = \frac{[A_T]}{[P_T]} \quad \delta = \frac{k_c^+ [A_T]^2}{LI^2 k_{Ar}} \quad K_{eq} = \frac{k_{Pr}^+}{k_{Pr}^-} \\ O = \frac{[O_2]}{K_O} \quad I = \frac{LI}{K_L} \quad K_O = \frac{k_{Ar}}{k_{Ao}} \quad K_L = \left( \frac{k_c^+ P_T}{k_c^-} \right)^{1/2} \end{array}$$

$A_T$  and  $P_T$  denote the total amounts of AppA and PpsR, respectively.

From Figures A.1 and A.2, it is apparent that both qualitative features of the simple model (3.12), namely peak formation in the steady state response curve and emergence of bistability, are still present in the model defined by Eqs. A.5 where two encounters between AppA molecules and one PpsR tetramer are required to achieve a full reduction of PpsR. The main difference compared to our simple model is that the fraction of fully oxidized PpsR ( $P_4^{++}$ ) is now markedly lowered, because a significant fraction of PpsR remains partially oxidized ( $P_4^{+-}$ ). Indeed, a closer analysis shows (see Subsection A.1) that both forms occur in steady state in a ratio of 2:1 ( $P_4^{+-} : P_4^{++}$ ).

## A.1 Quasi-Steady State Approximation

Under the assumption that the redox reactions in Eqs. A.1 and A.2 are much faster than any other processes in the system, we can assume that the partially reduced state reaches a quasi-steady state characterized by

$$\frac{d}{dt} [P_4^{+-}] \approx 0$$

which results in

$$\begin{aligned} [P_4^{+-}] &\approx 2 [P_4^{++}] \\ &= 2 \left( P_T - [P_4^{--}] - [P_4^{+-}] - \frac{1}{2} [AP_2] \right) \end{aligned}$$

or

$$[P_4^{+-}]_{qs} \approx \frac{2}{3} \left( P_T - [P_4^{--}] - \frac{1}{2} [AP_2] \right).$$

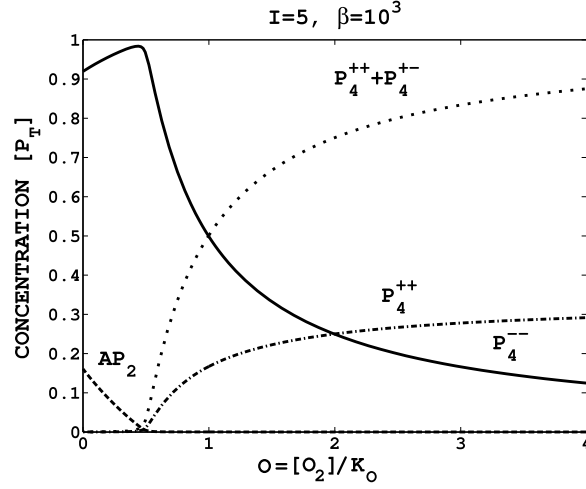


Figure A.1: *Steady state behaviour of Eqs. A.5. As in Fig. 3.3 for the simple model (Eq. 3.12), a peak develops in the steady state response curve of reduced PpsR ( $P_4^-$ ) at intermediate oxygen concentrations. Used parameters are:  $\alpha = 1 = \gamma$ ,  $\beta = 10^3$  and  $I = LI/K_L = 5$ . Note that the curves for  $AP_2$  and  $P_4^{--}$  are similar to those of Fig. 3.3D.*

Using this expression for  $P_4^{+-}$  in the ODE system in Eqs. A.3 results in

$$\begin{aligned}
 \frac{d}{dt} [A^-] &= k_{Ar} [A^+] - k_{Ao} [O_2] [A^-] - 2k'_{Pr} [A^-] [P_4^{++}] \\
 &\quad - 2 \left( \frac{k_c^+}{LI^2} [A^-]^2 [P_4^{--}] - k_c^- [AP_2]^2 \right) \\
 \frac{d}{dt} [P_4^{--}] &= -k_{Po} [O_2] [P_4^-] + k'_{Pr} [A^-] [P_4^{++}] \\
 &\quad - 2 \left( \frac{k_c^+}{LI^2} [A^-]^2 [P_4^{--}] - k_c^- [AP_2]^2 \right) \\
 \frac{d}{dt} [AP_2] &= 2 \left( \frac{k_c^+}{LI^2} [A^-]^2 [P_4^{--}] - k_c^- [AP_2]^2 \right)
 \end{aligned} \tag{A.6}$$

where

$$\begin{aligned}
 [P_4^{++}] &= P_T - [P_4^{--}] - [P_4^{+-}]_{qs} - \frac{1}{2} [AP_2] \\
 &= \frac{1}{3} \left( P_T - [P_4^{--}] - \frac{1}{2} [AP_2] \right).
 \end{aligned}$$

Note that Eqs. A.6 are almost identical to Eqs. 3.9. The combinatorial factor of 2 has been absorbed into the rate constant  $k'_{Pr}$  in Eqs. 3.9 leading to the

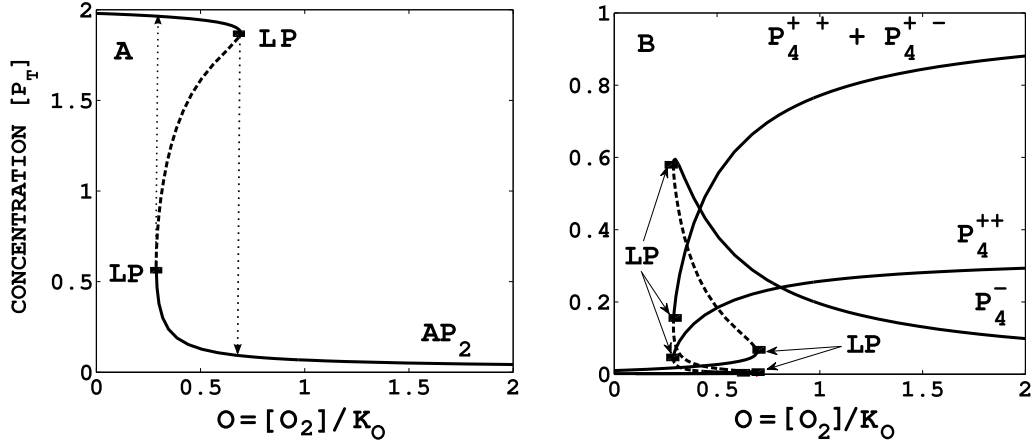


Figure A.2: *Bistable transition from anaerobic to aerobic growth conditions. In the region between the two limit points (LP) three stationary states coexist and the system exhibits hysteresis (indicated by dotted lines). Solid and dashed lines denote stable steady state and unstable steady state, respectively. Used parameters are:  $\alpha = 10$ ,  $\beta = 10^3$ ,  $\gamma = 4$  and  $I = LI/K_L = 0.1$ . Note that the curves in the left and the right panel are similar to those of Fig. 3.8A and B, respectively.*

rescaled parameter  $k'_{P_r} = 2k_{P_r}^+$ . Therefore, the main difference between the two ODE systems is the stoichiometric factor of 2 in front of the rescaled parameter  $k'_{P_r}$  in the equation for  $A^-$  which results from the fact that 2 AppA molecules are required to fully reduce one PpsR tetramer. However, as Figures A.1 and A.2 show this does not affect the qualitative behaviour of the system as predicted by the simple model.

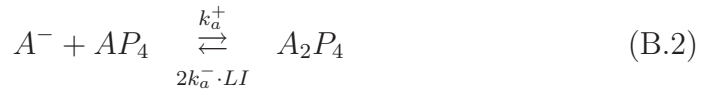
Furthermore, the pool of oxidized PpsR is now distributed between the fully oxidized form ( $P_4^{++}$ ) and the partially oxidized form ( $P_4^{+-}$ ). In principle, this could lead to interesting effects depending on the DNA-binding affinity of the partially oxidized form is comparable to that of the fully oxidized form ( $P_4^{++}$ ) or to that of the fully reduced form ( $P_4^{--}$ ). However, at the moment such details are not experimentally known.

# Appendix B

## Complex Formation as a Multi-Step Process

In Section 3.1.2, we have modeled the light-sensitive complex formation between the reduced forms of AppA and PpsR (Eq. 3.6) through an effective third-order reaction mechanism. Here, we examine the consequences of modeling the complex formation between AppA and PpsR by assuming a multi-step process (Eqs. 3.3, 3.4 and 3.5) instead of a lumped third order process (Eq. 3.6). In addition, we show how the effective parameters in Eq. 3.6 can be derived from the kinetic parameters of the multi-step process, through a quasi-equilibrium approximation for the intermediate species. Our results suggest that modeling the complex formation between AppA and PpsR in more detail does not alter our two main conclusions: The possibility of bistability in the AppA/PpsR system and the non-monotonic dependence of reduced PpsR on the oxygen concentration under sufficiently high light conditions.

We assume that complex formation proceeds by the following steps: First, two AppA molecules associate sequentially (in a two-step process) with one PpsR tetramer and, second, the so formed complex dissociates into the experimentally observed complex, where one AppA molecule is associated with one PpsR dimer.



Here, we consider PpsR as a tetramer composed of two identical dimer subunits. The first two equations describe the association of an AppA molecule to either of the two PpsR dimers. Since blue light illumination is known to inhibit complex formation (22), we have assumed (Eq. B.1-B.3) that the dissociation rate in Eqs. B.1 and B.2 is proportional to the light irradiance  $LI$ , hence  $k_a^- \cdot LI$  is a pseudo first order rate constant. The combinatorial factors of 2 in Eqs. (B.1) and (B.2) result from the fact that, in the first association event (Eq. B.1), there are two possibilities for an AppA molecule to bind one of the two PpsR dimers. Similarly, there are two possibilities for an AppA molecule to dissociate from the  $A_2P_4$  complex. For simplicity, we have assumed that binding of the second AppA molecule occurs independently from the first binding event such that the rate constants  $k_a^+$  and  $k_a^-$  are the same for both binding steps. The last equation (Eq. B.3) describes the formation of the AppA-PpsR complex ( $AP_2$ ) as observed experimentally.

After replacing the Eq. 3.6 by Eqs. B.1- B.3, the ODE system in Eqs. 3.9 read as (for  $K_{eq} = \infty$ )

$$\begin{aligned}
 \frac{d}{dt} [A^-] &= k_{Ar} [A^+] - k_{Ao} [O_2] [A^-] - 2k_a^+ [A^-] [P_4^-] + k_a^- \cdot LI [AP_4] \\
 &\quad - k_a^+ [A^-] [AP_4] + 2k_a^- \cdot LI [A_2P_4] - k_{Pr}^+ [A^-] [P_4^+] \\
 \frac{d}{dt} [P_4^-] &= -k_{Po} [O_2] [P_4^-] + k_{Pr}^+ [A^-] [P_4^+] - 2k_a^+ [A^-] [P_4^-] \\
 &\quad + k_a^- \cdot LI [AP_4] \\
 \frac{d}{dt} [AP_2] &= 2(k_d^+ [A_2P_4] - k_d^- [AP_2]^2) \tag{B.4} \\
 \frac{d}{dt} [AP_4] &= 2k_a^+ [A^-] [P_4^-] - k_a^- \cdot LI [AP_4] - k_a^+ [A^-] [AP_4] \\
 &\quad + 2k_a^- \cdot LI [A_2P_4] \\
 \frac{d}{dt} [A_2P_4] &= k_a^+ [A^-] [AP_4] - 2k_a^- \cdot LI [A_2P_4] - k_d^+ [A_2P_4] + k_d^- [AP_2]^2
 \end{aligned}$$

In addition, there are two conservation relations for the total amounts of AppA and PpsR, respectively which are given by

$$A_T = [A^+] + [A^-] + [AP_4] + 2[A_2P_4] + [AP_2] \tag{B.5}$$

$$P_T = [P_4^+] + [P_4^-] + [AP_4] + [A_2P_4] + \frac{1}{2}[AP_2]. \tag{B.6}$$

If we measure concentrations in terms of the total protein concentrations as

$$\begin{aligned} x_1 &= \frac{[A^-]}{[A_T]}, & x_2 &= \frac{[P_4^-]}{[P_T]}, & x_3 &= \frac{[AP_2]}{[P_T]}, & x_4 &= \frac{[AP_4]}{[A_T]} \\ x_5 &= \frac{[A_2P_4]}{[A_T]}, & x_6 &= \frac{[P_4^+]}{[P_T]}, & x_7 &= \frac{[A^+]}{[A_T]} \end{aligned} \quad (\text{B.7})$$

then ODE system in Eqs. B.4 becomes

$$\begin{aligned} \frac{d}{d\tau}x_1 &= x_7 - O x_1 + \mu \cdot LI \left[ x_4 - 2 \frac{x_1 x_2}{\gamma} \frac{1}{\bar{K}_a \cdot LI} - \frac{1}{\bar{K}_a \cdot LI} x_1 x_4 + 2x_5 \right] \\ &\quad - \frac{\beta}{\gamma} x_1 x_6 \\ \frac{d}{d\tau}x_2 &= \beta x_1 x_6 - \mu \cdot LI \left[ 2x_1 x_2 \frac{1}{\bar{K}_a \cdot LI} - \gamma x_4 \right] - \alpha O x_2 \\ \frac{d}{d\tau}x_3 &= 2\nu\mu\gamma \left( x_5 - \frac{1}{\bar{K}_d} \frac{x_3^2}{\gamma^2} \right) \\ \frac{d}{d\tau}x_4 &= \mu \cdot LI \left[ 2x_1 x_2 \frac{1}{\gamma} \frac{1}{\bar{K}_a \cdot LI} - x_4 - \frac{1}{\bar{K}_a \cdot LI} x_1 x_4 + 2x_5 \right] \\ \frac{d}{d\tau}x_5 &= \mu \cdot LI \left[ \frac{1}{\bar{K}_a \cdot LI} x_1 x_4 - 2x_5 - \frac{\nu}{LI} \left( x_5 - \frac{1}{\bar{K}_d} \frac{x_3^2}{\gamma^2} \right) \right] \end{aligned} \quad (\text{B.8})$$

where time ( $\tau$ ) is measured in units of  $1/k_{Ar}$  and

$$\begin{aligned} x_6 &= 1 - \left( x_2 + \frac{x_3}{2} \right) - \gamma(x_4 + x_5) \\ x_7 &= 1 - (x_1 + x_4 + 2x_5) - \frac{x_3}{\gamma} \end{aligned}$$

In Eqs. B.8  $LI$  and  $O$  denote the light irradiance and oxygen concentration, respectively. Here, oxygen concentration is measured in units of  $K_O = \frac{k_{Ar}}{k_{Ao}}$ .

The steady states of the ODE system defined by Eqs. B.8 depend on 7 dimensionless parameters. In addition to the 3 parameters introduced in the Chapter 3

$$\alpha = \frac{k_{Po}}{k_{Ao}}, \quad \beta = \frac{k_{Pr} [A_T]}{k_{Ar}}, \quad \gamma = \frac{[A_T]}{[P_T]}$$

they also depend on the dimensionless quantities

$$\begin{aligned} \bar{K}_d &= \frac{K_d}{A_T} = \frac{1}{A_T} \frac{k_d^+}{k_d^-}, & \bar{K}_a \cdot LI &= \frac{K_a \cdot LI}{A_T} = \frac{1}{A_T} \frac{k_a^- LI}{k_a^+} \\ \nu &= \frac{k_d^+}{k_a^-}, & \text{and } \mu &= \frac{k_a^-}{k_{Ar}}. \end{aligned} \quad (\text{B.9})$$

Figures B.1 and B.2 show that there are parameter combinations for which the steady state solutions of Eqs. (B.8) are similar to those of Eqs. 3.12. Therefore, consideration of multi-step process instead of single step for complex formation does not affect the main conclusions derived from the model discussed in Chapter 3.

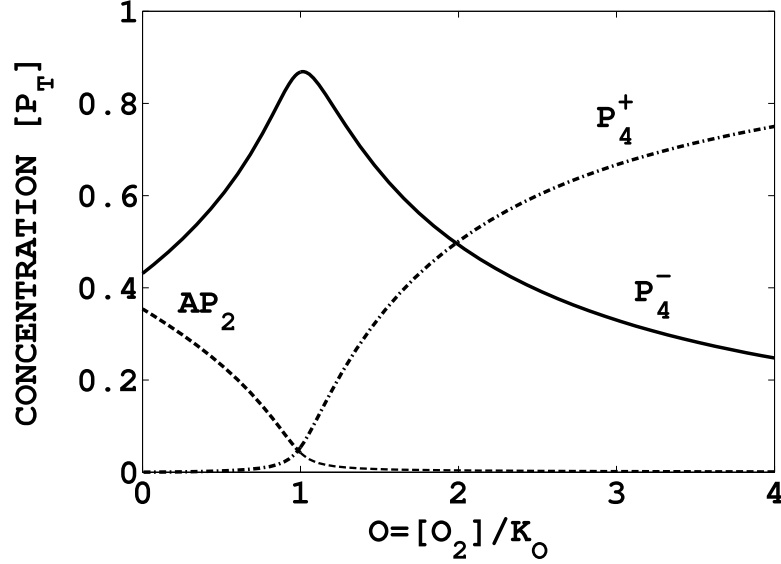


Figure B.1: *Steady state response curves calculated from Eqs. B.8. A peak develops in the steady state curve of reduced PpsR ( $P_4^-$ ) at intermediate oxygen concentrations. Used parameters are:  $\alpha = 1 = \gamma$ ,  $\beta = 10^3$ ,  $\bar{K}_d = 2$ ,  $\bar{K}_a = 0.1$ ,  $\nu = 1$ ,  $\mu = 20$  and  $LI = 5 \mu\text{mol}/\text{m}^2\text{s}$ .*

## B.1 Quasi-Equilibrium Approximation

We now show how the effective description used in the Chapter 3 (Eqs. 3.6) arises from the multi-step process introduced above. Therefore, we consider the case when the association steps between AppA and PpsR in Eqs. B.1 and B.2 are fast compared to all other processes in the system. Under this condition we can assume that the two reactions in Eqs. B.1 and B.2 are in quasi-equilibrium, i.e. we require that

$$\begin{aligned} 2k_a^+ [A^-] [P_4^-] - k_a^- LI [AP_4] &\stackrel{!}{=} 0 \\ k_a^+ [A^-] [AP_4] - 2k_a^- LI [A_2P_4] &\stackrel{!}{=} 0 \end{aligned} \quad (\text{B.10})$$

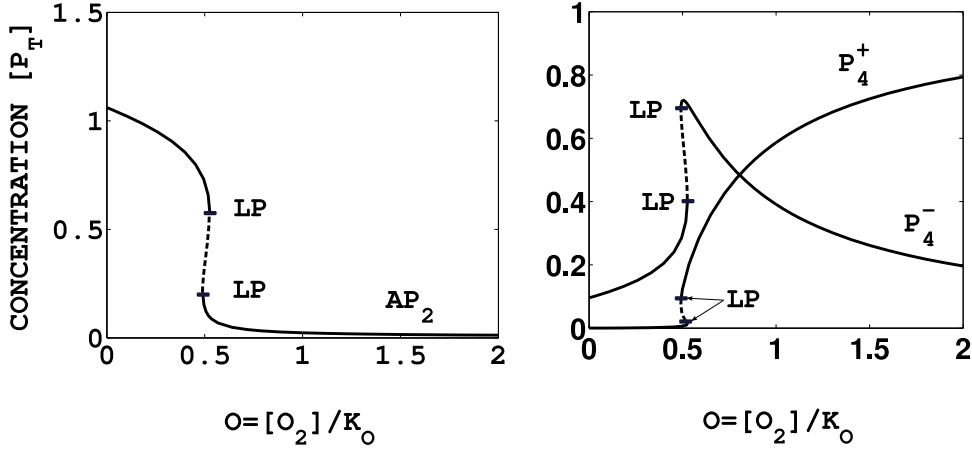


Figure B.2: Steady state response curves calculated from Eqs. B.8. The transition from anaerobic to aerobic growth conditions occurs via a bistable regime. In the region between the two limit points (LP) three stationary states coexist. Solid and dashed lines denote stable steady state and unstable steady state, respectively. Used parameters are:  $\alpha = 10$ ,  $\beta = 10^3$ ,  $\gamma = 4$ ,  $\bar{K}_d = 2$ ,  $\bar{K}_a = 0.1$ ,  $\nu = 1$ ,  $\mu = 20$  and  $LI = 5 \mu\text{mol}/\text{m}^2\text{s}$ .

In that case the intermediate complexes can be approximated as

$$[AP_4]_{eq} = 2 \frac{[A^-][P_4^-]}{K_a \cdot LI} \quad (\text{B.11})$$

$$[A_2P_4]_{eq} = \frac{1}{K_a^2 \cdot LI^2} [A^-]^2 [P_4^-] \quad (\text{B.12})$$

where  $K_a \cdot LI = k_a^- LI / k_a^+$  is the (light-dependent) dissociation constant for the association reaction between AppA and PpsR.

Additionally,

$$2k_a^+ [A^-] [P_4^-] - k_a^- LI [AP_4] = k_a^+ [A^-] [AP_4] - 2k_a^- LI [A_2P_4] \quad (\text{B.13})$$

$$k_a^+ [A^-] [AP_4] - 2k_a^- \cdot LI [A_2P_4] = k_d^+ [A_2P_4] - k_d^- [AP_2]^2 \quad (\text{B.14})$$

Using Eqs. B.11, B.12, B.13 and B.14 in Eqs. B.4, the latter can be approximated by

$$\begin{aligned}
 \frac{d}{dt} [A^-] &= k_{Ar} [A^+] - k_{Ao} [O_2] [A^-] - k_{Pr} [A^-] [P_4^+] \\
 &\quad - 2 \left( \frac{k_d^+}{K_a^2 \cdot LI^2} [A^-]^2 [P_4^-] - k_d^- [AP_2]^2 \right) \\
 \frac{d}{dt} [P_4^-] &= -k_{Po} [O_2] [P_4^-] + k_{Pr} [A^-] [P_4^+] \\
 &\quad - \left( \frac{k_d^+}{K_a^2 \cdot LI^2} [A^-]^2 [P_4^-] - k_d^- [AP_2]^2 \right) \\
 \frac{d}{dt} [AP_2] &= 2 \left( \frac{k_d^+}{K_a^2 \cdot LI^2} [A^-]^2 [P_4^-] - k_d^- [AP_2]^2 \right).
 \end{aligned} \tag{B.15}$$

These equations are the same as those in Eqs. 3.9 (for  $K_{eq} = \infty$ ) if (i) the equilibrium concentrations of the intermediate complexes  $AP_4$  and  $A_2P_4$  are sufficiently small ( $[AP_4]_{eq}, [A_2P_4]_{eq} \ll [A_T]$ ) such that they can be neglected in the conservation relations Eqs. B.5, B.6, and (ii) if we set

$$k_c^+ := \frac{k_d^+}{K_a^2} \quad \text{and} \quad k_c^- := k_d^-. \tag{B.16}$$

This shows explicitly how the effective rate constants introduced in Eqs. 3.6 are related to the kinetic parameters of an underlying multi-step process as defined by Eqs. B.1 and B.2. In addition, this analysis shows that the light irradiance would affect the forward rather than the backward rate as assumed in Eq. 3.6. Moreover, it gives a justification for the quadratic dependence of the dissociation constant on the light irradiance.

# Appendix C

## Descartes' Rule of Signs

Descartes' rule of sign has been used in Section 3.3. It is used for finding the number of real roots (i.e. number of positive and negative real roots) of the given polynomial. It states that

*“Let  $f(x) = a_0x^{b_0} + a_1x^{b_1} + \dots + a_nx^{b_n}$  denote a polynomial with nonzero real coefficients  $a_i$ , where the  $b_i$  are integers satisfying  $0 \leq b_0 < b_1 < \dots < b_n$ . Then the number of positive real zeros of  $f(x)$  (counted with multiplicities) is either equal to the number of changes in sign in the sequence  $a_0, \dots, a_n$  of the coefficients or less than that by an even whole number. The number of negative real roots of  $f(x)$  (counted with multiplicities) is either equal to the number of changes in sign in the sequence of the coefficients of  $f(-x)$  or less than that by an even whole number” (61).*

**Example:**  $f(x) = x^5 - 2x^4 + 6x^3 + 7x^2 - 8x + 2$ . In this polynomial  $f$ , there are four sign changes therefore,  $f$  can have 4, 2 or 0 positive real roots. Also,  $f(-x) = -x^5 - 2x^4 - 6x^3 + 7x^2 + 8x + 2$ . There is only one sign change in  $f(-x)$ , therefore  $f$  has exactly one negative real root.

# Appendix D

## Roots of the Polynomial 3.15

Here, we show how we reach to the conclusion that  $\alpha O > \gamma > 2$  is a necessary condition for all three roots of the polynomial  $f_\infty$  to fall within  $(0, 1)$  when  $\beta \gg 1$  (Section 3.3).

The fifth order polynomial when  $\beta \gg 1$  reads as

$$p_5 = f_\infty(y) = \left(1 - \frac{\alpha O}{\gamma} y^2\right) p_3(y) \quad (\text{D.1})$$

where

$$p_3(y) = I(1 + O)(1 - y^2) + y\left(1 - \frac{\gamma}{2}\right) - y^3\left(1 - \frac{\alpha O}{2}\right) \quad (\text{D.2})$$

By Descartes' rule of sign,  $\alpha O > 2$  is a necessary condition for the  $f_\infty$  to have three positive roots altogether. Following three relations are possible in  $\alpha O$  and  $\gamma$ : (i)  $\alpha O < \gamma$ , (ii)  $\alpha O = \gamma$  and (iii)  $\alpha O > \gamma$ . Let us discuss these cases one by one.

### Case 1. $\alpha O < \gamma$

Since,  $\gamma > \alpha O$  and  $\alpha O > 2$ , hence  $\gamma > \alpha O > 2$ . Assume  $\alpha O = (1 + \epsilon)\gamma$ , so that when  $\alpha O < \gamma$ ,  $\epsilon < 0$ . Also assume that  $\gamma = 2\omega$  with  $\omega > 1$ . Now, the fifth order polynomial  $f_\infty$  reads as

$$f_\infty(y) = (1 - (1 + \epsilon)y^2) \left[ (1 - y^2)(I(1 + O) + y(1 - \omega)) + y^3\epsilon\omega \right] \quad (\text{D.3})$$

Say  $Z(y) = [(1 - y^2)(I(1 + O) + y(1 - \omega)) + y^3\epsilon\omega]$   
Polynomial  $f_\infty$  has trivial zeros at  $y = \pm \frac{1}{\sqrt{1+\epsilon}}$ . Derivative of the polynomial

$f_\infty$  is given by

$$\frac{df_\infty(y)}{dy} = -(1 + \epsilon)2yZ + (1 - (1 + \epsilon)y^2) \frac{dZ}{dy} \quad (\text{D.4})$$

or

$$\frac{df_\infty(y)}{dy} = -(1 + \epsilon)2yZ \quad \text{at} \quad y = \pm \frac{1}{\sqrt{1 + \epsilon}} \quad (\text{D.5})$$

At  $y = \frac{1}{\sqrt{1 + \epsilon}}$

$$\frac{df_\infty(y)}{dy} = -2 \frac{\epsilon}{\sqrt{1 + \epsilon}} \left( I(1 + O) + \frac{1}{\sqrt{1 + \epsilon}} \right)$$

$\epsilon < 0$  and  $\epsilon > -1$  gives the lower bound of  $\epsilon$  (as  $\alpha O = \gamma(1 + \epsilon) > 2$ ). therefore,

$$\frac{df_\infty(y)}{dy} > 0$$

As, at  $y = \frac{1}{\sqrt{1 + \epsilon}}$ ,  $\frac{df_\infty(y)}{dy} > 0$  and the leading term in the polynomial D.3 is negative, therefore there will be another root in the interval  $(\frac{1}{\sqrt{1 + \epsilon}}, \infty)$ .

Consequently, we have four roots of the polynomial  $f_\infty$ : one between (0, 1), two at  $y = \pm \frac{1}{\sqrt{1 + \epsilon}}$ , and fourth in the interval  $(\frac{1}{\sqrt{1 + \epsilon}}, \infty)$ . So, three out of five roots are outside the interval (0, 1), which confirms that  $p_5$  (Eq. D.1) can not have three roots in (0, 1).

### Case 2. $\alpha O = \gamma$

As  $\alpha O > 2$  and  $\alpha O = \gamma$ , therefore in this case also  $\gamma > 2$ . Now, polynomial  $f_\infty$  (Eq.D.1) reads as

$$f_\infty = (1 - y^2) \left[ I(1 + O)(1 - y^2) + y \left( 1 - \frac{\gamma}{2} \right) - y^3 \left( 1 - \frac{\gamma}{2} \right) \right] \quad (\text{D.6})$$

or

$$f_\infty = (1 - y^2)^2 \left[ I(1 + O) + y \left( 1 - \frac{\gamma}{2} \right) \right] \quad (\text{D.7})$$

It is clear that  $f_\infty$  has double zeros at  $y = \pm 1$ . Hence, four out of the five roots of  $f_\infty$  are outside (0, 1), which confirms that when  $\alpha O = \gamma$ ,  $p_5$  (Eq. D.1) can not have three roots in (0, 1).

**Case 3.**  $\alpha O > \gamma$

In this case,  $\alpha O > 2$  and  $\alpha O > \gamma$ . Now there are two possibilities: either  $\gamma \leq 2$  or  $\gamma > 2$ . Assume  $\gamma \leq 2$ , then the polynomial  $p_3$  (Eq.D.2) satisfies

$$p_3 \geq y \left(1 - \frac{\gamma}{2}\right) - y^3 \left(1 - \frac{\alpha O}{2}\right) \quad \text{on } (0, 1)$$

because of  $I(1 + O) > 0$ , and  $(1 - y^2) > 0$  on  $(0, 1)$ .

This implies that  $f_\infty$  has precisely one root in  $(0, 1)$  namely  $\sqrt{\frac{\gamma}{\alpha O}}$ . Consequently, when  $\alpha O > 2$  and  $\alpha O > \gamma$ , along with  $\gamma \leq 2$ ,  $p_5$  (Eq. D.1) can not have three roots in  $(0, 1)$ .

*Hence, when  $f_\infty$  has three roots in  $(0, 1)$ , we are left with the only case  $\alpha O > \gamma > 2$ .*

# Appendix E

## Limit Point Bifurcation

For this section we follow Kuznetsov (62) and Strogatz (63). Limit points occur when we discuss the bifurcation diagram for the simple and the extended model in Chapter 3 and Chapter 4.

In this thesis we consider continuous-time dynamical systems of the form

$$\dot{y} = f(y, p) \quad \text{with} \quad y \in \mathbb{R}^n, \quad p \in \mathbb{R}^m \quad (\text{E.1})$$

We are interested in qualitative changes of the system's phase portrait as parameters are varied. In general, two possibilities can arise: (i) The phase portrait can either remain topologically equivalent to the original one, or (ii) its topology may differ from the original one.

The emergence of a topologically non-equivalent phase portrait under variation of parameters is called a *bifurcation*. The particular value of the parameter at which the system changes from one topology and to another one, is called *bifurcation point* or *critical point*.

There are many kinds of bifurcations, but here we will focus only on limit point bifurcation (saddle node bifurcation) as it is the only relevant bifurcation in this thesis.

In a saddle-node bifurcation, a pair of fixed (equilibrium) points of the system are *created* and *destroyed* as a parameter passes a bifurcation point. Such bifurcation point is called as saddle node or limit point. Alternative names are tangent or fold bifurcation and turning-point bifurcation.

Using the center manifold theorem (62) one can show that the system in Eq. E.1 is locally topologically equivalent to the one dimensional system

$$\dot{x} = \alpha \pm x^2, \quad \text{with} \quad x \in \mathbb{R}^1, \quad \alpha \in \mathbb{R}^1 \quad (\text{E.2})$$

which provides the normal form of a system exhibiting a saddle-node bifurcation.

Fig. E.1 shows the qualitative changes in the phase portrait of the system (Eq. E.2) for the '+' sign as  $\alpha$  passes through zero.

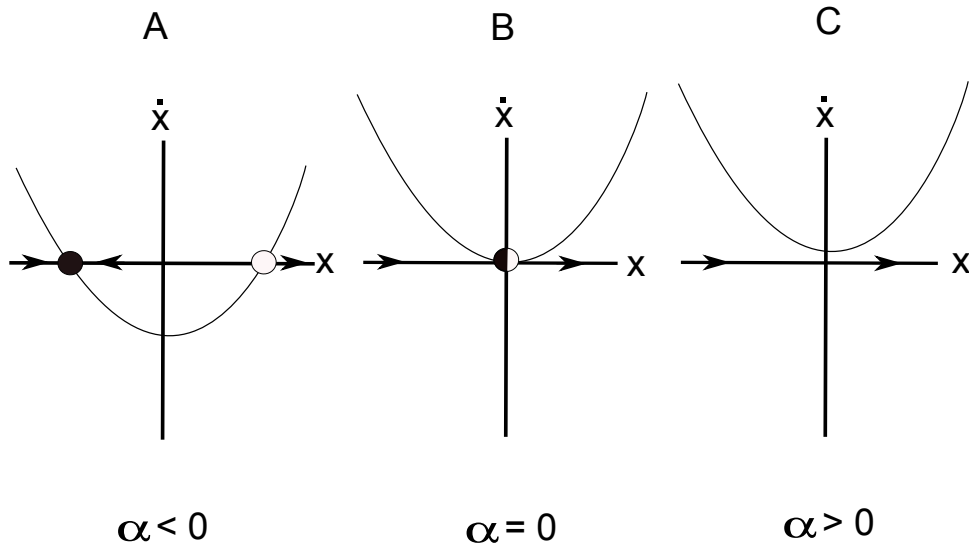


Figure E.1: *Demonstration of a saddle node bifurcation in a one dimensional dynamic system depending on one parameter ( $\alpha$ ). (A) When  $\alpha < 0$ , there are two fixed points: Stable (black circle) and unstable (white circle). (B) At  $\alpha = 0$ , both fixed points collide. (C) At  $\alpha > 0$ , there is no fixed point.*

When  $\alpha$  is negative ( $\alpha < 0$ ) then the system has two fixed points ( $x_{1,2} = \pm\sqrt{\alpha}$ ) one stable (black circle) and another (white circle) unstable. When  $\alpha$  approaches 0, the two fixed points move towards each other. At  $\alpha = 0$ , two fixed points collide and a new fixed point is formed which is very delicate since it disappears as soon as  $\alpha > 0$ . In this case  $\alpha = 0$  is the limit point. Alternatively, we can represent this bifurcation by a *bifurcation diagram* (Fig. E.2).

Note that the bifurcation diagrams shown in Chapter 3 and Chapter 4 contains two limit point bifurcations, which together create hysteresis curve and bistability.

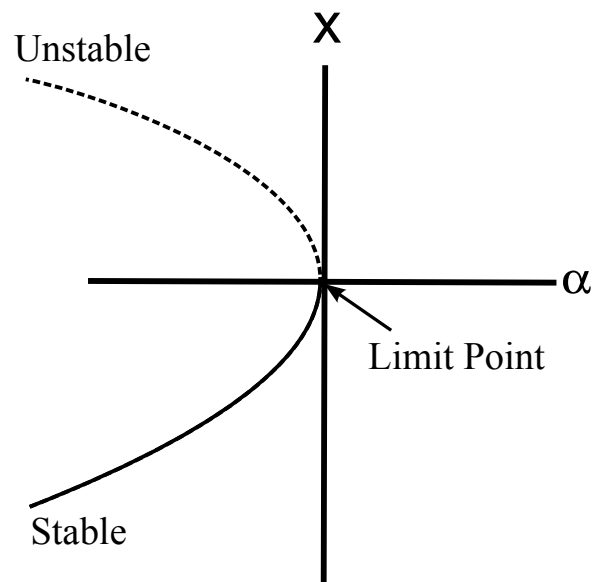


Figure E.2: *The bifurcation diagram of saddle node bifurcation.*

# Appendix F

## The Principle of Detailed Balance

The principle of detailed balance has been used in the Section 4.1.2 to set up the extended model. Here, we will follow Alberty (64), Onsager(65), Gorban et.al (66), van Kampen (67) and Reif (68).

The principle of detailed balance states that when a system is at equilibrium the rate of each elementary process is equal to the rate of its reverse process. This principle is founded upon the idea of the microscopic reversibility.

Let us consider an isolated system A and denote the probability that it will be found in state  $l$  at time  $t$  is  $P_l(t)$ . The probability  $P_l$  to find the system in state  $l$  at time  $t$  is increased by transitions from any other state  $m$  to  $l$ , which occur with rate  $W_{lm}$  (probability per unit time). Similarly,  $P_l$  is decreased by transitions from state  $l$  to other states  $m$  with rate  $W_{ml}$ . Then the temporal evolution of  $P_l$  is defined by

$$\frac{dP_l}{dt} = \sum_m (P_m W_{lm} - P_l W_{ml}) \quad \text{with } l \neq m \quad (\text{F.1})$$

Therefore, according to the principle of detailed balance, at equilibrium, the rate of the elementary process  $A_m \rightarrow A_l$  should be equal to the rate of the elementary process  $A_l \rightarrow A_m$ :

$$P_m^s W_{lm} = P_l^s W_{ml} \quad (\text{F.2})$$

To clarify, lets do one application of the principle of detailed balance on the interconversion of three isomers A, B, and C according to the following scheme

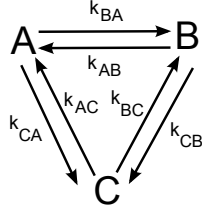


Figure F.1: *The cycle for the interconversion of three isomers A, B and C.*

Assume that the reactions obey a simple mass-action law. Then the rates of the change in the probability of occupation of the states A, B and C is given by

$$\begin{aligned}
 \frac{dP_A}{dt} &= -(k_{BA} + k_{CA})P_A + k_{AB}P_B + k_{AC}P_C \\
 \frac{dP_B}{dt} &= k_{BA}P_A - (k_{AB} + k_{CB})P_B + k_{BC}P_C \\
 \frac{dP_C}{dt} &= k_{CA}P_A + k_{CB}P_B - (k_{AC} + k_{BC})P_C
 \end{aligned} \tag{F.3}$$

where  $k_{BA}$  etc. are  $> 0$ .

The principle of detailed balance requires that the transition  $A \rightarrow B$  must take place with the same rate as the reverse elementary process  $B \rightarrow A$  occurs. Then the condition of detailed balancing imposes the following three relations among the transition rates:

$$\begin{aligned}
 k_{BA}P_A^s &= k_{AB}P_B^s \\
 k_{CB}P_B^s &= k_{BC}P_C^s \\
 k_{AC}P_C^s &= k_{CA}P_A^s
 \end{aligned} \tag{F.4}$$

Eq. F.4, is equivalent to the single relation among the transition rates.

$$k_{AB}k_{CA}k_{BC} = k_{BA}k_{CB}k_{AC} \tag{F.5}$$

Eq. F.5 is an intrinsic relation among the transition rates of cycle (Fig. F.1) and it holds under any condition, for example, steady state or a transient state (69) (despite the fact that it was derived using detailed balance). Further, this relation shows that the transition rates in the cycle are not completely independent of each other. In a self-consistent model, transition rates have to be chosen such that they satisfy this relationship (69).

# Appendix G

## Methods

For solving the ordinary differential equations (ODEs) in Chapters 3 and 4, XPPAUT (70) and MATCONT (71) simulation packages were used. Whenever XPPAUT was used to integrate the ODE system, the default integrator was set to “stiff”. While using MATCONT, the integration of the ODE system was performed with the ode15s and ode45 ODE solvers, when the ODE system was stiff and non-stiff, respectively. Other parameters such as tolerance and step size were set to their default values. To generate the bifurcation diagram, we performed numerical continuation of steady states or limit points using the Auto package, which is inbuilt in XPPAUTO or MATCONT.

# Bibliography

- [1] N. Hunter, F. Daldal, M. C. Thurnauer, and J. T. Beatty, *The Purple Phototrophic Bacteria*. Springer, P.O. Box 17, 3300 AA Dordrecht, The Netherlands, 2009.
- [2] M. T. Madigan and M. J. M., *Brock Biology of Microorganisms*. Pearson Prentice Hall, Pearson Education , Inc., Upper Saddle river, New Jersey 07458, 2006.
- [3] D. A. Bryant and N. U. Frigaard, “Prokaryotic photosynthesis and phototrophy illuminated,” *TRENDS in Microbiol.*, vol. 14(11), pp. 488–496, 2006.
- [4] J. Gregor and G. Klug, “Regulation of bacterial photosynthesis genes by oxygen and light,” *FEMS Microbiol. Lett.*, vol. 179, pp. 1–9, 1999.
- [5] Y. Han, M. H. F. Meyer, M. Keusgen, and G. Klug, “A haem cofactor is required for redox and light signaling by the AppA protein of *Rhodobacter sphaeroides*,” *Mol. Microbiol.*, vol. 64(4), pp. 1090–1104, 2007.
- [6] S. Braatsch, M. Gomelsky, S. Kuphal, and G. Klug, “A single flavo-protein, AppA, integrates both redox and light signals in *Rhodobacter sphaeroides*,” *Mol. Microbiol.*, vol. 45, pp. 827–836, 2002.
- [7] H. N. Happ, S. Braatsch, V. Broschek, L. Osterloh, and G. Klug, “Light-dependent regulation of photosynthesis genes in *Rhodobacter sphaeroides* 2.4.1 is coordinately controlled by photosynthetic electron transport via the PrrBA two-component system and the photoreceptor AppA,” *Mol. Microbiol.*, vol. 58, pp. 903–914, 2005.
- [8] J. Zeilstra-Ryalls, M. Gomelsky, J. M. Eraso, A. Yeliseev, J. O’Gara, and S. Kaplan, “Control of photosystem formation in *Rhodobacter sphaeroides*,” *J. Bacteriol.*, vol. 180, pp. 2801–2809, 1998.
- [9] C. L. Tavano and T. J. Donohue, “Development of the bacterial photosynthetic apparatus,” *Curr Opin Microbiol.*, vol. 9, pp. 625–631, 2006.

- 
- [10] J. I. Oh and S. Kaplan, "Generalized approach to the regulation and integration of gene expression," *Mol. Microbiol.*, vol. 39, pp. 1116–1123, 2001.
- [11] L. Gomelsky, O. V. Moskvina, R. A. Stenzel, D. F. Jones, T. J. Donohue, and M. Gomelsky, "Hierarchical regulation of photosynthesis gene expression by the oxygen-responsive *PrrBA* and *AppA-PpsR* system of *Rhodobacter sphaeroides*," *J. Bacteriol.*, vol. 190, pp. 8106–8114, 2008.
- [12] A. Verméglio and P. Joliot, "The photosynthetic apparatus of *Rhodobacter sphaeroides*," *Trends in Microbiology*, vol. 7, pp. 435–440, 1999.
- [13] S. Braatsch, O. V. Moskvina, G. Klug, and M. Gomelsky, "Responses of the *Rhodobacter sphaeroides* transcriptome to blue light under semiaerobic conditions," vol. 186, pp. 7726–7735, 2004.
- [14] M. Choudhary and S. Kaplan, "DNA sequence analysis of the photosynthesis region of *Rhodobacter sphaeroides* 2.4.1," *Nucleic Acids Res.*, vol. 28, pp. 862–867, 2000.
- [15] O. V. Moskvina, L. Gomelsky, and M. Gomelsky, "Transcriptome analysis of the *Rhodobacter sphaeroides* PpsR regulon: PpsR as a master regulator of photosystem development," *J. Bacteriol.*, vol. 187, pp. 2148–2156, 2005.
- [16] X. Zeng, M. Choudhary, and S. Kaplan, "A second and unusual *pucBA* operon of *Rhodobacter sphaeroides* 2.4.1: genetics and function of the encoded polypeptides," *J. Bacteriol.*, vol. 185, pp. 6171–6184, 2003.
- [17] S. Elsen, L. R. Swem, D. L. Swem, and C. E. Bauer, "*RegB/RegA*, a highly conserved redox-responding global two-component regulatory system," *Microbiol. Mol. Biol. Rev.*, vol. 68, pp. 263–279, 2004.
- [18] J. Wu and C. E. Bauer, "*RegB/RegA*, a global redox-responding two-component system," *Adv. Exp. Med. Biol.*, vol. 631, pp. 131–148, 2008.
- [19] J. H. Zeilstra-Ryalls and S. Kaplan, "Role of the *fnrL* gene in photosystem gene expression and photosynthetic growth of *Rhodobacter sphaeroides* 2.4.1," *J. Bact.*, vol. 180, pp. 1496–1503, 1998.
- [20] R. J. Penfold and J. M. Pemberton, "Sequencing, chromosomal inactivation, and functional expression in *Escherichia coli* of *ppsR*, a gene which represses carotenoid and bacteriochlorophyll synthesis in *Rhodobacter sphaeroides*," vol. 176, pp. 2869–2876, 1994.

- 
- [21] S. Elsen, M. Jaubert, D. Pignol, and E. Giraud, “*PpsR*: a multifaceted regulator of photosynthesis gene expression in purple bacteria,” *Mol. Microbiol.*, vol. 57, pp. 17–26, 2005.
- [22] S. Masuda and C. E. Bauer, “AppA is a blue light photoreceptor that antirepresses photosynthesis gene expression in *Rhodobacter sphaeroides*,” *Cell*, vol. 110, pp. 613–623, 2002.
- [23] M. Gomelsky and S. Kaplan, “appA, a novel gene encoding a transacting factor involved in the regulation of photosynthesis gene expression in *Rhodobacter sphaeroides* 2.4.1,” *J. Bacteriol.*, vol. 177, pp. 4609–4618, 1995.
- [24] S. Masuda, C. Dong, D. Swem, A. T. Setterdahl, D. B. Knaff, and C. E. Bauer, “Repression of photosynthesis gene expression by formation of a disulfide bond in CrtJ,” *Proc. Natl. Acad. Sci. USA*, vol. 99, pp. 7078–7083, 2002.
- [25] M. Gomelsky and S. Kaplan, “AppA, a redox regulator of photosystem formation in *Rhodobacter sphaeroides* 2.4.1, is a flavoprotein. Identification of a novel FAD binding domain,” *J. Biol. Chem.*, vol. 273, pp. 35319–35325, 1998.
- [26] M. Gomelsky and G. Klug, “BLUF: A novel FAD-binding domain involved in sensory transduction in microorganisms,” *Trends Biochem. Sci.*, vol. 27, pp. 497–500, 2002.
- [27] O. V. Moskvina, S. Kaplan, M. A. G. Gonzalez, and M. Gomelsky, “Novel heme-based oxygen sensor with a revealing evolutionary history,” *J. Biol. Chem.*, vol. 282, pp. 28740–28748, 2007.
- [28] H. Shimada, K. Iba, and K. Takamiya, “Blue-light irradiation reduces the expression of *puf* and *puc* operons of *Rhodobacter sphaeroides* under semi-aerobic conditions,” *Plant Cell Physiol.*, vol. 33, pp. 471–475, 1992.
- [29] M. Gomelsky and S. Kaplan, “Molecular genetic analysis suggesting interactions between AppA and PpsR in regulation of photosynthesis gene expression in *Rhodobacter sphaeroides* 2.4.1,” *J. Bacteriol.*, vol. 179, pp. 128–134, 1997.
- [30] S. N. Ponnampalam and C. E. Bauer, “DNA binding characteristics of CrtJ,” *J. Biol. Chem.*, vol. 272, pp. 18391–18396, 1997.

- 
- [31] C. E. Bauer, S. Elsen, L. R. Swem, D. L. Swem, and S. Masuda, “Redox and light regulation of gene expression in photosynthetic prokaryotes,” *Phil. Trans. R. Soc. Lond. B*, vol. 358, pp. 147–154, 2003.
- [32] S. Masuda, K. Hasegawa, and T. A. Ono, “Light-induced structural changes of apoprotein and chromophore in the sensor of blue light using FAD (BLUF) domain of AppA for a signaling state,” *Biochemistry*, vol. 44, pp. 1215–1224, 2005.
- [33] W. Laan, M. Gauden, S. Yeremenko, R. van Grondelle, J. T. M. Kennis, and K. J. Hellingwerf, “On the mechanism of activation of the BLUF domain of AppA,” *Biochem.*, vol. 45, pp. 51–60, 2006.
- [34] A. Jäger, S. Braatsch, K. Habertzettl, S. Metz, L. Osterloh, Y. Han, and G. Klug, “The AppA and PpsR proteins from *Rhodobacter sphaeroides* can establish a redox-dependent signal chain but fail to transmit blue-light signals in other bacteria,” *J. Bacteriol.*, vol. 189, pp. 2274–2282, 2007.
- [35] S. Metz, A. Jäger, and G. Klug, “In vivo sensitivity of blue-light dependent signaling mediated by AppA/PpsR or PrrB/PrrA in *Rhodobacter sphaeroides*,” *J. Bacteriol.*, vol. 191(13), pp. 4473–4477, 2009.
- [36] S. Metz, A. H. Hendriks, K. Hellingwerf, and G. Klug, “In vivo effects on photosynthesis gene expression of base pair exchanges in the gene encoding the light-responsive BLUF domain of AppA in *Rhodobacter sphaeroides*,” *Photochem. and Photobiol.*, vol. 86, pp. 882–889, 2010.
- [37] S.-K. Kim, J. T. Mason, D. B. Knaff, C. E. Bauer, and A. T. Setterdahl, “Redox properties of the *Rhodobacter sphaeroides* transcriptional regulatory proteins PpsR and AppA,” *Photosynth. Res.*, vol. 89, pp. 89–98, 2006.
- [38] M. Gomelsky and S. Kaplan, “Genetic evidence that PpsR from *Rhodobacter sphaeroides* 2.4.1 functions as a repressor of *puc* and *bchF* expression,” *J. Bacteriol.*, vol. 177, pp. 1634–1637, 1995.
- [39] J. E. Ferrell, Jr., “Self-perpetuating states in signal transduction: positive feedback, double-negative feedback and bistability,” *Curr. Opin. Cell Biol.*, vol. 14, pp. 140–148, 2002.
- [40] N. I. Markevich, J. B. Hoek, and B. N. Kholodenko, “Signaling switches and bistability arising from multisite phosphorylation in protein kinase cascades,” *J. Cell Biol.*, vol. 164, pp. 353–359, 2004.

- 
- [41] S. Legewie, B. Schöberl, N. Blüthgen, and H. Herzog, “Competing docking interactions can bring about bistability in the MAPK cascade,” *Biophys. J.*, vol. 93, pp. 2279–2288, 2007.
- [42] O. A. Igoshin, R. Alves, and M. A. Savageau, “Hysteretic and graded responses in bacterial two-component signal transduction,” *Mol. Microbiol.*, vol. 68, pp. 1196–1215, 2008.
- [43] E. M. Ozbudak, M. Thattai, H. N. Lim, B. I. Shraiman, and A. van Oudenaarden, “Multistability in the lactose utilization network of *Escherichia coli*,” *Nature*, vol. 427, pp. 737–740, 2004.
- [44] J. A. Megerle, G. Fritz, U. Gerland, K. Jung, and J. O. Rädler, “Timing and dynamics of single cell gene expression in the arabinose utilization system,” *Biophys. J.*, vol. 95, pp. 2103–2115, 2008.
- [45] M. Thattai and A. van Oudenaarden, “Stochastic gene expression in fluctuating environments,” *Genetics*, vol. 167, pp. 523–530, 2004.
- [46] E. Kussell and S. Leibler, “Phenotypic diversity, population growth, and information in fluctuating environments,” *Science*, vol. 309, pp. 2075–2078, 2005.
- [47] M. Acar, J. T. Mettetal, and A. v. Oudenaarden, “Stochastic switching as a survival strategy in fluctuating environments,” *Nat. Genet.*, vol. 40, pp. 471–475, 2008.
- [48] J. R. Pomeroy, “Uncovering mechanisms of bistability in biological systems,” *Curr. Opin. Biotechnol.*, vol. 19, pp. 381–388, 2008.
- [49] J. T. Mettetal, D. Muzzey, J. M. Pedraza, E. M. Ozbudak, and A. van Oudenaarden, “Predicting stochastic gene expression dynamics in single cells,” *Proc. Natl. Acad. Sci. USA*, vol. 103, pp. 7304–7309, 2006.
- [50] M. Jaubert, S. Zappa, J. Fardoux, J. M. Adriano, L. Hannibal, S. Elsen, J. Lavergne, A. Verméglio, E. Giraud, and D. Pignol, “Light and redox control of photosynthesis gene expression in *Bradyrhizobium*: Dual roles of two PpsR,” *J. Biol. Chem.*, vol. 279, pp. 44407–44416, 2004.
- [51] M. Gauden, S. Yeremenko, W. Laan, I. H. M. van Stokkum, J. A. Ihalainen, R. van Grondelle, K. J. Hellingwerf, and J. T. M. Kennis, “Photocycle of the flavin-binding photoreceptor AppA, a bacterial transcriptional antirepressor of photosynthesis genes,” *Biochemistry*, vol. 44, pp. 3653–3662, 2005.

- 
- [52] K. C. Toh, I. H. M. van Stokkum, J. Hendriks, M. T. A. Alexandre, J. C. Arents, M. Avila Perez, R. van Grondelle, K. J. Hellingwerf, and J. T. M. Kennis, “On the signaling mechanism and the absence of photoreversibility in the AppA BLUF domain,” *Biophys. J.*, vol. 95, pp. 312–321, 2008.
- [53] R. Pandey, D. Flockerzi, M. J. B. Hauser, and R. Straube, “Modeling the light- and redox-dependent interaction of PpsR/AppA in *Rhodobacter sphaeroides*,” *Biophys. J.*, vol. 100, pp. 2347–2355, 2011.
- [54] K. Henzler-Wildman and D. Kern, “Dynamic personalities of proteins,” *Nature*, vol. 450, pp. 964–972, 2007.
- [55] B. J. Kraft, S. Masuda, J. Kikuchi, V. Dragnea, G. Tollin, J. M. Zaleski, and C. E. Bauer, “Spectroscopic and mutational analysis of the blue-light photoreceptor appa: A novel photocycle involving flavin stacking with an aromatic amino acid,” *Biochemistry*, vol. 42, pp. 6726–6734, 2003.
- [56] W. Laan, M. A. van der Horst, I. H. van Stokkum, and K. J. Hellingwerf, “Initial characterization of the primary photochemistry of AppA, a blue-light-using flavine adenine dinucleotide-domain containing transcriptional antirepressor protein from *Rhodobacter sphaeroides*: A key role for the reversible intramolecular proton transfer from the flavin adenine dinucleotide chromophore to a conserved tyrosine?,” *Photochem. and Photobiol.*, vol. 78(3), pp. 290–297, 2003.
- [57] S. Masuda, Y. Tomida, H. Ohta, and K. Takamiya, “The critical role of a hydrogen bond between Gln63 and Trp104 in the blue-light sensing BLUF domain that controls AppA activity,” *J. Mol. Biol.*, vol. 368, pp. 1223–1230, 2007.
- [58] A. M. Stock, V. L. Robinson, and P. N. Goudreau, “Two-component signal transduction,” *Annu. Rev. Biochem.*, vol. 69, pp. 183–215, 2000.
- [59] Y. Han, S. Braatsch, L. Osterloh, and G. Klug, “A eukaryotic BLUF domain mediates light-dependent gene expression in the purple bacterium *Rhodobacter sphaeroides* 2.4.1,” *Proc. Natl. Acad. Sci. USA*, vol. 101, pp. 12306–12311, 2004.
- [60] A. Chatterjee, Y. N. Kaznessis, and W.-S. Hu, “Tweaking biological switches through a better understanding of bistability behavior,” *Curr. Opin. Biotechnol.*, 2008.

- 
- [61] X. Wang, “A simple proof of Descartes’s rule of signs,” *The American Mathematical Monthly*, vol. 111, pp. 525–526, 2004.
- [62] Y. A. Kuznetsov, *Elements of Applied Bifurcation Theory*. Springer-Verlag, New York, Inc., 1998.
- [63] S. H. Strogatz, *Nonlinear Dynamics And Chaos: With Applications to Physics, Biology, Chemistry, and Engineering*. Perseus Books, 1994.
- [64] R. A. Alberty, “Principle of detailed balance in kinetics,” *J. Chem. Edu.*, vol. 81, 2004.
- [65] L. Onsager, “Reciprocal relations in irreversible processes. i.,” *Phy. Rev.*, vol. 37, pp. 1446–1447, 1931.
- [66] A. N. Gorban and G. S. Yablonsky, “Extended detailed balance for systems with irreversible reactions,” *Chemical Engineering Science*, vol. 66, pp. 5388–5399, 2011.
- [67] N. G. Van Kampen, *Stochastic Processes in Physics and Chemistry*. Elsevier Science and Technology Books, 2007.
- [68] F. Reif, *Fundamentals of Statistical and Thermal Physics*. McGraw-Hill, Inc., USA, 1965.
- [69] T. L. Hill, *Free Energy Transduction and Biochemical Cycle Kinetics*. Dover Publications, Inc., New York (copyright 1989 by Springer-Verlag New York), 2005.
- [70] B. Ermentrout, *Simulating, Analyzing, and Animating Dynamical Systems: A Guide to XPPAUTO for Researchers and Students*. Society of Industrial and Applied Mathematics, Philadelphia, PA, 2002.
- [71] A. Dhooge, W. Govaerts, and Y. A. Kuznetsov, “MATCONT: A MATLAB package for numerical bifurcation analysis of odes,” vol. 29, pp. 141–164, 2003.

# List of Publications

1. **Rakesh Pandey**, Dietrich Flockerzi, Marcus J. B. Hauser and Ronny Straube.  
Modeling the Light- and Redox-Dependent Interaction of PpsR/AppA in *Rhodobacter sphaeroides*; *Biophys. J.* 100(10), 2347-2355, **2011**.
2. **Rakesh Pandey**, Dietrich Flockerzi, Marcus J. B. Hauser and Ronny Straube.  
An Extended Model for the Repression of Photosynthesis Genes by the AppA/PpsR System in *Rhodobacter sphaeroides*; *FEBS Journal* 279 (18), 3449-3461, **2012**.

# Curriculum Vitae

## Rakesh Pandey

Max Planck Institute for Dynamics of Complex Technical Systems

Sandtorstr. 1, D-39106 Magdeburg, Germany.

Email Id: pandey@mpi-magdeburg.mpg.de

Phone: ++49 (0)391 6110 457

---

## Personal Details

Date of Birth: 01.07.1983  
Place of Birth: Ballia, Uttar Pradesh, India  
Marital Status: Single  
Nationality: Indian

## Educational Details

### **April 2009 till Now: Ph. D. Student.**

Otto von Guericke University, Magdeburg.

Biophysics Group, Institute for Experimental Physics, PF 4120 D-39016  
Magdeburg, Germany.

### **October 2008 till Now: Ph. D. Student.**

Max Planck Institute for Dynamics of Complex Technical Systems Sand-  
torstr. 1, D-39106 Magdeburg, Germany.

**October 2008 till Now: Doctoral Student.**

International Max Planck Research School for Analysis, Design and Optimization in Chemical and Biochemical Process Engineering, Magdeburg.  
Max Planck Institute for Dynamics of Complex Technical Systems Sandtorstr. 1, D-39106 Magdeburg, Germany.

**July 2006-July 2008: Master of Technology in Computational and Systems Biology.**

Jawaharlal Nehru University, New Mehrauli Road, New Delhi 110067, India.

**July 2003-June 2005: Master of Science in Physics.**

V.B.S. Purvanchal University, Jaunpur 222001, Uttar Pradesh, India.

**July 2000-June 2003: Bachelor of Science in Physics, Chemistry and Mathematics.**

V.B.S. Purvanchal University, Jaunpur 222001, Uttar Pradesh, India.

**July 1998-June 2000: Intermediate (Class XII) with Physics, Chemistry, Mathematics, English and Hindi.**

Board of High School and Intermediate Education, Uttar Pradesh, India.

**July 1996-June 1998: High School (Class X) with Science, Mathematics, English, Hindi, Biology and Social Science.**

Board of High School and Intermediate Education, Uttar Pradesh, India.

Date, Place

Signature

# Erklärung

Rakesh Pandey  
Max Planck Institute for Dynamics  
of Complex Technical Systems Sandtorstr. 1,  
D-39106 Magdeburg, Germany.  
Email Id: pandey@mpi-magdeburg.mpg.de  
Phone: ++49 (0)391 6110 457

## Erklärung

Hiermit erkläre ich, das ich die von mir eingereichte Dissertation zum dem Thema

### **Modeling the AppA/PpsR Signal Transduction System of *Rhodobacter sphaeroides***

selbständig verfasst, nicht schon als Dissertation verwendet habe und die benutzten Hilfsmittel und Quellen vollständig angegeben wurden.

Weiterhin erkläre ich, dass ich weder diese noch eine andere Arbeit zur Erlangung des akademischen Grades doctor rerum naturalium (Dr. rer. nat.) an anderen Einrichtungen eingereicht habe.

Ort, Magdeburg

Unterschrift